PERIODICAL
2(2)
2(2)

Volume 2, No. 2 October 1955

new series

RECORDS OF OCEANOGRAPHIC WORKS IN JAPAN

Being the continuation of the
RECORDS OF OCEANOGRAPHIC WORKS IN JAPAN, Vol. 12, No. 2

Compiled by
Pacific Science Liaison Committee
of
Science Council of Japan

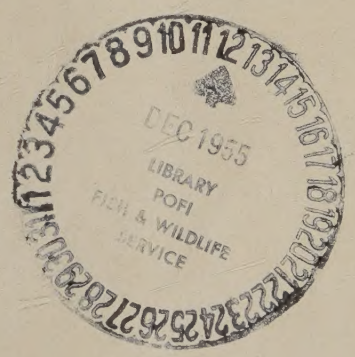

Published by

Japanese National Commission for Unesco

(4-3 Kasumigaseki, Chiyoda-ku, Tokyo, Japan)

BOARD OF EDITORS

Editor-in-Chief

Shinkishi Hatai

Editors

Yoshio Hiyama — Kōji Hidaka
Yasuo Miyake — Hiroshi Niino

With

the Co-operation of

(Physical Oceanography)
Kōji Fukutomi — Shōichirō Hayami
Mashito Nakano — Tadayoshi Sasaki
Kanji Suda — Ryūtarō Takahashi
Michitaka Uda

(Chemical Oceanography)
Masayoshi Ishibashi — Yasuo Matsudaira
Ken Sugawara

(Geological Oceanography)
Shōzaburō Hanzawa

(Biological Oceanography)
Denzaburō Miyadi — Yo K. Okada
Isao Taki — Yukio Yamada

(Fisheries)
Hiroaki Aikawa — Motosaku Fujinaga
Takeo Imai

Secretary

Buei Araya

SUGGESTION TO AUTHORS OF PAPERS FOR THE RECORDS OF OCEANOGRAPHIC WORKS IN JAPAN

An author wishing to contribute a paper to the RECORDS OF OCEANOGRAPHIC WORKS IN JAPAN should submit in compliance with the following suggestions :

1. Manuscripts will be accepted within the scope of
   Physical oceanography
   Geological oceanography
   Chemical oceanography
   Biological oceanography and Fisheries
2. An original and a copy of his munuscript should be type-written, double-spaced in 21×29.5 cm paper, within 12 sheets, making 6 printed pages including plates and tables.
3. The manuscript should be addressed to the competent editor and mailed to the official in charge of the Japanese National Commission for Unesco, 4-3 Kasumigaseki, Chiyoda-ku, Tokyo, Japan.
4. The author is asked to follow this publication for forms of headings and references, etc.
5. The editors reserve the right to accept the manuscrips and to make minior editorial changes in them, so that all papers may comform to over-all style of this publication.

CONTENTS

Why are the Thermocline and the Sea Surface Horizontal at the Equator ? ····HIDAKA, Koji····(1)

Coastal Upwelling off the California Coast ····YOSHIDA, Kozo····(8)

Note on the convective circulation (1) ····TAKANO, Kenzo····(21)

Drift and Diffusion of Radiologically Contaminated Water in the Ocean ····MIYOSHI, Hisashi, HORI, Sadakiyo and YOSHIDA, Shozo ····(30)

On a Simple Method for Estimating the Current Velocity at the Equator (II)····TSUCHIYA, Mizuki····(37)

Researches on the Fluctuation of the North Pacific Circulation
1. The Fluctuation of Oyasiwo Current in Relation to the Atmospheric Circulation and to the Distribution of the Dichothermal Waters in the North Pacific Ocean ····UDA, Michitaka····(43)

On the Theorem of Helland-Hansen and Ekman and Some of its Applications ····HAYAMI, Shoitiro, KAWAI, Hideo and OUCHI, Masao····(56)

On a Problem Concerning the Vertical Circulation of Sea Water Produced by Winds with Special Reference to its Bearing on Submarine Geology and Submarine Topography····NAKANO, Masito ····(68)

On the Possible Origin of the Intermediate Water in the Kuroshio···· ICIYE, Takashi····(82)

On the rapid determination of the dynamic depth anomaly in the Kuroshio Area····YASUI, Masashi····(90)

Notes on the Cross-Current Structure of the Kuroshio (Currents and Water Masses of the Kuroshio System V) ···· MASUZAWA, Jotaro and NAKAI, Toshisuke····(96)

Oceanic Condition in the North-Western Pacific Ocean (Preliminary Report) ···· FUKUOKA, Jiro···· (102)

The Radiochemical Analysis of Radio-Nuclides in Sea Water Collected Near Bikini Atoll···· MIYAKE, Yasuo and SUGIURA, Yoshio····(108)

On the First Larva of *parribucus Ursus-Major* (Herbst) ···· AIKAWA, Hiroaki and ISOBE, Kiyoshi····(113)

Distribution of Plankton Diatoms in Relation to Hydrographic Conditions in the Sea Area East of Honshu in the Summer of 1954····MARUMO, Ryuzo····(115)

On a Manganese Nodule and *Perotrochus* dredged from the Banks Near the Izu Islands, Japan···· NIINO, Hiroshi····(120)

Boric Acid in Bittern (I)····ISHIBASHI, Masayoshi, EMI, Koichi, KATAOKA, Hiroyoshi and KITADANI, Seizo····(127)

Optical properties of the water in the Kurrshio Current ····SASAKI, Tadayoshi, OKAMI, Noboru, WATANABE Seiichi and OSHIBA Gohachiro····(133)

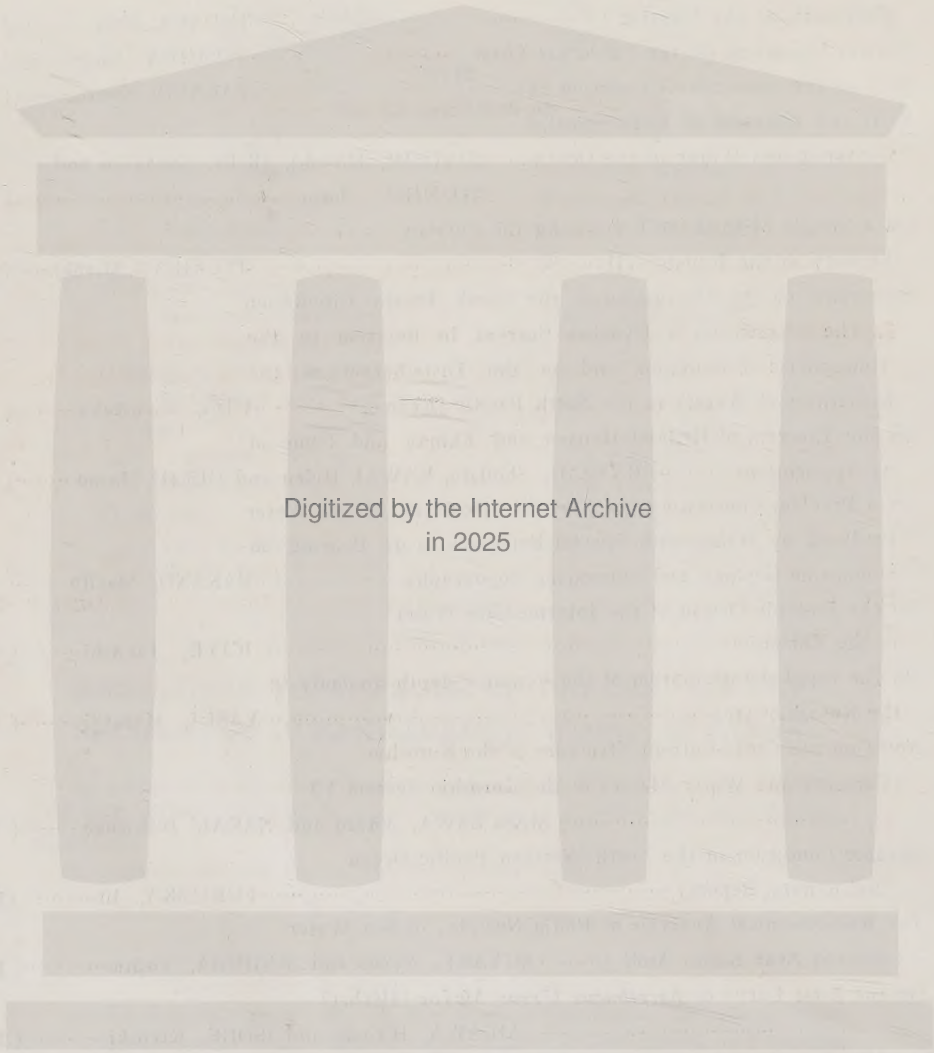

Digitized by the Internet Archive
in 2025

https://archive.org/details/records-of-oceanographic-works-in-japan-new-series_1955-10_2_2

Records of Oceanographic Works
in Japan, Vol. 2, No. 2.
October 1955

Why are the Thermocline and the Sea Surface Horizontal at the Equator ?

By

Koji Hidaka

(Geophysical Institute, Tokyo University)

Abstract-A dynamical explanation is given for the observed fact that the thermocline is horizontal and has no meridional slope at the equator, together with the conjecture that the sea surface also runs horizontal in the meridional direction.

1. Introduction Most of the recent hydrographic observations occupied across the Equator show that the thermocline is shallowest and has no meridional slope at the equator. This fact has been observed in the Carnegie sections (Sverdrup, Soule, eleming and Ennis, 1944) and more recent Albatros sections (Jerlov, 1953). Since 1951 the Pacific Ocean Fisheries Investigations, Fish and Wildlife Service in Hawaii have collected a large number of hydrographic sections across the equator and the results are being published recently (Cromwell, 1951, 1953 and 1954 ; Austin, 1954 a and b ; Stroup, 1954). All of these sections very distinctly show that the thermocline has no meridional slope at the equator.

It is frequently assumed that the same applies to the sea surface itself, though no special attempt has been possible to practically demonstrate this conjecture. Only positive evidence for this is that the Coriolis force vanishes at the equator and has different signs on both sides of the latter.

In this paper the author wishes to give a dynamical proof that both the thermocline and sea surface are horizontal at the equator and have no meridional slope there, by treating the dynamical equilibrium resulted in as the effect of a planetary wind system sweeping the surface of a zonal ocean consisting of two layers of different densittes.

In order to treat this problem, an integral expression for the current motion will be first derived.

2. An Integral Expression for the Ocean Currents. The hydrodynamical equations of stationary ocean currents in northern hemisphere are, when there is a slope on the sea surface corresponding to a definite wind distribution,

$$\mu\frac{\partial^2 u}{\partial z^2}+2\rho\omega\sin\varphi v=\frac{\partial p}{\partial x}, \tag{1}$$

$$\mu\frac{\partial^2 v}{\partial z^2}-2\rho\omega\sin\varphi u=\frac{\partial p}{\partial y} \tag{2}$$

where x and y are the coordinates in the horizontal, and z is taken vertically downwards, u and v are the components of horizontal velocity in x- and y-direction respectively, p the pressure, μ the coefficient of vertical eddy viscosity and ρ the density, of sea water, ω the angular velocity of the earth, φ the geographical latitude and g the acceleration of gravity.

On the sea surface we have

$$z=0: \quad -\mu\frac{\partial u}{\partial z}=\tau_x; \quad -\mu\frac{\partial v}{\partial z}=\tau_y, \tag{3}$$

where τ_x and τ_y are the stress components in both derections, and the bottom conditions are

$$z=h: u=v=0. \tag{4}$$

Combining the two equations (1) and (2) we have

$$\mu\frac{\partial^2 W}{\partial z^2}-2i\rho\omega\sin\varphi W=\frac{\partial p}{\partial x}+i\frac{\partial p}{\partial y} \tag{5}$$

where
$$W=u+iv \tag{6}$$

and the boundary conditions (3) and (4) now become

$$z=0: \quad -\mu\frac{\partial W}{\partial z}=\tau_x+i\tau_y \tag{7}$$

and

$$z=h: \quad W=0 \tag{8}$$

respectively.

A general solution of the equation (5) is

$$W=Ae^{-(1+i)az}+Be^{+(1+i)az}+\frac{1}{\mu}\int_0^z\left(\frac{\partial p}{\partial x}+i\frac{\partial p}{\partial y}\right)_s\frac{\sin(1-i)a)(z-s)}{(1-i)a}ds \tag{9}$$

where p is a function of z,

$$a=\sqrt{\frac{\partial\omega\sin\varphi}{\mu}}, \tag{10}$$

and A and B are constants to be determined by the conditions (7) and (8). In this solution we consider that the coefficient of vertical eddy viscosity μ is a constant from the surface down to the bottom and we do not distinguish between ρ_1 and ρ_2 in the quantity a as there would be only slight difference whichever value we may use. Ekman's "depth of frictional influence D"(Ekman, 1905) is given by

$$D=\frac{\pi}{a}. \tag{11}$$

By using the surface condition (7) we can determine A and (9) becomes

$$W=2B\cosh(1+i)az+\frac{\tau_x+i\tau_y}{(1+i)a\mu}e^{-(1+i)az}$$

$$+\frac{1}{\mu}\int_0^z\left(\frac{\partial p}{\partial x}+i\frac{\partial p}{\partial y}\right)_s\frac{\sin(1-i)a(z-s)ds}{(1-i)a} \tag{12}$$

Next, applying the bottom conditon (8) we have

$$0=2B\cosh(1+i)ah+\frac{\tau_x+i\tau_y}{(1+i)a_\mu}e^{-(1+i)ah}$$

$$+\frac{1}{\mu}\int_0^h\left(\frac{\partial p}{\partial x}+i\frac{\partial p}{\partial y}\right)_s\frac{\sin(1-i)a(h-s)}{(1-i)a}ds \qquad (13)$$

Multiplying $\cosh(1+i)ah$ on (12) and $-\cosh(1+i)az$ on (13) and adding them together, we have, after dividing by $\cosh(1+i)ah$

$$W=\frac{\tau_x+i\tau_y}{(1+i)a_\mu}\cdot\frac{\sinh(1+i)a(h-z)}{\cosh(1+i)ah}$$

$$-\frac{1}{\mu}\int_0^h\left(\frac{\partial p}{\partial x}+i\frac{\partial p}{\partial y}\right)_s\frac{\sinh(1+i)a(h-s)\cosh(1+i)az}{(1+i)a\cosh(1+i)ah}ds$$

$$+\frac{1}{\mu}\int_0^z\left(\frac{\partial p}{\partial x}+i\frac{\partial p}{\partial y}\right)_s\frac{\sinh(1+i)a(h-z)\cosh(1+i)as}{(1+i)a\cosh(1+i)ah}ds$$

This equation can be put in the folloving form:

$$M=\frac{\tau_x+i\tau_y}{(1+i)a_\mu}\cdot\frac{\sinh(1+i)a(h-z)}{\cosh(1+i)ah}-\frac{1}{\mu}\int_0^h\left(\frac{\partial p}{\partial x}+i\frac{\partial p}{\partial y}\right)_s G(z,s)ds \qquad (14)$$

where $G(z,s)$ is a symmetric kernel of the form:

$$\left.\begin{aligned}G(z,s)&=\frac{\sinh(1+i)a(h-z+s)+\sinh(1+i)a(h-z-s)}{2(1+i)a\cosh(1+i)ah},\quad s<z\\&=\frac{\sinh(1+i)a(h+z-s)+\sinh(1+i)a(h-z-s)}{2(1+i)a\cosh(1+i)ah},\quad s>z.\end{aligned}\right\} \qquad (15)$$

So far there is no particular restriction imposed on the form of the prssure p in the expression (14) except it is a function of depth z. We consider that this pressure distribution has been resulted in by the effect of wind stress distribution. In an actual ocean the winds give rise to certain slopes on the surface of the sea and a certain pressure distribution in the sea. The currents responding these slope and pressure distribution combine themselves with the pure drift currents, thus giving rise to the total circulation of the ocean.

It is therefore evident that two terms on the right-hand member of (14) cannot be independent each other. There must be some relationships to connect them.

3. Realation between the Wind Stresses and the Pressure Field in the Sea.

Ekman (1905) derived the relation between the wind stresses and those slopes produced by the former on the sea surface of a homogeneous water in two cases. For an enclosed sea he could connect the wind stresses and surface slopes in a stationary state by the condition that both the east-west and north-south components M_x and M_x of mass transport must vanish simultaneously. For an infinitely long straight coast, he solved the problem assuming that the mass transport in a direction perpendicular to the coast must vanish.

But these assumptions are only valid when we assume with Ekman that both the drift and slope currents do not vary from place to place. A more general condition applicable to an open ocean and variation of winds from place to place,

will be

$$\frac{\partial M_x}{\partial x}+\frac{\partial M_y}{\partial y}=0 \tag{16}$$

which means the absence of divergence in mass transport, and can be derived from the equation of continuity in astationary state:

$$\frac{\partial}{\partial x}(\rho u)+\frac{\partial}{\partial y}(\rho v)+\frac{\partial}{\partial z}(\rho w)=0 \tag{17}$$

by integrating it with respect to z from the surface ($z=0$) down to the bottom ($z=h$).

4. An application to a Two-Layer Zonal Ocean. in an actual ocean the winds have approximately zonal distribution, that is, the wind stress components over the ocean are functions of latitude only. Suppose a zonal ocean completely covering the earth at a constant depth h. Then this zonal wind distribution necessarily gives rise to a zonal system of drift currents in this ocean and certain distributions of surface slopes giving rise to a pressure gradient in the meridional direction, which in turn would produce slope currents at the same time. Of course, we need not there to emphasize that no east-west gradients in current velocity and the slopes of sea surface would be produced.

Another salient feature of the tropical and subtropical waters of the world's oceans is that an interface called the "thermocline" separates an upper layer of lower density from a heavier underlying water. This stratification seems to be important sometimes for interpreting the actual situation of motion of water in low and middle latitudes.

In order to represent this structure, suppose that the sea consists of an upper layer of lower density and heavier water below it. (Fig. 1) Let the densities of these two layers be ρ_1 and ρ_2 respectively($\rho_2>\rho_1$). Suppose the thickness of the upper layer when there is no wind stress on the sea surface be h_1, and this thickness is small compared with the total depth h of the ocean. Actually the thermocline is located at a depth of about 100 to 150 meters, and the mean depth of the oceans is about 4000 meters.

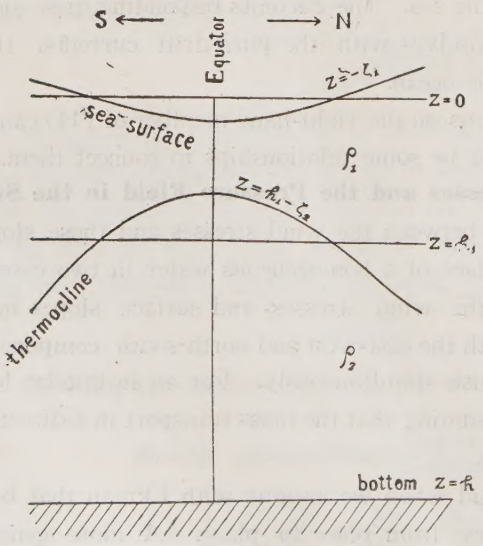

Fig. 1

In actuality the density of water in the upper mixed layer is nearly uniform, while that of lower layer is larger and slightly increases downwards.

This structure is approximately represented by the model under consideration.

Owing to the disturbances of winds, these two surfaces will be deformed. Let the equations of the sea surface and the interface be $z=-\zeta_1$ and $z=h_1-\zeta_2$ respectively. Then the pressure gradient at a point z in the lighter upper and heavier lower water will be given by

$$\frac{\partial p}{\partial y}=g\rho_1\frac{\partial \zeta_1}{\partial y}, \quad (-\zeta_1<z<h_1-\zeta_2) \tag{18}$$

$$=g\rho_1\frac{\partial \zeta_1}{\partial y}+g(\rho_2-\rho_1)\frac{\partial \zeta_2}{\partial y}, \quad (h_1-\zeta_2<z<h). \tag{19}$$

If ζ_1 anf ζ_2 are not large, the integral expression (14) for the ocean currents becomes approxlmately

$$W=\frac{\tau_x+i\tau_y}{(1+i)a\mu}e^{-(1+i)az}-\frac{i}{\mu}\int_0^{h_1}\frac{\partial p}{\partial y}G(z,s)ds$$

$$-\frac{i}{\mu}\int_{h1}^{h}\frac{\partial p}{\partial y}G(z,s)ds \tag{20}$$

because we have $\frac{\partial p}{\partial x}=0$ in a zonal ocean. Substituting from (18) and(19), we have

$$W=\frac{\tau_x+i\tau_y}{(1+i)a\mu}e^{-(1+i)az}-\frac{i}{\mu}g\rho_1\frac{\partial \zeta_1}{\partial y}\int_0^{h_1}G(z,s)ds$$

$$-\frac{i}{\mu}\left\{g\rho_1\frac{\partial \zeta_1}{\partial y}+g(\rho_2-\rho_1)\frac{\partial \zeta_2}{\partial y}\right\}\cdot\int_{h1}^{h}G(z,s)ds \tag{21}$$

Thus the currents we are looking for are now expressed in terms of the stress components τ_x and τ_y, and the slopes of sea surface $\frac{\partial \zeta_1}{\partial y}$ and that of interfacce $\frac{\partial \zeta_2}{\partial y}$. In order to determine the relation between these quantities the expression (16) will be employed. In a zonal ocean it is evident that there can be no east-west variation in wind stress and currents. We can therefore assume $\frac{\partial M_x}{\partial x}=0$, so that it follows $\frac{\partial M_y}{\partial y}=0$ from (16). Thus M_y is independent of both x and y. But if the ocean is limited this constant cannot have other value than 0. Moreover, we consider that this relation is fulfilled in each of the two layers separately, or

$$\int_0^{h_1}\rho_1 v dz=0 \tag{22}$$

and

$$\int_{h1}^{h}\rho_2 v dz=0\ . \tag{23}$$

Integrating the right-hand member of (21) with respect to z from $z=0$ to $z=h_1$, and from $z=h_1$ to $z=h$, and equating their imaginary parts to zero, we have

$$(1-\cos ah_1e^{-ah_1})\,\tau_x-\sin ah_1e^{-ah_1}\tau_y-g\rho_1\frac{\partial \zeta_1}{\partial y}\cdot\frac{1-(\cos 2ah_1+\sin 2ah_1)e^{-2ah_1}}{4a}$$

$$+\left\{g\rho_1\frac{\partial \zeta_1}{\partial y}-g(\rho_2-\rho_1)\frac{\partial \zeta_2}{\partial y}\right\}\cdot\frac{1-(\cos 2ah_1+\sin 2ah_1)e^{-2ah_1}}{4a}=0, \tag{24}$$

and

$$\cos ah_1 e^{-ah_1}\tau_x+\sin ah_1 e^{-ah_1}\tau_y-g\rho_1\frac{\partial\varsigma_1}{\partial y}\cdot\frac{1-(\cos 2ah_1+\sin 2ah_1)e^{-2ah_1}}{4a}$$

$$+\left\{g\rho_1\frac{\partial\varsigma_1}{\partial y}-g(\rho_2-\rho_1)\frac{\partial\varsigma_2}{\partial y}\right\}\frac{3-(\cos 2ah_1+\sin 2ah_1)e^{-2ah_1}}{4a}=0. \qquad (25)$$

In obtaining these equations is made a certain number of reasonable simplifications coming from neglecting e^{-ah} against 1 and e^{-ah_1} because h_1 is supposed to be small compared with h, the total depth to the bottom.

Solving the two equations (24) and (25) as simultaneous, the slopes of the sea surface and interface are obtained as follows :

$$g\rho_1\frac{\partial\varsigma_1}{\partial y}=-\left\{\frac{\tau_x}{2}+\frac{(1-\cos ah_1 e^{-ah_1})\tau_x-\sin ah_1 e^{-ah_1}\tau_y}{1-(\cos 2ah_1+\sin 2ah_1)e^{-2ah_1}}\right\}\cdot 4a \qquad (26)$$

and

$$g(\rho_2-\rho_1)\frac{\partial\varsigma_2}{\partial y}=\frac{(1-\cos ah_1)e^{-ah_1}\tau_x-\sin ah_1 e^{-ah_1}\tau_y}{1-(\cos 2ah_1+\sin 2ah_1)e^{-2ah_1}}\cdot 4a \qquad (27)$$

or

$$g\rho_1\frac{\partial\varsigma_1}{\partial y}+g(\rho_2-\rho_1)\frac{\partial\varsigma_2}{\partial y}=-\frac{\tau_x}{2}\cdot 4a \qquad (28)$$

7. No Meridional Slope of the Sea Surface and Thermocline at the Equator.

The expression (26) tends, when $\varphi\to 0$ or $a\to 0$, to

$$g\rho_1\frac{\partial\varsigma_1}{\partial y}\to 2a\tau_y \qquad (29)$$

giving

$$\frac{\partial\varsigma_1}{\partial y}=0 \qquad \text{at } \varphi=0. \qquad (30)$$

This means that the sea surface is horizontal and has no meridional slope at the Equator. In a similar way it follows from (27) and (28)

$$\frac{\partial\varsigma_2}{\partial y}=0 \qquad \text{at } \varphi=0,$$

showing tht thermocline is also horizontal and has no meridional slope at the Equator.

The present interpretation is based upon the assumption that the ocean is zonal, there being no continents and islands in it, and that the motion of water has no east-west variation. Of course, there can be no longitudinal slope. Since the east-west slope of the sea surface is not large in the Equatorial Pacific Ocean, we may conclude that our theory would furnish us with a fairly good dynamical explanation of the observed facts.

References

Austin, Thomas S.,

1954a Mid-Pacific oceanography III, Transequatorial waters, August-October 1951. U. S. Fish and Wildlife Service, Spec. Sci. Rep.: Fish. No. 131

1954b Mid-Pacific oceanography, V. Transequatorial waters, May-June 1952,

August, 1952. U. S. Fish and Wildlife Service Spec. Sci. Rep.: Fish. No. 136

Cromwell, Townsend,

1951. Mid-Pacific oceanography. January-March 1950. U. S. Fish and Wildlife Service Spec. Sci. Rep.: Fish. No. 54,

1953. Circulation in a meridional plane in the central Equatorial Pacific. Jour. of Mar. Res., 12 (2): 196-213

1954. Mid-Pacific oceanography II. Transequatorial waters, June-August 1950, January-March 1951. U. S. Fish and Wildlife Service, Spec. Sci. Rep.: Fish. No.131

Ekman, V. W.

1905. On the influence of the Earth's rotation on ocean currents. Arkiv för Matemetik, Astronomi och Fysik., Band 2. No. 11.

Jerlov, N. G.,

1953. Studies of the equatorial currents in the Pacifific. Tellus, 5 (3):308-314.

Stroup, E. D.,

1954. Mid-Pacific oceanography IV, Transequatorial waters, January-March 1952. U. S. Fish and Wildlife Service, Spec. Sci. Rep.:Fisheries No. 135.

Sverdrup, H. U., F. M. Soule, R. H. Fleming and C. C. Ennis,

1944. Observations and results in physical oceanography. Sci. Res. of Cruise VII of the Carnegie during 1928-29 under Command of Captain J. P. Ault. Oceanography-1-A, Washington, D. C.

Records of Oceanographic Works
in Japan, Vol. 2, No. 2,
October 1955

COASTAL UPWELLING OFF THE CALIFORNIA COAST

By

Kozo Yoshida

(Geophysical Institute, Tokyo University)

ABSTRACT

It is indicated that the coastal upwelling as a boundary phenomenon may take place within a narrow strip close to the coast, or within a distance less than 100 km from the coast, when north-westerly winds parallel to the coast prevail longer than a week. The speed of this upwelling is measured by wind data averaged over this coastal zone. The variations in surface currents and in thickness of the mixed layer during the period of upwelling are derived and are found reasonable in comparison with observed conditions.

INTRODUCTION

It was indicated by the present author and Mao (Yoshida and Mao, 1955) that upwelling off the California coasts is essentially ascribed to the local wind stress curl over the inshore areas. Subtropical Convergence which occurs further in the open ocean in these latitudes, 25° to 45°N, is partially compensated by coastal divergence due to local wind field modified by coastal effects on winds. It appears that this mechanism is in essential contrast to that so far accepted as a boundary phenomenon.

It should be noted, however, that the above applies only to the average vertical motion over a scale of month and of 100km. Some local and instantaneous features are smoothed out from those results, and it is suspected that there might be some small-scale, localized, upwelling which has escaped from our previous results of average upwelling.

In fact, the upwelling which was indicated by Sverdrup and Fleming (1941) from cruise data in 1937 is confined within a distance from the coast of nearly 50 to 100km. Conspicuous cold and saline water in the surface layer which is very likely to indicate upwelling, is, in many cases, present within a narrow region close to the coast, perhaps less than 100km. The station plan of the CCOFI cruise, revised since 1950, includes more nearshore stations than before, and it appears that the above features have been more clearly indicated. Thus, there appears to be certain indications that "coastal upwelling" is present which is confined within a distance less than 100km or so (Figs 1 a, b, c). Although our

average upwelling or offshore upwelling may be important on dynamical balance in the California current system, the coastal upwelling might be of more practical significance on productivity of the waters along the coasts.

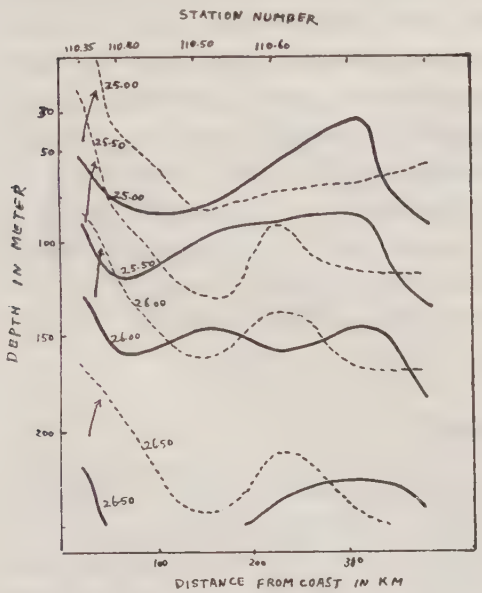

Fig 1a. Section showing distribution of density (σ_t) above 200m.
(a) ——— : CCOFI cruise 5003, March, 1950
(b) ····· : CCOFI cruise 5004, April, 1950.

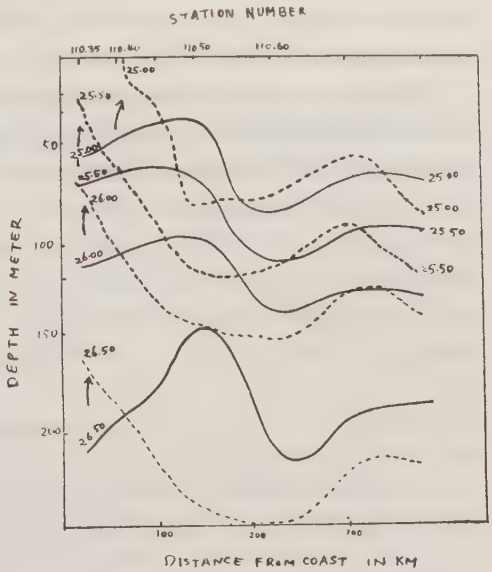

Fig 1b. Section showing distribution of density (σ_t) above 200m.
(a) ——— : CCOFI cruise 5101, January, 1951
(b) ····· : CCOFI cruise 5103, March, 1951.

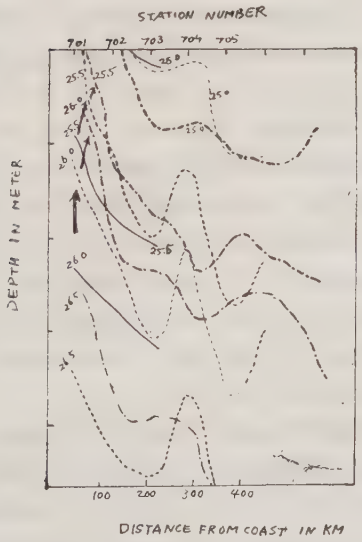

Fig 1c. Section showing distribution of density (σ_t) above 200m.
(a) ——— : CCOFI cruise 4903, March, 1949.
(b) ····· : CCOFI cruise 4904, April, 1949.
(c) —·—·— : CCOFI cruise 4905, May, 1949.

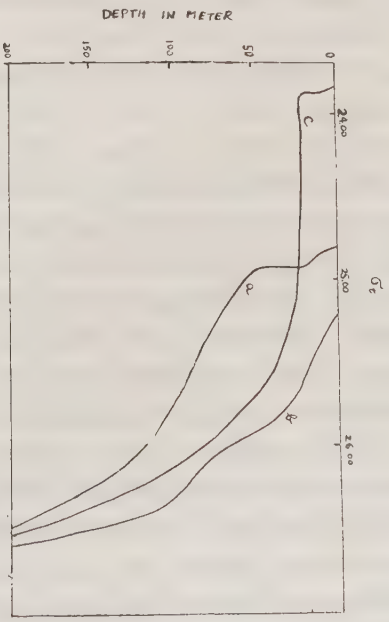

Fig 2. Vertical distribution of density (σ_t) at Station 110.35, CCOFI cruises : (a) Cruise 5003, March, 1950, (b)Cruise 5005, May, 1950, (c) Cruise 5009, September, 1950.

Those small-scale processes are difficult to deal with, since observations are not available to such detailed features yet, and various unknown factors seem to be involved for any theoretical approach. However, it appears that a simple model for coastal upwelling can be derived which may possibly account for the characteristic features of the observed facts so far obtained in the California waters.

Now let us confine ourselves to the problem of coastal processes. Various outstanding features of variations in oceanographic conditions such as in surface currents, surface swirls and subsurface density field have been observed which may probably be associated with upwelling, especially in the waters off California. It is then the principal purpose of the present paper to go into the possible processes of upwelling as a boundary phenomenon of which the occurrence may be limited within a narrow strip close to the coast, and to see whether the results could be in accord with the observed facts.

THEORY

Upwelling along the coasts of California, Peru, Southwest Africa and Morocco has been interpreted as the following processes: (The Oceans, 1942)

> "……a wind in the Northern Hemisphere which blows parallel to the coast, with the coast on the left-hand side. In this case the light surface water will be transported away from the coast and must, owing to the continuity of the system, be replaced near the coast by heavier subsurface water……".

This may probably apply to an early stage during a period of upwelling. When a duration of winds is as short as a few hours, offshore component of surface water transport will not be considerable since drift current may not fully develop. When the winds are more or less steady as long as several hours to one day, drift current may develop, but considerable upwelling will not follow due to oscillation of thermocline. The processes during ***a few days to a week*** which may be associated with a wind of duration not less than a week will then be quite essential to the mechanism involved above. If the wind continues more or less steadily for much longer than a week, the surface currents will approach to be steady. The period of a few days to a week may be characterized by that during which geostrophic balance is approached, while local time change in relative vorticity is not negligible in the vorticity equation.

Let us assume at first a model for the California waters in which the coastline runs in north-south direction. This assumption will not modify the results materially as far as the scale of the processes of our concern is so small, within a narrow strip close to the coast, that the effects of planetary vorticity is negligible. Some errors might enter from this assumed model, since the California coastline bends at Point Conception.

The origin of the coordinate is taken at any arbitrary point along the coastline, x and y axes pointing positively eastward and northward. z axis directs

positively downward, $z=0$ being placed along a mean sea level.

The present discussion is at first intended to derive quantitative results, of which the qualitative descriptions have been established by the foregoing authors (Sverdrup and Fleming, 1941). Hence, following the foregoing mechanism, the model is further idealized : essentially there is no variations in conditions in north-south direction. We are still interested in processes of scale of order of several days to a week and of 10km, so that processes of much smaller scale would escape our scope. Rough estimates of order of magnitude for the general conditions in this locality may indicate that the balance in the upper mixed layer is between the terms

$$-fv=-\frac{\partial p}{\partial x} \qquad (1)$$

$$\frac{\partial v}{\partial t}+fu=\frac{\partial}{\partial z}\left(A\frac{\partial v}{\partial z}\right)\approx\frac{\tau_y}{H} \qquad (2)$$

where f is Coriolis parameter, p is pressure, A is eddy viscosity, τ_y is the northward component of wind stress τ, u and v are the x and y components of current velocity, and H is an average thickness of the mixed layer.

The corresponding vorticity equation and divergence equations are respectively

$$\frac{\partial \zeta}{\partial t}-f\frac{w_h}{H}\approx\frac{curl_z\,\tau}{H} \qquad (3)$$

and

$$f\zeta\approx\frac{\partial^2 p}{\partial x^2} \qquad (4)$$

where ζ is a vertical component of relative vorticity, and w_h is vertical velocity at $z=h$ (a depth of thermocline).

Equation of continuity and a condition of quasi-isostatic adjustment lead to

$$w_h\approx\frac{1}{g\Delta\rho}\frac{\partial p}{\partial t} \qquad (5)$$

This equation (5) is quite essential to the process under consideration, and it is based on two assumptions : (1) penetration of water, momentum, heat or salt from subsurface depths to surface layer will be negligible at this stage, and (2) surface slope will occur to diminish pressure gradient in greater depths, so that surface slope and thermocline slope will establish nearly isostatic condition. These are not obviously acceptable assumptions because time constants involved are not well known. However, it might appear reasonable to assume such conditions at a stage during a week, as there seems to be some reason to accept it when we consider a model of processes of mutual adjustment between pressure and current (Yoshida, 1955b:). Defant estimated from the data off the California coasts that the time constant might be one or two days.*

Now it is quite obvious that coastal upwelling depends also upon wind distributions at some distances from the coast. It would be expected that field of

* Albert Defant : Memorandum concerning the work of the Marine Life Research Program, La Jolla, 1950.

wind stress curl somewhat offshore may intensify or reduce the coastal upwelling, or may even lead to coastal sinking, even when the narrow northerly winds exist along the coast. The combination of eqs. (3), (4) and (5) immediately yield

$$\frac{\partial^2 w}{\partial x^2} - k^2 w = \frac{k^2}{f} \frac{\partial \tau_y}{\partial x} \tag{6}$$

where $k = \dfrac{f}{\sqrt{gH\Delta\rho}}$.

The boundary condition along the coast ($u=0$) is seen to require

$$\left.\frac{\partial w}{\partial x}\right|_{x=0} = \left.\frac{k^2}{f}\tau_y\right|_{x=0}. \tag{7}$$

Under the condition that $w \to 0$ as $x \to -\infty$, the solution is

$$w = \frac{k^2}{2f}\left[+ \int_0^x \tau_y e^{k(x-\xi)} d\xi + \int_{-\infty}^x \tau_y e^{-k(x-\xi)} d\xi + e^{kx} \int_{-\infty}^0 \tau_y e^{k\xi} d\xi \right] \tag{8}$$

This may imply that w at a locality x is given by a difference between some weighted mean of τ_y west of the locality x and the mean of τ_y east of x (to the coast). Where the locality is far off the coast, that is $|kx| \gg 1$, this difference will be well approximated by $\dfrac{\partial \tau_y}{\partial x}$ ***at the locality.***

Along the coastline, on the other hand, we have

$$w_0 = \frac{k^2}{f} \int_{-\infty}^0 \tau_y e^{kx} dx. \tag{9}$$

It is seen from above that uniform northerly wind over offshore water lead to the coastal upwelling in amount of

$$w_0 = \frac{\tau_y|_0}{\sqrt{gH\Delta\rho}} \tag{10}$$

In this case, upwelling velocity is proportional to the intensity of northerly wind and does not explicitly upon latitude. With the assumed numerical values $g\Delta\rho = 2.5$, $H = 4 \times 10^3$ and $\tau_y|_0 = -0.5$, one obtains

$$w|_{x=0} \approx -5 \times 10^{-3} \text{ cm/sec}$$

In five days, this amount of upwelling give an upward displacement of a thermocline by 22 meters. This rise of a thermocline will not continue with the above rate after an earlier transient stage is over, but will approach to an equlibrium condition probably in a week or so, as will be seen in later sections of this paper. Then the resultant displacement of the thermocline would not materially differ from the above during a whole stage for a month or two, in rough agreement with the observed amount of displacement detected from two cruises with interval of nearly one month. However, it should be noted that the region where this coastal upwelling occurs is practically ***limited within a narrow strip*** close to the coast, if there is no wind stress curl offshore. The numerical values assumed above give $k \sim 0.7 \times 10^{-6} \text{cm}^{-2}$, and it follows that at distance 40km w is reduced to 6 percent of the one at the coast, and only 3 percent at 50km. Thus the process is practically limited within 40 to 50km from the coast at latitudes of California. An effective width of coastal upwelling is measured by k, so that L,

a characteristic width, may be introduced by

$$L=\pi/k \tag{11}$$

or

$$L=\frac{\pi\sqrt{gH\Delta\rho}}{f} \tag{12}$$

which may suggest that coastal upwelling extends wider in lower latitudes than in higher. Approximate values of L will be listed in the following :

L (in 100 km)

latitude(°) \ $gH\Delta\rho(10^4\times)$	0.5	1.0	2.0	4.0	6.0
10	1.0	1.4	2.0	2.8	3.4
30	0.3	0.5	0.7	0.9	1.1
50	0.2	0.3	0.4	0.6	0.7
70	0.1	0.2	0.3	0.4	0.5

In most coastal regions in the oceans, the values of $gH\Delta\rho$ may fall within the range listed above. The values probably vary with latitude, and, perhaps, may occur most frequently with those around 1.0. The length L may be similar as "the radius of deformation" called by Rossby (1938).

CHANGES IN SURFACE CONDITIONS

Eddies, Currents in surface layer.

Various characteristics of changes in surface currents and eddies during a period of upwelling have been observed (Suerdrup and Fleming, 1941; Sverdrup and Allen, 1939, the Oceans. 1942). In this connection, it may be of some interest to remark on the changes in those surface conditions which are derived from the above model of transient state of upwelling process. At these early stages, days to week, those changes are expressed by

$$\frac{\partial v}{\partial t}=\frac{g\Delta\rho}{f}\frac{\partial w}{\partial x} \tag{13}$$

$$\frac{\partial \zeta}{\partial t}=f\frac{w}{H}+\frac{curl\,\tau}{H} \tag{14}$$

$$\frac{\partial h}{\partial t}=w \tag{15}$$

In the inshore region, very close to the coast, they are roughly

$$\frac{\partial v}{\partial t}\approx\frac{\tau_y}{H}\Big|_0 \tag{16}$$

$$\frac{\partial \zeta}{\partial t}\approx\frac{\tau_y|_0\,k}{H} \tag{17}$$

$$\frac{\partial h}{\partial t}\approx\frac{\tau_y|_0\,k}{f} \tag{18}$$

all of which indicate quite appreciable amount of changes.

On the other hand, outside the inshore region, the changes are smaller in currents and vorticity, even in the regions of considerable upwelling. They are given approximately by

$$\frac{\partial v}{\partial t} \approx -\frac{g\Delta\rho}{f^2}\frac{\partial^2 \tau_y}{\partial x^2} \tag{19}$$

$$\frac{\partial \zeta}{\partial t} \approx -\frac{g\Delta\rho}{f^2}\frac{\partial^3 \tau_y}{\partial x^3} \tag{20}$$

$$\frac{\partial h}{\partial t} \approx -\frac{1}{f}\frac{\partial \tau_y}{\partial x} \tag{21}$$

A rise of isopycnal is not uniform near the coast, but it is largest along the coast due to coastal upwelling. Thus, ***the variations in surface features are practically confined within the narrow coastal regions.*** In other words, the coastal upwelling asscociates considerable changes in surface conditions within the coastal waters of width L, while upwelling or sinking outside this strip will not give rise to such significant changes during such a length of time as a week or so.

It should be observed that surface southward current is accelerated, as seen from (16), increasing southward component of velocity by some 50cm/sec in a week. Negative vorticity will be accelerated under the corresponding conditions. A depth of thermocline will rise by some 20m in a week. These results are roughly in agreement with the observed facts so far obtained in the considered areas. Of course, it is not evident that such changes do take place in actuality since observed data are scarce in confirming such changes over days to a week. The rough comparison described in the present paper is, therefore, only based on empirical informations of changes from month to month.

BALANCED STATE

Obviously, the changes described above will not continue very long. Perhaps, the early stage will represent the processes which occur during a week or so. This estimate must, however, depend largely upon factors which contribute to check the changes and bring a new balance. It should be noticed in this connection that the distribution of vertical velocity is kept ***unchanged*** during the above stage, while appreciable changes take place in surface currents, and a depth of thermocline. This would be valid as far as we assume that nearly "isostatic adjustment" is at least partially established during a period of a few days to a week. It may follow then that upwelling develops during periods earlier than those concerned here, perhaps one to a few days.

The surface divergence, of which the essential portion is due to wind driven currents, will occur without much delay as wind develops, perhaps hours to a day. Vertical motion thus developed will change the density distributions considerably. Especially, a thermocline layer will be raised and then sea surface will be lowered, leading to a shrinking of the mixed layer.

Factors which might control the processes during later stages of coastal upwelling are not well known. One of the most probable factors would be supposed to be ***lateral mixing*** in the inshore region. Owing to the changes at early stages, the conspicuous gradients in surface currents, vorticity and a depth of thermocline

are produced in a narrow coastal zone. During periods after a week duration of nearly steady winds, lateral mixing is assumed to be more important than local time acceleration, and the processes discussed in the followings will represent nearly steady state when quasi-equilibrium condition is established for the system. Of course, there must be transient stages from the early stages to this final stage, which perhaps concern a period of 5 days to two weeks. Transient stage will only briefly be described later on.

Dynamical equations are now

$$-fv=-\frac{\partial p}{\partial x} \tag{22}$$

$$fu=\frac{\tau_y}{H}+B\frac{\partial^2 v}{\partial x^2} \tag{23}$$

where B is a coefficient of lateral mixing.

The corresponding vorticity equation and divergence equation are

$$-f\zeta=-\frac{\partial^2 p}{\partial x^2} \tag{24}$$

$$-f\frac{w}{H}=\frac{1}{H}\frac{\partial \tau_y}{\partial x}+B\frac{\partial^2 \zeta}{\partial x^2} \tag{25}$$

respectively.

The process of lateral mixing which is assumed to play a significant role in bringing the system initially disturbed into quasi-balanced state may perhaps be caused by inshore eddies of various scale and by internal waves. The latter process might deserve attention. The rise of thermocline due to ascending motion will cause a sharp horizontal gradient of density. When conditions fluctuate as encountered usually, internal waves will develop and cause intense mixing ***across*** the thermocline. The horizontal boundary waves, or meandering, may also be generated, which produce mixing.

The ascending motion at early stages leads to a marked variation of a depth of thermocline which in many cases is raised up to the very surface. Lateral mixing across the inclined thermocline would follow, and the equation for conservation of mass may become (Yoshida, 1955a)

$$w\frac{\partial \rho}{\partial z}=B\frac{\partial^2 \rho}{\partial x^2} \tag{26}$$

where ρ is defined as a function of T and S essentially.

This may approximately lead to (Yoshida, 1955a)

$$w=-B\frac{\partial^2 h}{\partial x^2} \tag{27}$$

The boundary condition at the coast is still given by (7) for w, which, on the other hand, lead to

$$\left.\frac{\partial^2 v}{\partial x^2}\right|_0=-\frac{\tau_y|_0}{BH} \tag{28}$$

or,

$$v|_0=0 \tag{29}$$

Owing to the relations:

$$w_h = -B\frac{\partial^2 h}{\partial x^2} = -\frac{B}{g\Delta\rho}\frac{\partial^2 p}{\partial x^2} = -\frac{fB}{g\Delta\rho}\frac{\partial v}{\partial x} = -\frac{fB}{g\Delta\rho}\zeta, \qquad (30)$$

the equation for w will again become the same as at the earlier stage, indicating that the distribution of vertical velocity will be kept unchanged throughout the whole stage of the processes as far as winds are kept steady.

As stated before, vertical motion is maintained quasi-steadily by winds, unless winds vary abruptly during a period less than one day. Ascending water is subject to mixing with the surrounding water and thermocline layer will not be raised appreciably. At this established stage, vorticity in the surface layer is proportional to vertical velocity. Upwelling is thus associated with cyclonic vorticity in surface layer, in contrast to the inshore initial increase of negative vorticity due to coastal upwelling. Negative vorticity initially developed will be completely changed into steady positive vorticity.

Since surface currents at the coast are small in later stages, the established positive vorticity will not be associated with ***eddy*** or swirl.

This may appear to agree with the facts observed by Sverdrup and others that the countercurrent tends to disappear and uniform southward current develops when upwelling takes place, while, when upwelling ceases, countercurrent appears and eddies are formed.

It appears that the processes depend essentially upon two dimensionless parameters of time and space, represented by

$$T = k\sqrt{Bt} \quad \text{and} \quad X = -kx$$

respectively. The region $X<1$ represents that of significant coastal upwelling where changes in vorticity are appreciable. Then $T=1$ may give a characteristic time which practically divides the processes into two stages, earlier stage and final stage. The absolute value of time for $T=1$ depends upon B and k, and is found to be of order of several days, perhaps. In lower latitudes, and in regions closer to the coast, the final stage will be attained earlier.

North-south Variations

The above model is somewhat hypothetical, and, in actuality, various other factors might be important in bringing out the features observed. One of the most probable would be the north-south variations in conditions which are present probably due to north-south variations in winds and geographic features. In fact, abnormally cold surface water is present in most cases at various localities along coasts and not everywhere along the coast. Upwelling is also supposed very likely to occur in the similar manner. Increased vorticity in surface layer may tend to lead to change the large horizontal shear of north-south flow into eddies, which would yield north-south variations in conditions. Eddies may also

be formed by topographic conditions. For examples, cyclonic eddy prefers to be formed to the south of Point Conception, a rather sharp bending point, where the eddy is frequently observed between the coastline and southward California current which flows quite apart from the coast. To the south, the Biscaino Bay and the Point Eugenia may also lend significant disturbances to the features.

There might also be some possibility that north-south pressure gradient balances the vertical mixing of meridional component of momentum, along the coast, although the existing data seem to be insufficient to test this balance. At this situation, the present theory may only provide a first approximation to the process under the assumption that north-south variations are secondary.

SUBSURFACE CURRENTS

What would be the situations in the lower layer which correspond to the processes in the upper layer? A main difference is that there may not be appreciable wind-stirred mixing in the lower layer, especially in earlier stages of the process. There must be a definite rise or fall of thermocline at this stage due to vertical motion induced by surface winds, and this will necessarily introduce vertical motion in the layer below. Owing to a lack of stress curl, in the lower layer, an introduced vertical motion must lead to a change of vorticity. At some early stages, when upwelling takes place, relative vorticity will increase with time, northward currents being accelerated inshore. Subsurface northward current thus developed associates subsurface convergence, due to planetary vorticity which will tend to take a part to balance the horizontal divergence.

It is then understood readily that subsurface countercurrent develops inshore when upwelling takes place, in accord with our previous theory and observations (Yoshida and Mao, 1955).

In contrast to the foregoing results (The Oceans, 1942), a recent study of density distributions in the areas appeared to suggest that southward flow is present below 200m level in many cases when our previous estimate showed sinking inshore (Yoshida and Mao, 1955). It might be roughly be estimated that subsurface balance between planetary vorticity and horizontal divergence is established in a week to a month.

DISCUSSIONS AND CONCLUSIONS

It is suggested from the above discussions that upwelling may occur within a narrow strip of some 50km in width close to the coast during periods when northerly (parallel to the coastline) winds prevail off the coast. The mechanism involved in this process is essentially similar as accepted before. In the earlier stages, the changes in surface currents, vorticity and a depth of thermocline will be essential to the process practically limited within the zone. Such local pheno-

mena of boundary upwelling were neglected in the estimate of average upwelling in the preceding paper (Yoshida and Mao). Such boundary upwelling which is ***not due to curl*** of wind stress, however, will not extend by any means to distances greater than 100km from the coast. As mentioned before, vertical motion at distances greater than 100km is essentially due to wind stress curl ***at the locality***, also in accord with the results in preceding paper. Therefore, upwelling somewhat offshore and that close to the coastal boundary is somewhat different from each other in its mechanism, though not entirely independent of each other. In most cases, owing to the general conditions in the wind field off the coast, offshore upwelling may be accompanied by coastal upwelling. In some cases, however, offshore upwelling and coastal upwelling are separated from each other by a trough of sinking water between them. In some other cases, either of them will be absent. In general, the coastal upwelling is somewhat smaller in its scale of the covered area, though more intense. Wind data at the coast station as well as those at one to several stations offshore would provide a good means of estimating coastal upwelling velocity. Eq. (14) may suggest that some averaged wind data over 50 to 100km from the coast, if available, will be useful. This might further suggest that somewhat smoothed wind informations from weather maps could be used for this purpose on the basis of eq. (14). It might be mentioned that the distribution of wind stress curl will practically determine the vertical motion up to the coast, though the boundary upwelling is somewhat more intense. The] width of boundary upwelling will be narrower when an axis of northerly wind approaches closer to the coast, and wider when the axis is present further away from the coast.

Sverdrup and Fleming (1941) found that upwelling takes place between the coast and the boundary region where the swift northerly current exists. Their interpretation presumes an offshore boundary wall which moves slowly away from the coastside and causes a subsurface transport toward the inner region. On the other hand, our interpretation is that the boundary wall corresponding to the one assumed by them is provided by a vertical column of water where surface northerly wind has its maximum intensity. In the regions of no wind stress curl, or of the maximum wind stress, horizontal divergence is small. Moreover, our interpretion may imply that surface horizontal divergence is fed by subsurface ***northward*** transport rather than by subsurface coastward transport.

It was assumed in the present discussion that the adjustment or an equilibrium is approached through lateral mixing in the coastal zone, and it was suggested that a week or two would be sufficient duration of the winds to bring a new balance. Such lateral mixing in coastal zone is suggested to occur owing to coastal friction (including bottom friction in shallow water regions), horizontal eddies of various dimensions, and internal waves. Instead of lateral mixing, planetary vorticity in lower layers would probably be an important factor which brings

the system to a balance through compensating surface divergence, and it may be implied that the time constant may not be much longer than two weeks as far as the scale of wind disturbances is of the order of that concerned here. The fairy good agreement between seasonal variations in upwelling and in wind stress curl which was found in the California waters might support this estimate for the time constants. Outside of the narrow coastal zone, vertical motion occurs quasisteadily due to curl τ, and slow variations in surface currents, vorticity and the mixed layer thickness take place. (Yoshida, 1955b). The changes in those surface conditions will not be appreciable in a week or so, except for the coastal zone. They will reveal, however, seasonal changes of considerable amount in response to the seasonal changes in wind conditions. Within the coastal strip, on the other hand, the changes may respond appreciably to the changes in winds of which the dominant periods are longer than weeks to a month. It may appear that the changes in surface currents inshore will be appreciable when more or less steady winds last far longer than a week, whereas those outside the strip, the average winds for several months would yield appreciable changes in the oceanographic conditions in the mixed layer.

When we are concerned with more local processes, non-linear effects might be essential. Such small scale processes, however, could be disregarded for the present purposes. The coastal upwelling revealed in the present study, though it occurs in narrow zone, will be important, since it may associate the considerable changes in surface currents or eddies. It has occasionally been stated that "productivity" of the California waters may depend greatly upon upwelling, and in some occasions the eddies or the countercurrents have been thought to be responsible. It is likely, however, that these factors are closely interrelated and cannot by any means be regarded as independent phenomena. Since each of them may have its own significance on the productivity of the waters, it would be highly desirable to find the relationship present between them.

Among various other possible factors which might control the coastal upwelling, one may think of (1) coastal and bottom friction, and (2) variations in vertical stratification with distance from the coast.

It might be worthwhile to mention that a thermocline often reaches the surface in the region close to the coast. Such is found probably during periods of upwelling. The area within which a thermocline reaches the surface is confined within a limited distance from the coast, and this will roughly measure the extent where "coastal upwelling" takes place. (Figs. 1, 2). This might lead to a speculation that, after the thermocline reaches the surface, wind-drift-current does not fully develop along the coast owing to a great vertical stability which was brought out by coastal upwelling, and the processes for balances might be somewhat different from those discussed above.

Acknowledgements

The writer has benefited greatly by many discussion, on the data in the California waters, with Paul L. Horrer and Joseph L. Reid, of the Scripps Institution of Oceanography, La Jolla, California, where this paper was partly prepared. He is also indebted to Dr. Robert S. Arthur of the Scripps for the suggestion as to the coastal effects on upwelling which were obscured in our previous work (Yoshida and Mao, 1955).

REFERENCES

Rossby, C. G.
1938 On the mutual adjustment of pressure and velocity distributions in certain simple current system, II. J. Mar. Res., **1** (3) : 239-263.

Sverdrup, H. U., and W. E. Allen
1939 Distribution of diatoms in relation to the character of water masses and currents off southern California in 1938. J. Mar. Res. **2** (2) : 131-144.

Sverdrup, H. U., and R. H. Fleming
1941 The waters off the coast of southern California, March to July, 1937. Scripps Inst. Oceanogr., Bull., **4** (10) : 261-378.

Sverdrup, H. U., M. W. Johnson, and R. H. Fleming
1942 The Oceans. Prentice Hall, Inc., New York. 1087 pp.

Yoshida, Kozo and Han-Lee Mao
1955 A new measurement of upwelling with examples in the California current region. (In press).

Yoshida, Kozo
1955a An example of variations in oceanic circulation in response to the variations in wind field. (In press)

Yothida, Kozo
1955b A discussion on responses of the oceanic circulation to a fluctuating wind stress. (unpublished)
1955c Interaction between the mixed layer and the lower layer. (unpublished)

Records of Oceanographic Works
in Japan, Vol. 2, No. 2,
October 1955

Note on the convective circulation (I)

by
Kenzo Takano
(Geophysical Institute, Tokyo University)

Abstract: A convective circulation due to density differences maintained at the surface in a rectangular basin of water comparable in size to the Pacific Ocean is treated on the assumption that the Coriolis parameter is a constant, the eddy viscosity is equal to the eddy diffusivity, the density is uniform at the bottom and as a first approximation the advection terms are negligible in comparison with the diffusion terms in the equation of density diffusion. It is found that the intense upwelling occurs near the western boundary from the surface down to the bottom, the intense sinking near the eastern boundary, the width of these regions increases with the horizontal eddy viscosity and such a circulation seems to be of importance in the actual ocean circulation.

1. A thermal convective current due to temperature differences given to the surface has been obtained in a zonal basin of water extending infinitely in the east-west direction, on neglecting the non-linear terms, the vertical eddy viscosity and the meridional variation of the Coriolis parameter (Takano, 1955). The present note will give a convective circulation in a rectangular basin comparable in size to the Pacific instead of that in a zonal basin. In order to simplify the calculation, the Coriolis parameter is assumed to be a constant and the advection terms in the equation of density diffusion are neglected as a first approximation, because as is inferred from the previous study these terms appear small in comparison with the diffusion terms. Of course, the meridional variation of the Coriolis parameter can play an important rôle and non-linear terms are not always negligible.
The present note is a first slight attempt to estimate the convective circulation in the actual ocean.

2. Let the x-axis be positive eastward along the equator, the y-axis northward and the z-axis vertically downward. If the non-linear terms and the terms including the vertical motion are neglected, the equations of motion are given by

$$A_h\left(\frac{\partial^2}{\partial x^2}+\frac{\partial^2}{\partial y^2}\right)u+A_v\frac{\partial^2 u}{\partial z^2}+\rho f v=\frac{\partial p}{\partial x}, \qquad (1)$$

$$A_h\left(\frac{\partial^2}{\partial x^2}+\frac{\partial^2}{\partial y^2}\right)v+A_v\frac{\partial^2 v}{\partial z^2}-\rho f u=\frac{\partial p}{\partial y}, \qquad (2)$$

$$0=\frac{\partial p}{\partial z}-g\rho, \qquad (3)$$

where u, v are the components of the current velocity in the x- and y-directions, p the pressure, ρ the density, A_v and A_h the coefficients of vertical and horizontal mixings and f the Coriolis parameter. The equations (1) to (3) lead to

$$A_h\left(\frac{\partial^2}{\partial x^2}+\frac{\partial^2}{\partial y^2}\right)\frac{\partial u}{\partial z}+A_v\frac{\partial^3 u}{\partial z^3}+f\frac{\partial}{\partial z}(\rho v)=g\frac{\partial \rho}{\partial x}, \qquad (4)$$

$$A_h\left(\frac{\partial^2}{\partial x^2}+\frac{\partial^2}{\partial y^2}\right)\frac{\partial v}{\partial z}+A_v\frac{\partial^3 v}{\partial z^3}-f\frac{\partial}{\partial z}(\rho u)=g\frac{\partial \rho}{\partial y}. \qquad (5)$$

The equation of density diffusion is

$$\frac{\partial}{\partial x}(\rho u)+\frac{\partial}{\partial y}(\rho v)+\frac{\partial}{\partial z}(\rho w)=A_h\left(\frac{\partial^2}{\partial x^2}+\frac{\partial^2}{\partial y^2}\right)\rho+A_v\frac{\partial^2 \rho}{\partial z^2}. \qquad (6)$$

When as a first approximation ρ is assumed independent of x, the advection terms are sufficiently small and the variation in the density is concerned with the gravity terms only, the above equations (4) to (6) are reduced to

$$\left\{A_h\left(\frac{\partial^2}{\partial x^2}+\frac{\partial^2}{\partial y^2}\right)+A_v\frac{\partial^2}{\partial z^2}\right\}^2\frac{\partial u}{\partial z}+f^2\frac{\partial u}{\partial z}=-fg\frac{\partial \rho}{\partial y}, \qquad (7)$$

$$A_h\frac{\partial^2 \rho}{\partial y^2}+A_v\frac{\partial^2 \rho}{\partial z^2}=0. \qquad (8)$$

The boundary conditions are as follows:

$$u=v=0, \qquad \text{at } x=0,\ L \text{ and } y=0,\ l, \qquad (9)$$

$$A_v\frac{\partial u}{\partial z}=A_v\frac{\partial v}{\partial z}=0, \qquad \text{at } z=-H,\ H, \qquad (10)$$

$$w=0, \qquad \text{at } z=-H,\ H, \qquad (11)$$

$$\rho=-\Delta\rho\cos my+\rho_{-H}, \qquad \text{at } z=-H, \qquad (12)$$

$$\rho=\rho_H, \qquad \text{at } z=H. \qquad (13)$$

Here L, l, $-H$ and H denote the length in the east-west direction, the width in the north-south direction, the surface and the bottom of the basin, respectively, w the vertical velocity, $\Delta\rho$, ρ_{-H}, ρ_H are pure constants and $m=\frac{\pi}{l}$.

Then, the density and the horizontal velocity are expressed by

$$\rho=-\frac{4\Delta\rho}{\pi}(\rho_1\sinh\gamma z+\rho_2\cosh\gamma z)\cos my\sum_{s=1}^{\infty}\frac{1}{2s-1}\sin\frac{2s-1}{L}\pi x+\frac{\rho_H-\rho_{-H}}{2H}z+\frac{\rho_H+\rho_{-H}}{2}$$

$$=-\frac{4\Delta\rho}{L}(\rho_1\sinh\gamma z+\rho_2\cosh\gamma z)\cos my\sum_n\frac{\sin nx}{n}+\frac{\rho_H-\rho_{-H}}{2H}z+\frac{\rho_H+\rho_{-H}}{2}, \qquad (14)$$

$$u=\sin my\sum_{s=1}^{\infty}u_s\sin\frac{2s-1}{L}\pi x=\sin my\sum_n u_s\sin nx, \qquad (15)$$

$$v=\mathrm{sid}\ my\sum_{s=1}^{\infty}v_s\sin\frac{2s-1}{L}\pi x=\sin my\sum_n v_s\sin nx, \qquad (16)$$

where $\rho_1=\frac{-1}{2\sinh\gamma H}$, $\rho_2=\frac{1}{2\cosh\gamma H}$, $\gamma=m\sqrt{\frac{A_h}{A_v}}$, $n=\frac{2s-1}{L}$,

u_s and v_s are unknown functions of z only.

The equation of continuity:

$$\frac{\partial}{\partial x}(\rho u)+\frac{\partial}{\partial y}(\rho v)+\frac{\partial}{\partial z}(\rho w)=A_h\left(\frac{\partial^2}{\partial x^2}+\frac{\partial^2}{\partial y^2}\right)\rho+A_v\frac{\partial^2\rho}{\partial z^2} \tag{17}$$

is approximately simplified as

$$\frac{\partial u}{\partial x}+\frac{\partial v}{\partial y}+\frac{\partial w}{\partial z}=0 \tag{18}$$

which is transformed into

$$\begin{aligned} w&=-\int\left(\frac{\partial u}{\partial x}+\frac{\partial v}{\partial y}\right)dz \\ &=-\left[\sin my\Sigma n\cos nx\int u_s dz+m\cos my\Sigma\sin nx\int v_s dz\right] \\ &=-\left[\sin my\Sigma n\cos nx\cdot w_{1s}+m\cos my\Sigma\sin nx\cdot w_{2s}\right], \end{aligned} \tag{19}$$

where $w_{1s}=\int u_s dz$ and $w_{2s}=\int v_s dz$. (20)

Hence, the conditions (10) and (11) are replaced by

$$\left.\begin{aligned} &A_v\frac{du_s}{dz}=A_v\frac{dv_s}{dz}=0, \\ &w_{1s}=w_{2s}=0, \end{aligned}\right\}\ \text{at}\quad z=-H,\ H, \tag{21}$$

and the equation (7) leads to an equation

$$\left\{-A_h(m^2+n^2)+A_v\frac{d^2}{dz^2}\right\}^2\frac{du_s}{dz}+f^2\frac{du_s}{dz}=-\frac{4gf\Delta\rho m}{Ln}(\rho_1\sinh\gamma z+\rho_2\cosh\gamma z), \tag{22}$$

of which the solution is written as

$$\begin{aligned} u_s=&c_1\cosh p_1z+c_2\sinh p_1z+c_3\cosh p_2z+c_4\sinh p_2z+c_5 \\ &+U_s(\rho_1\cosh\gamma z+\rho_2\sinh\gamma z), \end{aligned} \tag{23}$$

where $U_s=-\frac{4gfm}{L\gamma n}\cdot\frac{\Delta\rho}{A_h{}^2n^4+f^2}$,

$$p_1=\sqrt{\frac{A_h(m^2+n^2)+if}{A_v}}\quad\text{and}\quad p_2=\sqrt{\frac{A_h(m^2+n^2)-if}{A_v}}. \tag{24}$$

Substituting the above solution into the equation (4), we have

$$\begin{aligned} v_s=-\frac{1}{f}\Big[&\left\{A_h(m^2+n^2)-A_vp_1{}^2\right\}(c_1\cosh p_1z+c_2\sinh p_1z) \\ &+\left\{A_h(m^2+n^2)-A_vp_2{}^2\right\}(c_3\cosh p_2z+c_4\sinh p_2z) \\ &+U_sA_hn^2(\rho_1\cosh\gamma z+\rho_2\sinh\gamma z)+c_7\Big], \end{aligned} \tag{25}$$

and from (20)

$$\begin{aligned} w_{1s}=&\frac{1}{p_1}(c_1\sinh p_1z+c_2\cosh p_1z)+\frac{1}{p_2}(c_3\sinh p_2z+c_4\cosh p_2z) \\ &+\frac{U_s}{\gamma}(\rho_1\sinh\gamma z+\rho_2\cosh\gamma z)+c_5z+c_6, \end{aligned} \tag{26}$$

$$\begin{aligned} w_{2s}=\frac{1}{f}\Big[&\frac{A_h(m^2+n^2)-A_vp_1{}^2}{p_1}(c_1\sinh p_1z+c_2\cosh p_1z) \\ &+\frac{A_h(m^2+n^2)-A_vp_2{}^2}{p_2}(c_3\sinh p_2z+c_4\cosh p_2z) \\ &+\frac{U_sA_hn^2}{\gamma}(\rho_1\sinh\gamma z+\rho_2\cosh\gamma z)+c_7z+c_8\Big]. \end{aligned} \tag{27}$$

The boundary conditions give

$$c_1=\frac{U_s\rho_1\gamma(\gamma^2-p_2^2)}{p_1(p_2^2-p_1^2)}\cdot\frac{\sinh\gamma H}{\sinh p_1H},\quad c_2=\frac{U_s\rho_2\gamma(\gamma^2-p_2^2)}{p_1(p_2^2-p_1^2)}\cdot\frac{\cosh\gamma H}{\cosh p_1H},$$

$$c_3=-\frac{U_s\rho_1\gamma(\gamma^2-p_1^2)}{p_2(p_2^2-p_1^2)}\cdot\frac{\sinh\gamma H}{\sinh p_1H},\quad c_4=-\frac{U_s\rho_2\gamma(\gamma^2-p_1^2)}{p_2(p_2^2-p_1^2)}\cdot\frac{\cosh\gamma H}{\cosh p_2H},$$

$$c_5=\frac{U_s\rho_1\sinh\gamma H}{H}\left(\gamma\frac{p_1^2+p_2^2-\gamma^2}{p_1^2p_2^2}-\frac{1}{\gamma}\right),\quad c_6=U_s\rho_2\cosh\gamma H\left(\gamma\frac{p_1^2+p_2^2-\gamma^2}{p_1^2p_2^2}-\frac{1}{\gamma}\right),\tag{28}$$

$$c_7=-\frac{1}{H}\Big[\frac{c_1}{p_1}\sinh p_1H\left\{A_h(m^2+n^2)-A_vp_1^2\right\}+\frac{c_3}{p_2}\sinh p_2H\left\{A_h(m^2+n^2)-A_vp_2^2\right\}$$
$$+\frac{U_s\rho_1}{\gamma}A_hn^2\sinh\gamma H\Big],$$

$$c_8=-\Big[\frac{c_2}{p_2}\cosh p_1H\left\{A_h(m^2+n^2)-A_vp_1^2\right\}+\frac{c_4}{p_2}\cosh p_2H\left\{A_h(m^2+n^2)-A_vp_2^2\right\}$$
$$+\frac{U_s\rho_2}{\gamma}A_hn^2\cosh\gamma H\Big].$$

After neglecting the small terms and putting $p_1=\alpha+\beta i$, $p_2=\alpha-\beta i$, the solutions (23), (25) to (27) are in the form:

$$u_s=\frac{U_s\gamma A_v}{f(\alpha^2+\beta^2)}\Big[(\rho_1\sinh\gamma H+\rho_2\cosh\gamma H)e^{\alpha(z-H)}\left\{\beta(\gamma^2-3\alpha^2+\beta^2)\cos\beta(H-z)\right.$$
$$\left.+\alpha(\gamma^2-\alpha^2+3\beta^2)\sin\beta(H-z)\right\}+(\rho_1\sinh\gamma H-\rho_2\cosh\gamma H)e^{-\alpha(z+H)}$$
$$\times\left\{\beta(\gamma^2-3\alpha^2+\beta^2)\cos\beta(H+z)+\alpha(\gamma^2-\alpha^2+3\beta^2)\sin\beta(H+z)\right\}\Big]$$
$$+U_s\Big[\frac{\rho_1}{H}\sinh\gamma H\left(\gamma\frac{p_1^2+p_2^2-\gamma^2}{p_1^2p_2^2}-\frac{1}{\gamma}\right)+\rho_1\cosh\gamma z+\rho_2\sinh\gamma z\Big],\tag{29}$$

$$v_s=\frac{2\alpha\beta U_s\gamma A_v^2}{f^2(\alpha^2+\beta^2)}\Big[(\rho_1\sinh\gamma H+\rho_2\cosh\gamma H)e^{\alpha(z-H)}\left\{\alpha(\gamma^2-\alpha^2+3\beta^2)\cos\beta(H-z)\right.$$
$$\left.-\beta(\gamma^2-3\alpha^2+\beta^2)\sin\beta(H-z)\right\}+(\rho_1\sinh\gamma H-\rho_2\cosh\gamma H)e^{-\alpha(z+H)}$$
$$\times\left\{\alpha(\gamma^2-\alpha^2+3\beta^2)\cos\beta(H+z)-\beta(\gamma^2-3\alpha^2+\beta^2)\sin\beta(H+z)\right\}\Big]$$
$$+\frac{U_s}{f}\Big[A_hn^2(\rho_1\cosh\gamma z+\rho_2\sinh\gamma z)+\frac{\rho_1}{H}A_h(m^2+n^2)\sinh\gamma H$$
$$\times\left(\gamma\frac{p_1^2+p_2^2-\gamma^2}{p_1^2p_2^2}-\frac{1}{\gamma}\right)\Big],\tag{30}$$

$$w_{1s}=\frac{U_s\gamma A_v}{f(\alpha^2+\beta^2)^2}\Big[(\rho_1\sinh\gamma H+\rho_2\cosh\gamma H)e^{\alpha(z-H)}\left\{\beta(\gamma^2-3\alpha^2+\beta^2)(\alpha\cos\beta\overline{H-z}\right.$$
$$\left.-\beta\sin\beta\overline{H-z})+\alpha(\gamma^2-\alpha^2+3\beta^2)(\beta\cos\beta\overline{H-z}+\alpha\sin\beta\overline{H-z})\right\}$$
$$+(\rho_1\sinh\gamma H-\rho_2\cosh\gamma H)e^{-\alpha(z+H)}\left\{\beta(\gamma^2-3\alpha^2+\beta^2)(-\alpha\cos\beta\overline{H+z}\right.$$
$$\left.+\beta\sin\beta\overline{H+z})+\alpha(\gamma^2-\alpha^2+3\beta^2)(-\beta\cos\beta\overline{H+z}+\alpha\sin\beta\overline{H+z})\right\}\Big]$$
$$+U_s\Big[\frac{1}{\gamma}(\rho_1\sinh\gamma z+\rho_2\cosh\gamma z)+\left(\gamma\frac{p_1^2+p_2^2-\gamma^2}{p_1^2p_2^2}-\frac{1}{\gamma}\right)\left(\rho_2\cosh\gamma H\right.$$
$$\left.+\frac{\rho_1}{H}z\sinh\gamma H\right)\Big],\tag{31}$$

$$w_{2s}=\frac{2\alpha\beta U_s\gamma A_v^2}{f^2(\alpha^2+\beta^2)^2}\Big[(\rho_1\sinh\gamma H+\rho_2\cosh\gamma H)e^{\alpha(z-H)}\Big\{\alpha(\gamma^2-\alpha^2+3\beta^2)(\alpha\cos\beta\overline{H-z}$$
$$-\beta\sin\beta\overline{H-z})-\beta(\gamma^2-3\alpha^2+\beta^2)(\beta\cos\beta\overline{H-z}+\alpha\sin\beta\overline{H-z})\Big\}$$
$$+(\rho_1\sinh\gamma H-\rho_2\cosh\gamma H)e^{-\alpha(z+H)}\Big\{\alpha(\gamma^2-\alpha^2+3\beta^2)(-\alpha\cos\beta\overline{H+z}$$
$$+\beta\sin\beta\overline{H+z})-\beta(\gamma^2-3\alpha^2+\beta^2)(-\beta\cos\beta\overline{H+z}+\alpha\sin\beta\overline{H+z})\Big\}\Big]$$
$$+\frac{U_s}{f}\Big[\frac{A_hn^2}{\gamma}(\rho_1\sinh\gamma z+\rho_2\cosh\gamma z)+A_h(m_2+n_2)\Big(\gamma\frac{p_1^2+p_2^2-\gamma^2}{p_1^2p_2^2}$$
$$-\frac{1}{\gamma}\Big)\Big(\frac{z}{H}\rho_1\sinh\gamma H+\rho_2\cosh\gamma H\Big)\Big]. \tag{32}$$

If A_h is of the order of 10^8 to 10^{12} C. G. S, the above solutions are shortened in part; for example, at the surface in the central portion of the basin, it follows approximately that

$$u_s\fallingdotseq\frac{4gm}{\gamma fLn}\Delta\rho\Big(1-\frac{1}{2H\gamma}\Big), \tag{33}$$

$$u\fallingdotseq\sin my\sum\frac{4gm}{\gamma fLn}\Delta\rho\Big(1-\frac{1}{2H\gamma}\Big)\sin nx,$$
$$=\Big(1-\frac{1}{2H\gamma}\Big)\frac{g}{f}\sqrt{\frac{A_v}{A_h}}\Delta\rho\cdot\sin my, \tag{34}$$

$$v_s\fallingdotseq\frac{4gm}{f^2Ln}\alpha A_v\Delta\rho(\rho_1\sinh\gamma H-\rho_2\cosh\gamma H), \tag{35}$$

$$v\fallingdotseq\frac{g\gamma A_v}{\sqrt{2}f^{3/2}}\Delta\rho(\rho_1\sinh\gamma H-\rho_2\cosh\gamma H)\sin my. \tag{36}$$

Of course, for great numbers of n, u_s or v_s are not expressed by (33) or (35) and u_s tends progressively to decrease with $\frac{1}{n^5}$ and v_s with $\frac{1}{n^3}$. However, if (33) and (35) hold for about the first dozen of terms, the velocity given by these terms will represent an approximate solution except in the close neighbourhood of the boundaries. In this case, the horizontal eastward velocity at the surface in the central part of the basin depends on the ratio $\frac{A_h}{A_v}$ only.

When we choose

$A_h=10^8 g\ cm^{-1}\ sec^{-1}$, $L=3\pi\times10^8\ cm$, $f=6,962\times10^{-5}\ sec^{-1}$,
$A_v=10^2 g\ cm^{-1}\ sec^{-1}$, $H=2\times10^5\ cm$, $l=2\pi\times10^8\ cm$,
$g=980\ cm\ sec^{-2}$,

the surface velocity is given by

$$u\fallingdotseq72\times10^2\Delta\rho\sin my, \tag{37}$$
$$v\fallingdotseq64\Delta\rho\sin my, \tag{38}$$

and the eastward velocity at the bottom is given by

$$u\fallingdotseq-\Big\{(\rho_1\cosh\gamma H+\rho_2\sinh\gamma H)+\frac{1}{2H\gamma}\Big\}\frac{g}{f}\sqrt{\frac{A_v}{A_h}}\Delta\rho\sin my \tag{39}$$
$$=-31\times10^2\Delta\rho\sin my$$

in the central part of the basin.

On the other hand, in the previous note, neglecting the terms including the vertical eddy viscosity, we have

$$u = 74 \times 10^2 \Delta\rho \sin my,$$

$$v = 0.25 \Delta\rho \sin my$$

at the surface in a zonal basin with the same numerical values. These results imply that, so far as the eastward velocity is concerned, the effect of the vertical eddy viscosity is not important, the solution excluding this effect in a zonal basin can be applied to the central portion of an enclosed basin and its vertical distribution is determined by the pressure gradient $\frac{\partial}{\partial y}\int g\rho dz$ only ; however, the eddy viscosity plays an important role in the northward velocity at the surface layer, though at the lower layer its vertical structure depends on the pressure gradient only.

In the figures 1 to 4 is represented a numerical example for $A_h = 10^{11}$ and $A_v = 10^3$ instead of $A_h = 10^8$ and $A_v = 10^2$, on assuming large coefficients of vertical and horizontal mixings so that the rapid convergence takes place in the series and the first fifteen terms indicate a sufficiently approximate solution. It is seen that the intense upwelling occurs near the western boundary and the intense sinking near the eastern boundary, these regions narrow with decreasing coefficient of horizontal mixing, the region of upwelling at the surface may not always coincide with that at $2000m$ in depth; though the horizontal velocity is nearly uniform except in the vicinity of the boundaries, it decreases slightly at the center. For smaller value of A_h the velocity will increase and the regions of the intense vertical motion become narrower.

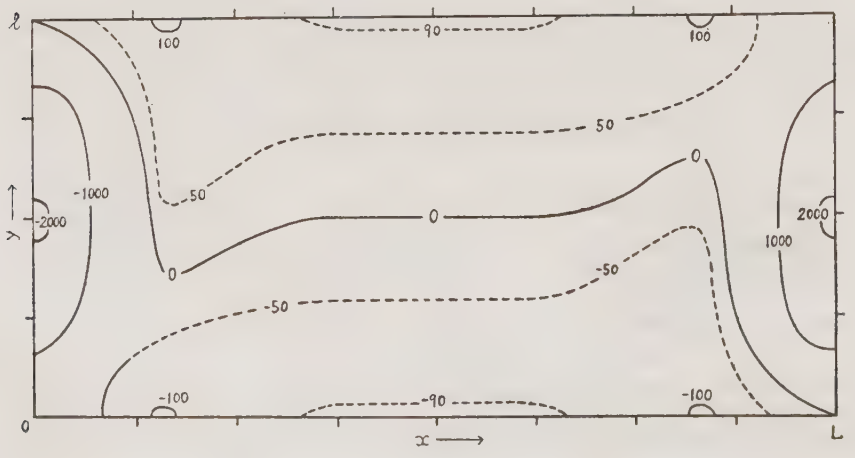

Fig 1. Distribution of $\frac{\partial w}{\partial z} \times \frac{10^8}{\Delta\rho}$(sec^{-1}) at the surface.
(−) : upwelling ; (+) : sinking.

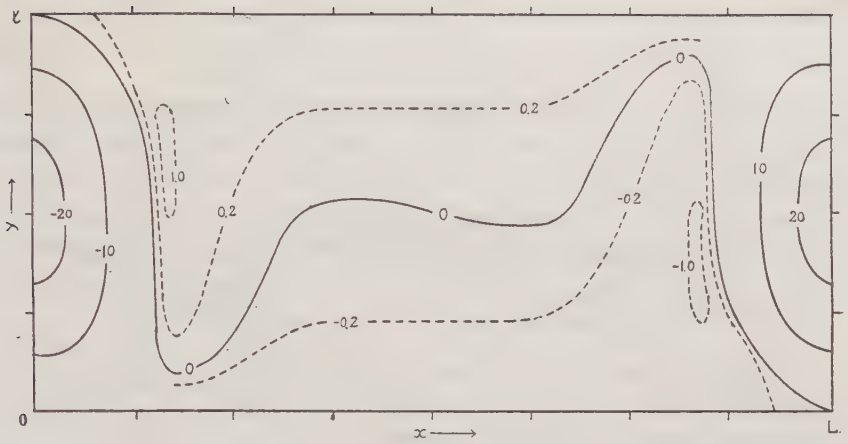

Fig 2. Distribution of $w \times \frac{10^2}{\Delta\rho}(cm\,sec^{-1})$ at 2000m in depth.
(−) : upwelling ; (+) : sinking.

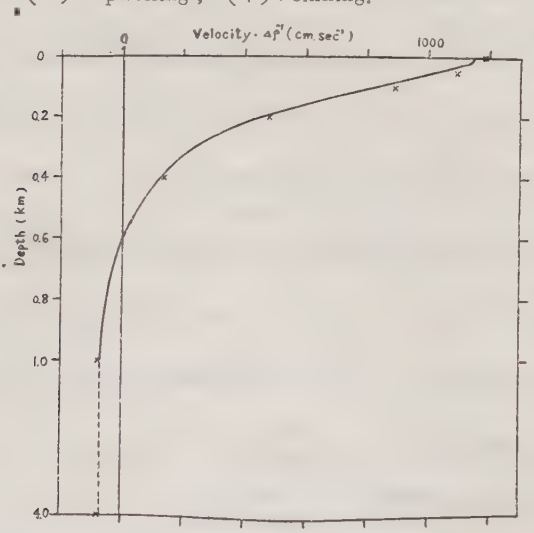

Fig 3. Vertical profile of $\frac{u}{\Delta\rho}$ at $x=\frac{L}{2}$, $y=\frac{l}{2}$(full line) and at $x=\frac{L}{6}$, $\frac{5L}{6}$, $y=\frac{l}{2}$(cross marks).

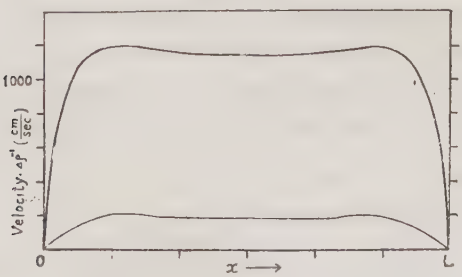

Fig 4. Horizontal variation of $\frac{u}{\Delta\rho}$(upper curve) and $\frac{v}{\Delta\rho}$(lower curve) at $y=\frac{l}{2}$.

In the second approximation the additive density ρ_a is given by

$$v\frac{\partial \rho}{\partial y}+w\frac{\partial \rho}{\partial z}=A_h\left(\frac{\partial^2}{\partial x^2}+\frac{\partial^2}{\partial y^2}\right)\rho_a+A_v\frac{\partial^2 \rho_a}{\partial z^2}, \tag{40}$$

where ρ is the density (14) and v, w are the velocity components obtained above.

If u_s, v_s, w_{1s} and w_{2s} are assumed to be constant in order to avoid the tedious calculation, ρ_a is written as

$$\begin{aligned}
\rho_a=-\Delta\rho\Big[&\frac{m}{2}\Big\{\sum\frac{v_n}{A_h n^2-A_v\gamma^2}\sin nx\Big(-\rho_2\frac{\cosh\gamma H}{\sinh\delta_1 H}\cosh\delta_1 z-\rho_1\frac{\sinh\gamma H}{\sinh\delta_1 H}\sinh\delta_1 z\Big)\\
&+\cos 2my\sum\frac{v_n}{-A_h(n^2+4m^2)+A_v\gamma^2}\sin nx\Big(-\rho_2\frac{\cosh\gamma H}{\cosh\delta_2 H}\cosh\delta_2 z\\
&-\rho_1\frac{\sinh\gamma H}{\sinh\delta_2 H}\sinh\delta_2 z\Big)+(\rho_1\sinh\gamma z+\rho_2\cosh\gamma z)\Big(\sum\frac{v_n}{A_h n^2-A_v\gamma^2}\sin nx\\
&+\cos 2my\sum\frac{v^u}{-A_h(n^2+4m^2)+A_v\gamma^2}\sin nx\Big)\Big\}\\
&+\gamma m\Big\{\sum\frac{w_{2s}}{-A_h(n^2+4m^2)+A_v\gamma^2}\sin nx\Big(\rho_1\frac{\cosh\gamma H}{\cosh\delta_2 H}\cosh\delta_2 z\\
&+\rho_2\frac{\sinh\gamma H}{\sinh\delta_2 H}\sinh\delta_2 z\Big)+\frac{1}{2}\sum\frac{w_{2s}}{-A_h n^2+A_v\gamma^2}\sinh nx\Big(\rho_1\frac{\cosh\gamma H}{\cosh\delta_1 H}\cosh\delta_1 z\\
&+\rho_2\frac{\sinh\gamma H}{\sinh\delta_1 H}\sinh\delta_1 z\Big)-\frac{1}{2}(\rho_1\cosh\gamma z+\rho_2\sinh\gamma z)\Big(\sum\frac{w_{2s}}{-A_h n^2+A_v\gamma^2}\sin nx\\
&+\cos 2my\sum\frac{w_{2s}}{-A_h(n^2+4m^2)+A_v\gamma^2}\sin nx\Big)\Big\}\\
&-\frac{\gamma}{2}\sin 2my\Big\{\sum\frac{nw_{1s}}{-A_h(n^2+4m^2)+A_v\gamma^2}\cos nx\Big(-\rho_1\frac{\cosh\gamma H}{\cosh\delta_2 H}\cosh\delta_2 z\\
&-\rho_2\frac{\sinh\gamma H}{\sinh\delta_2 H}\sinh\delta_2 z\Big)+(\rho_1\cosh\gamma z+\rho_2\sinh\gamma z)\sum\frac{nw_{1s}}{-A_h(n^2+4m^2)+A_v\gamma^2}\cos nx\Big\}\\
&+\frac{\rho_H-\rho_{-H}}{2H}\Big\{\sin my\sum\frac{nw_{1s}}{A_h(n^2+m^2)}\cos nx+m\cos my\sum\frac{w_{2s}}{A_h(n^2+m^2)}\sin nx\\
&-\sin my\sum\cos nx\frac{\cosh\delta_3 z}{\cosh\delta_3 H}\frac{nw_{1s}}{A_h(m^2+n^2)}\\
&+m\cos my\sum\sin nx\frac{\cosh\delta_3 z}{\cosh\delta_3 H}\frac{w_{2s}}{A_h(m^2+n^2)}\Big\}\Big],
\end{aligned} \tag{41}$$

where $\delta_1{}^2=\frac{A_h}{A_v}n^2$, $\delta_2{}^2=\frac{A_h}{A_v}(4m^2+n^2)$ and $\delta_3{}^2=\frac{A_h}{A_v}(m^2+n^2)$.

According to an assumption in the first approximation, the additive density ρ_a has to be small as compared with ρ. This assumption seems to hold up to $\Delta\rho=10^{-3}$ or $\Delta\rho=2\times10^{-3}$ and $\rho_{-H}-\rho_H=2\times10^{-3}$, even for the maximum values of u_s, v_s, w_{1s} and w_{2s} with $A_h=10^8$ and $A_v=10^2$. Therefore, from (37) and (38) we have, at a distance off the boundaries, the nearly uniform surface velocity

$$u_{surf}=7.2\sin my, \tag{42}$$

$$v_{surf}=0.064\sin my, \tag{43}$$

and the nearly uniform velocity in the east-weat direction at the bottom

$$u_b=-3.1\sin my, \tag{44}$$

with $\Delta\rho=10^{-3}$, $A_h=10^8$ and $A_v=10^2$;

while in the same way, with $\Delta\rho=10^{-3}$, $A_h=10^{11}$ and $A_v=10^3$,

$$u_{surf}=1.2\sin my, \tag{45}$$

$$v_{surf}=0.2\sin my, \tag{46}$$

$$u_b=-0.1\sin my. \tag{47}$$

3. Although the boundary condition that the stress vanishes at the bottom adopted for simplicity may not be reasonable, yet the gross features of the velocity field will not be entirely altered in the case of putting the condition that the velocity itself vanishes at the bottom. In our case, there is no horizontal volume transport at every point, viz. $\int_{-H}^{H} udz=0$ and $\int_{-H}^{H} vdz=0$.

According to the result of K. Hidaka who has obtained the divergence of the surface drift currents in terms of the wind stress over the Pacific Ocean, the divergence is of the order of $\pm10^{-8}\,\mathrm{sec}^{-1}$. Our result illustrated in the figure 1 gives about $2\times10^{-8}\,\mathrm{sec}^{-1}$ at the maximum for the numerical values $\Delta\rho=10^{-3}$, $A_h=10^{11}$ and $A_v=10^3$. If we take $A_h=10^8$ and $A_v=10^2$ instead of $A_h=10^{11}$ and $A_v=10^3$, the absolute value of the divergence may be made several times as large as $2\times10^{-8}\,\mathrm{sec}^{-1}$ near the boundaries.

These results are not immediately applied to the actual ocean circulation in the Pacific or other oceans, because the meridional variation in the Coriolis parameter, the wind stress and the effect of the homogeneous layer in low latitudes are not taken into account, moreover, actually, the minimum density at the surface is not found at the equator.

References

Hidaka, Koji:

1955, Divergence of Surface Drift Currents in Terms of Wind Stresses, with Special Application to the Location of Upwelling and Sinking., Japanese Journal of Geophysics, Vol. 1, 47-56

Takano, Kenzo:

1955, An Example of Thermal Convective Current., Records of Oceanographic Works in Japan, Vol. 2, 76-79.

Records of Oceanographic Works
in Japan, Vol. 2, No. 2
October 1955

Drift and Diffusion of Radiologically Contaminated Water in the Ocean.

By
Hisashi Miyoshi*, Sadakiyo Hori**, and Shozo Yoshida**.

Abstract: An immense quantity of radiologically contaminated water spreading in a fan-shaped horizontal distribution away from (Bikini) atoll in Marshall Islands area, was found by a Japanese survey ship, in May and June, 1954. And the radioactive matter proved an excellent tracer of the currents and the phenomena of diffusion. Its distribution compels us to think the vertical eddy coefficient of diffusivity was only 5cm²/sec. or so, in the upper mixed layer of this area.

The contaminated stratosphere water found near Bikini is, besides due to the vertical diffusion, considerably due to the passing through of the calcite particles which fell down from the sky following the explosions. So, we calculated the times, using the Stokes's law, required by the calcite particles of various sizes to fall through sea water from the surface to the depths of 200m and 500m.

Finally, contaminated water spread rather two-dimensionally, and reached the large distances. The survey ship detected contaminated water some 800km to the east northeast of Bikini Atoll. This fact can be explained either by an additional counter current or by a large elliptic vortex the minor axis of which is the straight line connecting Bikini and Wake. One of the present authors prefers the former.

§ 1. Introduction.

On June 12, 1954, 38 days after the last of the experiments of American atomic weapons, which were performed (perhaps on March 1, March 27†, April 26, and May 5 at Bikini Atoll) in Marshall Islands area, a Japanese survey ship (Shunkotsu-Maru) went north along the meridian 163°50′E which lies some 150km to the west of Bikini Atoll, and found an immense quantity of drifting radiologically contaminated sea water and clear atmosphere above it.

Contaminated water which formed a thin stratum was continuously detected during the course along this meridian, from 10°55′N to 12°09′N, at the sea surface of some stations while at the certain depths of other stations. This region is shown by the double line B in Fig. 1. This region around Bikini Atoll is situated at the middle of the predominant North Equatorial Current. When our survey

* Tokyo University of Fisheries.
** Hydrographic Office, Maritime Safety Agency Tokyo.
† It is also said that on April 6, an experiment was performed, but this is inaccurate.

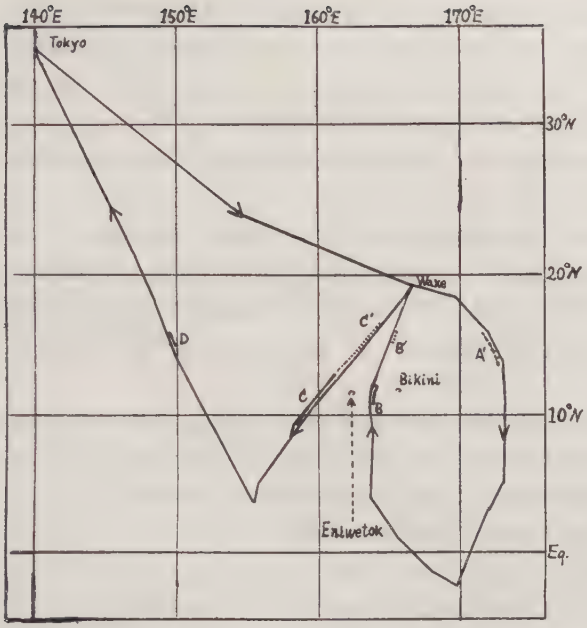

Fig 1. The course of the survey ship.

was performed, therefore, sea water contaminated by the dusts which fell down from the sky following the explosions, might have flowed away in the distance. We infer the detected contaminated water was the lagoon water emitted from the eastern atoll and conveyed by the North Equatorial Current, diffusing principally along the isopycnal surface and forming a fan-shaped horizontal distribution.

We found the radiologically contaminated water was an excellent tracer of the currents and the phenomena of diffusion. Because the concentration of the matter in the ocean can be determined within an error of ±5% by a G-M tube and scaler "32".

The most remarkable appearance of the distribution of contaminated water along the double line B is its slight vertical thickness. Up to the present, the vertical eddy coefficient of diffusivity has been thought to be very large (310cm²/sec. : Defant 1932) in the upper mixed layer of the equatorial ocean, and actually W. H. Munk et al(1949) verified its value to be 200~300cm²/sec. in Bikini lagoon. Our data, however, compel us to think it was only 5cm²/sec. or so in the mixed layer of this area.

Passing through this area and the next rather clear area, the survey ship encountered a secondary contaminated band shown by a dotted line B′ in Fig. 1. The examples of the surface water contamination in the clear area and the secondary contaminated band were 70 and 692 cpm/1, respectively. Across this secondary contaminated band and towards Wake Island, we found sea was very clear. On the returning way, C′ and C are the secondary contaminated band and the principal contaminated area, respectively. But in this case, we met with no distinctly clear area lying between C′ and C, while the lengths of the double lines B and C were proportional to their distances to Bikini Atoll. And along the last course, only one weakly contaminated area D was encountered.

Besides this general tendency, the most remarkable fact was that contaminated band was met with, at the dotted line A′ in Fig. 1, which lies some 800km to the east northeast of Bikini Atoll. The maximum value along this line was 450 cpm/1. On the other hand, consistent easterly currents were found at C′ and B′

(0.5 knot~0.7 knot) by our current meter, and at A′ judging from the easterly drift of the ship against the northeast trade wind. The two ways of thinking to explain this fact are as follows.

1. An additional counter current may exist near the latitude of 15°N.
2. A large elliptic vortex the minor axis of which is a straight line connecting Wake and Bikini may exist.

These two possible phenomena may superpose each other. But one of the authors (H. Miyoshi) prefers the former. Expecting the future studies, concerning this problem, we will now treat the vertical diffusion of contaminated water in the troposphere and the cause of the contamination of the stratosphere found especially along B line.

In this report, we will not regard the conditions of counting, and will deal with the data represented by the arbitrary unit. We should remember that both the reality of the additional counter current and the westward flowing away of the water contaminated by the dusts which fell down from the sky, as well as the contamination of the stratosphetre water due to the passing through of the dusts (calciteparticles), indicate that the considerable part of the whole radioactive matter created by the bombs was missed by the survey ship, and cannot by extrapolated.

§ 2. Vertical Diffusion of Contaminated Water in the Troposphere.

The artificial conditions which A. E. C. could not publish, are the differences between the types of the four (or five) bombs, types of the explosions (underwater, on the coral, or in the air) and the existence of the atoll besides Bikini Atoll at which the experiment was done. We will lead, therefore, the general and common conclusions which don't depend upon these conditions.

Now we will show the data, which represent the contamination of sea water at 8 stations along B line in Table 1.

No. of st. (lat.) / Depth (m)	17-1 (10°55′N)	17-2 (11°09′)	17-3 (11°18′)	17-4 (11°28′)	17-5 (11°39′)	17-6 (11°49′)	17-7 (11°59′)	17-8 (12°09′)
0	84	1610	566	859	1539	1792	5500	260
20		982	810	641	1841	1877	6048	1091
25	254							
40		169	1160	1563	1792	516	923	452
50	5780	50	503	1683	1221	470	356	580
60		23	273		517	216	375	346
75	67							
80		12	1283	840	182	48	55	39
100	25	8	368	939	25	20	14	32
200	28	27	11	59	65	50	64	49
300	23					110		
500						116		

Table 1. Unit : cpm/1 (counts per minute per litre). This table shows the data of sea water contamination on June 12, 1954, along the meridian lying some 150km to the west of Bikini.

As an important factor for the analysis of the features of diffusion, W.S. von Arx (1948) reported the mean depth of the paincipal passes around Bikini Atoll through which lagoon water is emitted as the jet streams during the ebb tides. This depth is, according to him, 29.4m, so we assume that a uniformly contaminated water plate which is 30m thick, started and diffused downward for 3 days, being conveyed westwards by the North Equatorial Current. Then the concentration at depth z is given as follows,

$$s=\frac{1}{\sqrt{\pi}}\int_{\frac{-z}{2\sqrt{A_V t}}}^{\infty} f(z+2\sqrt{A_V t}\cdot\xi)e^{-\xi^2}\cdot d\xi+\int_{\frac{z}{2\sqrt{A_V t}}}^{\infty} f(-z+2\sqrt{A_V t}\cdot\xi)e^{-\xi^2}\cdot d\xi \quad (1)$$

here

$$\left.\begin{aligned} f(x)&=c \qquad 0<z<3000\\ &=0 \qquad z>3000 \end{aligned}\right\} \quad (2)$$

Now, putting $t=3\times24\times60\times60$ (velocity of the westward current at this area was 1.2 knot, and the distance between this meridian and Bikini Atoll is some 150km), we will show the three concentration-depth curves corresponding to $A_V=$ 100cm²/sec., =10cm²/sec., and =5cm²/sec., in Fig. 2. Here, A_V is the vertical eddy coefficient of diffusivity. And as the relative values of the concentrations at many places are represented by their radioactivities, we plotted the observed values of the latters on the same figure. The curve corresponding to $A_V=$ 100 cm²/sec., is far-off from the observed values. And the curve corresponding to $A_V=5$cm²/sec., seems to be the most suitable for the data at Stations 17-6 and 17-7. Here, we adopted the concentrations at 20m, the most radioactive layers of the observed ones, as the standard values (100%), and showed the other values by their relative figures. The computed values increase from 20m to the surface, contrasting with the observed tendencies. These discrepancies might result from the fact that heavier lagoon water might have slightly sunk, be covered by the thin layer of ocean water and be mixed with the latter sufficiently by the surface waves. We need not, therefore, mind these discrepancies.

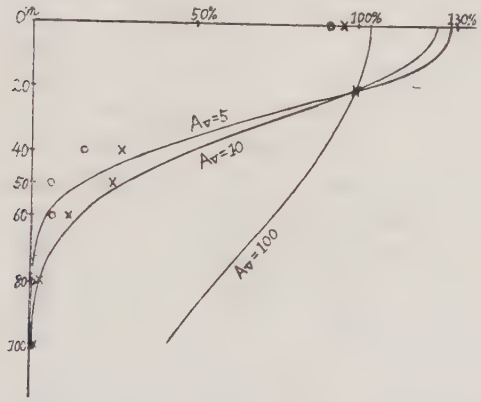

Fig 2. The concentration-depth curves corresponding to $A_v=100$cm²/sec., =10cm²/sec., =5 cm²/sec., × and ○ show the data at Stations 17-6 and 17-7, respectively.

§3. Contamination of Water in the Stratosphere.

In Table 1, when one looks over the data of radioactivity of water from the surface to the stratosphere at Station 17-6, one will find that radioactivity increases with depth passing through its neck point (100m) and into the strathsphere. Excluding one by one the various possibilities of the causes which might have

invited this increase (For example, the possibility that the survey ship might catch the particles sinking through the stratosphere on June 12 can be excluded by Fig. 3. That is, the rather coarse particles which could select the courses $\overrightarrow{A'B}$ or $\overrightarrow{AB}$, might have sunk deeper than C, perhaps to the ocean bottom on June 12. Here A is the bottom of the passes around Bikini Atoll.), we can suppose the following two possibilities which remain.

(1) By only the passing through of the calcite particles, the water of the stratosphere as well as that of the troposphere might be radiologically contaminated, and the latter might be washed away and be taken place of by the ocean water growing more and more diluted day by day, while the former might remain here.

(2) Soon after the explosions, intensely contaminated water passed through the point S (Fig. 3) growing diluted day by day. This contamination might be due to the radioactive lagoon water, at first to a considerable part, then to the whole part. As is indicated by the analysis in §2, the ratio of the concentration at B to that at S, as well as the ratio of the concentration at S to thah at AA'' (the exits of lagoon water), is constant. If the concentration at AA'', therefore, decays exponentially day, that at B may also decay in the same manner. Concering this, when we pay attention to the spacial distribution of radioactivity, we need not consider about its physical decay, except the differences among the constants C_i (concentration$=C_i\times$radioactivity) which are characteristic to each concentration produced by the bomb exploded on a certain day. Here, we only point out the decay of concentration being emitted from the atoll. This fact that the concentration at B decays, is similar to the phenomenon that the temperature at the ground surface falls towards night. In the latter case, as is well known, the temperature below the surface rises higher than that at the surface. In the case of Fig. 3, the concentration at C may grow denser than that at B, the stratosphere corresponding to ground.

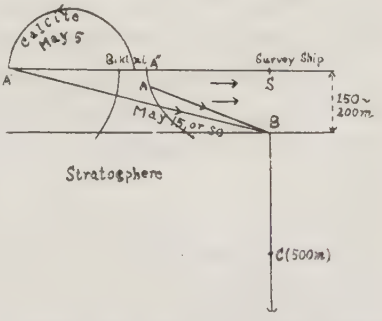

Fig 3. Bikini Atoll and the survey ship, which is coming to the rader.

The two causes (1) and (2) may both participate in rising the concentration in the stratosphere. We can think that (1) has played the more important rôle, judging from the data at other areas showing the similar tendencies which are not so remarkable as that of Station 17-6, in spite of the fact that the vertical diffusion at the formers to the depths corrsponding to B in Fig. 3 is more sufficint than that at the latter. So, we will perform an analysis, adopting as the value of 100cm^2/sec. and neglecting the covering effect of the thermocline where Av is very small. When we take the origin of z-axis at the uppermost layer of the thermocline, the boundary condition is given by an exponential function. When the ratio of water volume transported into and out of the lagoon per one day to

the whole volume of lagoon water (being reported by W.S. von Arx to be more than 7% and being thought to be small as about 5% thwards summer) is $n\%$, we can define the following quantity

$$\theta = 1 - \frac{n}{100} \qquad (3),$$

then the function of time t

$$\theta^{t/T} = e^{\frac{\log\theta}{T}t} = e^{-k^2 t} \quad \because \log\theta < 0 \qquad (4)$$

can be used once a standard as the ratio of the quantity of the matter which remains in lagoon water to the whole quantity pooled at the explosion, time t after the contaminated matter spread in the lagoon. Here T means one day. The concentration of the matter contained in the emitted water from the atoll may be proportional to this value. This may be called the oceanographical decay. Considering the many factors and thinking only the last two bombs (April 36 and May 5) were effective on June 12, we can get the equation which relative value of radioactivity at the depth $150\text{m} + l \times 50\text{m}$, as follows,

$$s = 0.480l\left\{s_2\int_{11}^{20}\frac{e^{-0.05130n}\cdot e^{-\frac{0.7235}{(47-n)}l^2}}{\sqrt{(47-n)^3}}dn + s_3\int_{20}^{47}\frac{e^{-0.05130n}\cdot e^{-\frac{0.7235}{(47-n)}l^2}}{\sqrt{(47-n)^3}}dn\right\} \qquad (5),$$

here

$$s_2 = \frac{1}{1+\sqrt{\left(\frac{47}{38}\right)^3 e^{9k^2}}}s_3 = 0.314s_3 \qquad (6),$$

for the physical decay is known to be given by $t^{-1.5}$.

Numerical caluculation shows that

$$[s]_{150m} : [s]_{200m} : [s]_{300m} : [s]_{500m} = 17 : 40 : 33 : 6 \qquad (7).$$

Thinking the observed contamination of the stratosphere water might have a steady distribution, and be reliable, we cannot apply the ratios given by (7), especially $[s]_{300m}/[s]_{500m}$. So we may think the contamination of the stratosphere water which is comparable to that of the troposphere water, being integrated vertically, is principally due to tne passing through of the calcite particles. This indicates that the area to which the calcite particles fell down can be guessed by surveying the stratosphere water contamination, and that much radioactive particles might lie on the bottom of this area.

Diameters (μ) of the particles	Times from surface to 200m	Times from surface to 500m
840	6.18 min. >	0.317 h
250	1.16 h	3.58 〃
150	3.23 〃	9.94 〃
75	12.9 〃	39.8 〃
33	66.8 〃	205 〃
16	284 〃	874 〃
8	1140 〃	3500 〃
5	2910 〃	8950 〃

Table 2. The times required by the calcite particles to fall through sea water from surface to the depths of 200m and 500m. Unit : hour

Then we calculated the times, as the fundamental data, required by the calcite particles of various sizes, to fall through sea water from surface to the depths of 200m and 500m, which are shown in Table 2.

Water viscosity is almost determined by water temperature and hydrostatic pressure. The effect of the latter is once neglected (so the re-calculation is desirable), Cl is assumed to be 20‰, and the vertical distribution of water temperature is assumed as Fig. 4, in which we can see the observed values fit well the theoretical ones.

§ 4. Conclusions.

1. In May and June, 1954, a survey ship found an immense quantity of drifting radiologically contaminated water and clear atmosphere above it, around Bikini Atoll. The additional counter current and the westward flowing away of the water contaminated by the dusts which fell down from the sky, as well as the contamination of the stratosphere water due to the passing through of the dusts (calcite particles), indicate that the considerable part of the whole radioactive matter created by the bombs was missed by the survey ship, and cannot be extrapolated.

2. The radioactive matter proved an excellent tracer of the currents and the phenomena of diffusion. The vertical distribution of radioactivity near Bikini compels us to think the vertical eddy coefficient of diffusivity was only $5cm^2/sec.$ or so in the upper mixed layer of this area.

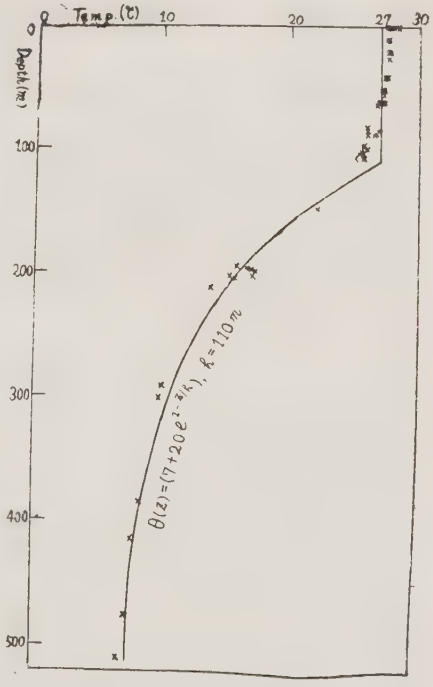

Fig 4. The vertical distribution of water temperature at the area which is some 150km to the west of Bikini, and its approximate equations.

§ 5. Acknowledgements.

The present authors wish to express their hearty thanks to Dr. Y. Miyake, Professor M. Uda, Dr. T. Ichie, Dr. G. Yoshii, Mr. M. Tsuchiya and Mr. S. Okano for their kindness to discuss with them.

References.

Jerlov, N. G. (1953) : "Studies of the Equatorial Currents in the Pacific", Tellus, **5** (3).

Miyake, Y. and M. Koizumi (1948) : "The Measurement of the Viscosity Coefficient of Sea Water", Journ. Mar. Res., **7** (2), pp. 63—66.

Von Arx, W. S. (1948) : "The Circulation System of Bikini and Rongelap Lagoons", Trans. Amer. Geophys. Union, **29** (6), pp. 861—870.

Records of Oceanographic Works
in Japan, Vol. 2, No. 2,
October 1955

On a Simple Method for Estimating the Current Velocity at the Equator.

(II)

By

Mizuki Tsuchiya

(Geophysical Institute, Tokyo University)

Abstract: The effect of the inertial and the frictional terms upon the previously proposed method for estimating the current velocity at the equator is studied. The inertial and the frictional terms do not seem to alter the previous result. Therefore, the geostrophic approximation of ocean current can be applied far closer to the equator than so far considered. Further more, at the equator and its immediate vicinity, the E-W component of current velocity is determined by the curvature of the isobaric surface in the meridional vertical section instead of its slope.

1. The geostrophic approximation of ocean current velocity had been considered to fail near the equator due to the vanishing of the Coriolis parameter. In 1953, Jerlov (1953) removed the uncertainty of the current velocity at the equator by differentiation of Helland-Hansen's formula with respect to the latitude. Recently Hidaka (1955) gave a formula of numerical computation for the practical analysis by this method. In the previous paper, the author (Tsuchiya, 1955) discussed the same problem and showed some of the results of analyses from actual data. In the present paper, he takes the effect of the inertia terms and the friction terms which was neglected in the previous paper into consideration and examines the validity of this method in detail.

2. We take x-axis along the equator directed toward the east, y-axis along a meridian directed toward the north and z-axis vertically downward. Then the equations of motion in steady state are given with a sufficient approximation by

$$u\frac{\partial u}{\partial x}+v\frac{\partial u}{\partial y}+w\frac{\partial u}{\partial z}-fv=-\frac{1}{\rho}\frac{\partial p}{\partial x}+A\frac{\partial^2 u}{\partial z^2}+B\nabla^2 u, \qquad (1)$$

$$u\frac{\partial v}{\partial x}+v\frac{\partial v}{\partial y}+w\frac{\partial v}{\partial z}+fu=-\frac{1}{\rho}\frac{\partial p}{\partial y}+A\frac{\partial^2 v}{\partial z^2}+B\nabla^2 v, \qquad (2)$$

where $\nabla^2=\frac{\partial^2}{\partial x^2}+\frac{\partial^2}{\partial y^2}$, u, v and w are the x, y and z components of current velocity respectively, f the Coriolis parameter, p the pressure, ρ the density, A

and B are the vertical and the horizontal eddy viscosity respectively.

We can estimate the magnitude of every term in (1) and (2) with sufficient accuracy for the present purpose. Assuming the orders of the quantities in (1) and (2) as $u \sim 5\times 10$, $v \sim 10$, $w \sim 10^{-3}$, $H \sim 10^{4}$, $L_x \gg L_y \sim 10^{7}$, $A \sim 10^{2}$, $B \sim 10^{7}$ (later, all units in c. g. s.), where H, L_x and L_y are typical lengths in z, x and y directions respectively, we obtain

$$u\frac{\partial}{\partial x} \sim \frac{u}{Lx} \ll 5\times 10^{-6}, \quad v\frac{\partial}{\partial y} \sim \frac{v}{Ly} \sim 10^{-6},$$

$$w\frac{\partial}{\partial z} \sim \frac{w}{H} \sim 10^{-7}, \qquad A\frac{\partial^2}{\partial z^2} \sim \frac{A}{H^2} \sim 10^{-6},$$

$$B\nabla^2 \sim B\left(\frac{1}{Lx^2} + \frac{1}{Ly^2}\right) \sim B\frac{1}{Ly^2} \sim 10^{-7}.$$

Therefore, we have

$$\left.\begin{aligned} &u\frac{\partial u}{\partial x} \ll 2.5\times 10^{-4}, \quad v\frac{\partial u}{\partial y} \sim 5\times 10^{-5}, \quad w\frac{\partial u}{\partial z} \sim 5\times 10^{-6}, \\ &A\frac{\partial^2 u}{\partial z^2} \sim 5\times 10^{-5}, \qquad B\nabla^2 u \sim 5\times 10^{-6} \end{aligned}\right\} \qquad (3)$$

in (1) and

$$\left.\begin{aligned} &u\frac{\partial v}{\partial x} \ll 5\times 10^{-5}, \quad v\frac{\partial v}{\partial y} \sim 10^{-5}, \quad w\frac{\partial v}{\partial z} \sim 10^{-6}, \\ &A\frac{\partial^2 v}{\partial z^2} \sim 10^{-5}, \qquad B\nabla^2 v \sim 10^{-6} \end{aligned}\right\} \qquad (4)$$

in (2).

The distribution of $\frac{1}{\rho}\frac{\partial p}{\partial y}$ is determined by oceanographic data. Under the assumption that the 1000 db surface is horizontal we can replace the pressure

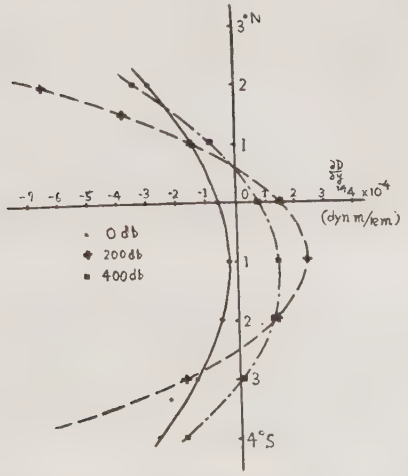

Fig 1. Meridional gradient of the isobaric surfaces (0 db, 200 db and 400 db surfaces) referred to the 1000 db surface. 172°W. July, 1950. The values in dynamic meter /km are equivalent to those in c. g. s.

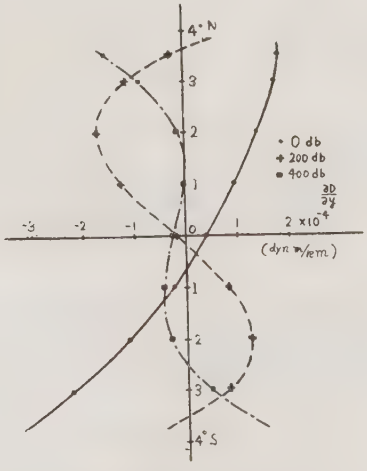

Fig 2. Meridional gradient of the isobaric surfaces (0 db, 200 db and 400 db surfaces) referred to the 1000 db surface. 158°W. July, 1950.

gradient $\frac{1}{\rho}\frac{\partial p}{\partial y}$ by the slope of the isobaric surface $\frac{\partial D}{\partial y}$, where D is the geopotential distance of the isobaric surface from the 1000 db surface. In practice we approximte D with a polynomial of degree three or four with respect to y, i.e. $D=a+by+cy^2+dy^3$ or $D=a+by+cy^2+dy^3+ey^4$. If there are several oceanographic stations on a same meridian across the equator, the constants a, b, c, d and e are determined from the observed D-values at these stations by the method of least squares. Then $\frac{\partial D}{\partial y}$ is readily calculated.

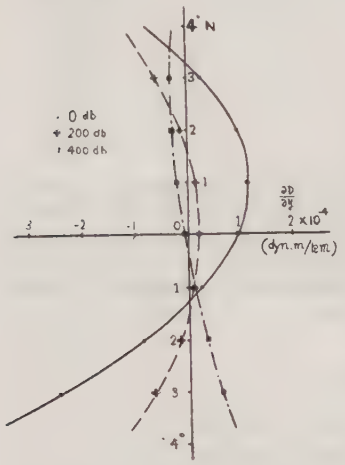

Fig 3. Meridional gradient of the isobaric surfaces (0 db, 200 db and 400 db surfaces) referred to the 1000 db surface. 168°W. January, 1951.

The analyses of the data of Hugh M. Smith Cruises executed by the Pacific Oceanic Fishery Investigations during 1950-1952 and Japanese surveying vessel Kôsyû in 1933 and 1936, show that $\frac{\partial D}{\partial y}$ becomes small as y approaches to zero. Some examples of the distribution of $\frac{\partial D}{\partial y}$ are illustrated in fig. 1-3. From them we can see the meridional pressure gradient at the equator is less than the order of 10^{-4}. If we consider the equation (2) with (4), it is supposed that this small pressure gradient is balanced by the friction terms and the inertia terms. On the other hand, except within the narrow belt between 1°N and 1°S, the pressure gradient is larger than the inertia terms and the friction terms but so small that it can be in balance with the small Coriolis term in low latitudes. This fact is confirmed almost without exception in many examples which the author dealt with hitherto. Hence the geostrophic approximation may be able to be applied far closer to the equator than so far considered, perhaps to 1°N and 1°S.

Comparison of thus calculated current speed in low latitudes with the observed is made for only one example. Direct measurement of current speed by the method of two current meters was executed by the Kôsyû at a station located 1° 49′S and 155°44′E. The results of observations and calculations are shown in fig. 4. An unreasonably large value of observed current speed at 10m depth may be excluded because the other two give a well accordance. The agreement of both observed and calculated values is fairly well, particularly above 300m, which may indicate the validity of the application of the geostrophic approximation to low latitudes.

With respect to the E-W gradient of pressure, which is supposed to be small compared with the meridional gradient, we have not sufficient data to determine it, because each station is separated so widely in x direction and the date of each observation differs so much. Its value, however, may be of same order as the

inertia terms and the friction terms given in (3). Therefore if we could know the value of $\frac{1}{\rho}\frac{\partial p}{\partial x}$, it would not be possible to determine v by the geostrophic approximation. Thus we can not say anything about the meridional component of the current velocity in low latitudes on the cotrary to the case of the E-W component.

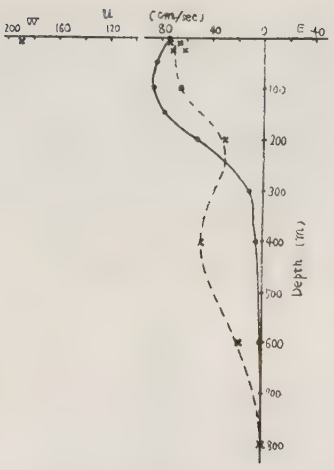

Fig 5. E-W component of current velocity at 1°49′S and 155°44′E. Sept., 1933. The dynamic calculations(dots) refer to 800 db and the direct measurements(crosses) are relative to 800m.

3. At the equator and its immediate vicinity, we can not determine the current velocity by the above described method, because all terms in the equations (1) and (2) become of same orders in magnitudes. Now we can transform (1) and (2) into the vortcity and the divergence equations as follows:

$$u\frac{\partial\varsigma}{\partial x}+v\frac{\partial\varsigma}{\partial y}+w\frac{\partial\varsigma}{\partial z}+\beta v+(f+\varsigma)Q-\xi\frac{\partial w}{\partial x}-\eta\frac{\partial w}{\partial y}=-\frac{1}{\rho^2}\frac{\partial(p.\rho)^*}{\partial(x.y)}+A\frac{\partial^2\varsigma}{\partial z^2}+B\nabla^2\varsigma, \tag{5}$$

$$u\frac{\partial Q}{\partial x}+v\frac{\partial Q}{\partial y}+w\frac{\partial Q}{\partial z}-f\varsigma+\beta u+Q^2-2\frac{\partial(u.v)^*}{\partial(x.y)}+\frac{\partial w}{\partial x}\frac{\partial u}{\partial z}+\frac{\partial w}{\partial y}\frac{\partial v}{\partial z}=-\frac{1}{\rho}\nabla^2 p+\frac{1}{\rho^2}(\nabla p\cdot\nabla\rho)^{**}+A\frac{\partial^2 Q}{\partial z^2}+B\nabla^2 Q, \tag{6}$$

where

$$\xi=\frac{\partial w}{\partial y}-\frac{\partial v}{\partial z},\quad \eta=\frac{\partial u}{\partial z}-\frac{\partial w}{\partial x},\quad \varsigma=\frac{\partial v}{\partial x}-\frac{\partial u}{\partial y},\quad Q=\frac{\partial u}{\partial x}+\frac{\partial v}{\partial y}$$

and β is the Rssby parameter defined by $\frac{df}{dy}$.

We can estimate the magnitude of every term in (5) and (6) by the same manner as described above. Assuming sea water is incompressible, we obtain $\frac{\partial u}{\partial x}+\frac{\partial v}{\partial y}+\frac{\partial w}{\partial z}=0$. This is written in the form $Q=-\frac{\partial w}{\partial z}$, and $Q\sim\frac{w}{H}\sim10^{-7}$ is obtained. On the other hand, $\frac{\partial u}{\partial x}\sim\frac{u}{Lx}\ll5\times10^{-6}$ and $\frac{\partial v}{\partial y}\sim\frac{v}{Ly}\sim10^{-6}$. Therefore $\frac{\partial u}{\partial x}$ and $\frac{\partial v}{\partial y}$ have a tendency to cancel each other. In the same way, following estimations are obtained.

$$\xi\sim10^{-3},\quad \eta\sim5\times10^{-3},\quad \varsigma\sim5\times10^{-6}.$$

Hence, we have

$$u\frac{\partial\varsigma}{\partial x}\ll2.5\times10^{-11},\ v\frac{\partial\varsigma}{\partial y}\sim5\times10^{-12},\ w\frac{\partial\varsigma}{\partial z}\sim5\times10^{-13},\ \beta v\sim10^{-12},\ \varsigma Q\sim5\times10^{-13},$$
$$\xi\frac{\partial w}{\partial x}\ll10^{-13},\ \eta\frac{\partial w}{\partial y}\sim5\times10^{-13},\ A\frac{\partial^2\varsigma}{\partial z^2}\sim5\times10^{-12},\ B\nabla^2\varsigma\sim5\times10^{-13} \tag{7}$$

---

* $\frac{\partial(\alpha.\beta)}{\partial(x.y)}=\frac{\partial\alpha}{\partial x}\frac{\partial\beta}{\partial y}-\frac{\partial\alpha}{\partial y}\frac{\partial\beta}{\partial x}$. ** $(\nabla p\cdot\nabla\rho)=\frac{\partial p}{\partial x}\frac{\partial\rho}{\partial x}+\frac{\partial p}{\partial y}\frac{\partial\rho}{\partial y}$.

in (5), and the baroclinic effect $\frac{1}{\rho^2}\frac{\partial(p.\rho)}{\partial(x.y)}$ is supposed to be less than the order of 10^{-16}. In (6), we have

$$\left.\begin{aligned} &u\frac{\partial Q}{\partial x}\ll 5\times10^{-13},\ v\frac{\partial Q}{\partial y}\backsim 10^{-13},\ w\frac{\partial Q}{\partial z}\backsim 10^{-14},\ \beta u\backsim 5\times10^{-12},\ Q^2\backsim 10^{-14},\\ &\frac{\partial w}{\partial x}\frac{\partial u}{\partial z}\ll 5\times10^{-13},\ \frac{\partial w}{\partial y}\frac{\partial v}{\partial z}\backsim 10^{-13},\ \frac{1}{\rho^2}(\nabla p\cdot\nabla\rho)\backsim 10^{-16},\ A\frac{\partial^2 Q}{\partial z^2}\backsim 10^{-13},\\ &B\nabla^2 Q\backsim 10^{-14}\end{aligned}\right\}\quad(8)$$

The term $\frac{\partial(u.v)}{\partial(x.y)}=|\nabla u|\cdot|\nabla v|\sin\psi$ represents the solenoidal effect of the lines $u=$ const and $v=$const, where $|\nabla u|=\sqrt{\left(\frac{\partial u}{\partial x}\right)^2+\left(\frac{\partial u}{\partial y}\right)^2}$, $|\nabla v|=\sqrt{\left(\frac{\partial v}{\partial x}\right)^2+\left(\frac{\partial v}{\partial y}\right)^2}$ and ψ is the angle between the both lines. Since $|\nabla u|\backsim 5\times10^{-6}$, $|\nabla v|\backsim 10^{-6}$ and $\sin\psi$ is supposed to be 10^{-1} in order, $\frac{\partial(u.v)}{\partial(x.y)}$ may be of the order of 10^{-13}.

We can calculate $\nabla^2 p\fallingdotseq\frac{\partial^2 p}{\partial y^2}$ from the oceanographic data, but it will be quite uncertain because of the errors introduced by differentiating two times. If we use D instead of p, differentiations of the expression for D by the polynomial obtained above may give the most reliable and objective value of $\frac{\partial^2 D}{\partial y^2}$. Thus $\frac{\partial^2 D}{\partial y^2}$ at the equator is estimated as 10^{-12} in magnitude.

As will be seen from (7) all terms in (5) are nearly of same orders, and we can not say, here again, anythig about the meridional component of current velocity. But in the equation (6), this is not the case. From (8) it is readily seen that effective terms in (6) are only βu and $\frac{1}{\rho}\nabla^2 p$. In other words, βu and $\frac{1}{\rho}\nabla^2 p$ balance each other. This balance will hold not only at the equator but also in the regions where f is not exactly zero as far as $f\varsigma$ is less than 10^{-12}.

Thus at the equator and its immediate vicinity, the E-W component of the current velocity can be expressed by

$$\beta u=-\frac{1}{\rho}\nabla^2 p,\qquad(9)$$

and if it is permitted to put $\nabla^2 p=\frac{\partial^2 p}{\partial y^2}$ with sufficient accuracy, (9) becomes

$$\beta u=-\frac{1}{\rho}\frac{\partial^2 p}{\partial y^2}.$$

For the practical purpose, replacing $\frac{1}{\rho}\frac{\partial^2 p}{\partial y^2}$ by $\frac{\partial^2 D}{\partial y^2}$, we have

$$\beta u=-\frac{\partial^2 D}{\partial y^2}.\qquad(10)$$

This is the exactly the same as derived by Hidaka (1955) and by the author in his previous paper.

4. Some examples of the E-W component of the current velocity in a vertical section, calculated by (10) at the equator and by the geostrophic approximation

in the region outside the narrow belt between 1°N and 1°S, are shown in the previous paper. Above discussion and these examples seem to indicate the validity of the present method for calculating ocean current velocity. A more precise discussion, however, should be made after many systematic oceanographic observations in the equatorial region.

Acknowledgement

The author wishes to express his sincerest thanks to Dr. K. Hidaka and Dr. K. Yoshida for their encouragement and valuable discussions. He also indebts to Dr. O. E. Sette of Pacific Oceanic Fishery Investigations who made the data of the Hugh M. Smith available to him.

References

Hidaka, K, 1955 : Dynamical Computation of Ocean Currents in a Vertical Section Occupied Across the Equator. Japanese Journ. Geophys., **1**, (2) : 57-60.

Jerlov. N. G. 1953 : Studies of the Equatorial Currents in the Pacific. Tellus, **5** : 308-314.

Tsuchiya, M. 1955 : On a Simple Method of Estimating the Current Velocity at the Equator. Journ. Oceanogr. Soc. Japan, **11**, (1) : 1-4.

Records of Oceanographic Works
in Japan, Vol. 2, No. 2,
October 1955

RESEARCHES ON THE FLUCTUATION OF THE NORTH PACIFIC CIRCULATION.

I. THE FLUCTUATION OF OYASIWO CURRENT IN RELATION TO THE ATMOSPHERIC CIRCULATION AND TO THE DISTRIBUTION OF THE DICHOTHERMAL WATERS IN THE NORTH PACIFIC OCEAN.

By

Michitaka Uda

(Tokyo University of Fisheries)

Introduction

In order to predict the fluctuation of Kurosiwo and Oyasiwo with the bearing on the forecast of the agicultural and fisheries yields, the interrelationship between the water circulation in the North Pacific Ocean with its adjacent seas and the atmospheric circulation over them should be studied closely. In the northern Japan during the past historical ages the frequent occurrence of bad harvest years of rice crop due to the cool summer was experienced, e. g. in the years of 1755, 1783, 1833, 1836, 1866, 1869, 1884, 1902, 1905, 1913, (1923), 1931, 1934, 1941, 1945, 1953, (Hokkaidō 1954). Hitherto many authors (K. Andō,[1] T. Okada[2] and others)[3) 4) 5)] have been investigated on this problem and its ultimate causes. Their results for the characteristic features of the cool summer years can be summarized as follows;

(1) The prevalence of the cold Oyasiwo Current and the cold northeasterly wind sent from the Okhotsk High.

(2) In winter the abnormal development of the Aleutian Low (e. g. in the years of 1833, 1866, 1869, 1884, 1902, 1905, 1913, 1931, 1934). [1) 2) 3) 4) 5) 6)]

(3) In winter the general development of the Siberian High stronger than normal.

(4) In early summer the development of the North Pacific High (the Middle Latitude High) weaker than normal.

(5) In summer, contrary to the lower water temperature than normal in the Oyasiwo Current in the North-Eastern Sea Region of Japan (including the adjacent waters to Kuril) and Okhotsk Sea, the higher water temerature than normal in the Bering Sea and the neighbouring waters to Aleutian Islands. (e. g. 1931, 1934, 1941, 1953). [3) 4) 5) 6)]

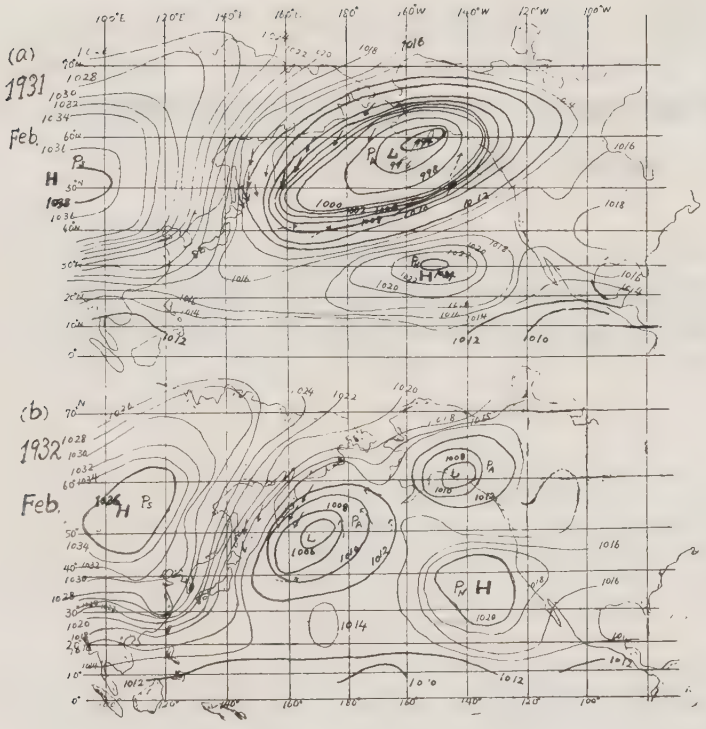

Fig. 1 a, b Distribution of Atmospheric Pressure in February (1931-34). (Arrows mean winds around Aleutian Low).

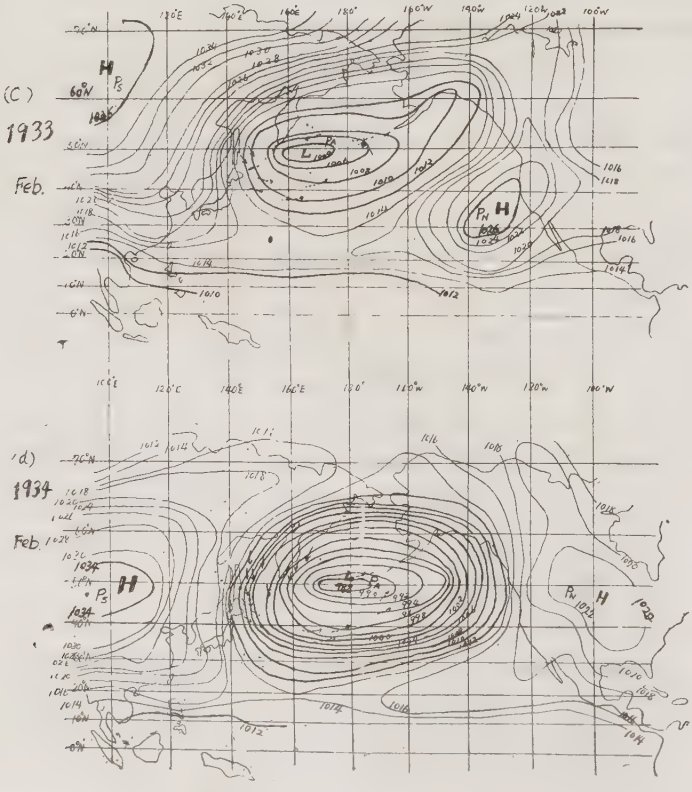

Fig. 1 c, d Distribution of Atmospheric Pressure in February (1931~1934). (Arrows mean winds around Aleutian Low).

Consequently we can conclude the development of the Aleutian Low in the North Pacific fed by the northerly prevalence of the Kurosiwo Current in correspondence to the case of the Icelandic Low in the North Atlantic fed by the warm waters of Gulf Stream.

I. *The fluctuation of Oyasiwo Current in Relation to the Atomospheric Circulation.*

Basing on the barometric table in the northern hemisphere (C. M. O)[7] the present author plotted the distribution maps of the atmospheric pressure in February during 1931-1934 (see Fig. 1) and found the conspicuous prosperity of the Aleutian Low (P_A) and the Siberian High (P_s) in the yeras 1931 and 1934 of cool summer compared to that of the warm summer years.

Following the anticyclonic circulation around the developed center of the Aleutian Low, the winter monsoon (westerlies) (W) prevails in proportional to the pressure gradient (P_s-P_A) (see Tab. 1) and consequently the more abundantly produced cold waters by severe monsoon flow southward strongly than normal as Oyasiwo Cold Current. (V). i. e. $V=KW=K'\sqrt{(P_s-P_A)}$.

Table 1.
The Pressure Difference between Aleutian High (P_A) and Siberian High (P_S). $\Delta P=P_S-P_A$

Year / Month	1931	1932	1933	1934
Jan.	+ 48.5mb	+25.1mb	+31.2mb	+ 39.5mb
Feb.	+ 43.7	+21.2	+26.8	+ 41.5
Mar.	+ 18.3	+28.3	+18.7	+ 28.3
Apr.	+ 1.8	+13.0	+ 8.7	+ 12.9
May.	+ 3.1	+ 4.6	− 0.7	− 5.0
Jun.	− 3.4	− 6.1	− 5.2	− 4.4
Jul.	− 11.5	−15.7	−11.7	− 11.7
Aug.	− 7.3	− 2.7	− 5.5	+ 2.5
Sept.	+ 2.6	+ 2.7	+ 6.8	+ 9.9
Oct.	+ 14.5	+16.8	+19.3	+ 18.0
Nov.	+ 23.1	+18.7	+17.0	+ 28.8
Dec.	+ 22.3	+37.4	+15.4	+ 30.0
J. F. Mar. $\Sigma\Delta P$	+110.5	+74.6	+76.7	+109.3
J. F. $\Sigma\Delta P$	+ 92.2	+46.3	+58.0	+ 81.0
Summer	Cool	Warm	Warm	Cool

In the years of cool summer we can see the regional correlation such that the water colder than normal in the North-western Pacific west to Kamchatka Penn. contrary to the water warmer than normal in the Eastern Pacific east to Aleutian (inclusive) and seemingly the successive or alternative occurrence of warm, cold

and cold, warm years according to the intensity of the winter monsoon and the northery prevalence of warm current or to the values of $(P_S\text{-}P_A)$ and $(P_A\text{-}P_N)$ i. e. zonal indices.

II. *The Distribution and the fluctuation of the Dichothermal Waters in the North Pacific.*

Formerly[8] the present author has shown that dichothermal water (intermediate minimum of the water temperature) is important as the index of the prevalence of the subarctic cold water masses in the North Pacific produced by the winter cooling and mixing due to the westerly monsoon, by the coincidence of the values of water temperature, dissolved oxygen and σ_t, and the methothermal water (ca 3°C 34‰) in the deeper layer of the Okhotsk Sea corresponds to the O_2-minimum continuing to the deep water in the North Pacific Ocean. After the World War II several authors (Yukimasa Saitō,[9] Yositada Takeuti,[10] Nobuo Watanabe[11] et al) discussed on the nature of the Oyasiwo Current but very few on the nature of the dichothermal layer in question. Recently under the guidance of the present author H. Miwa of the Tōkyō University of Fisheries found the relation between the favourable salmon fishing grounds and the frontal locality of the dichothermal water in the adjacent waters of Aleutian Islands.[12]

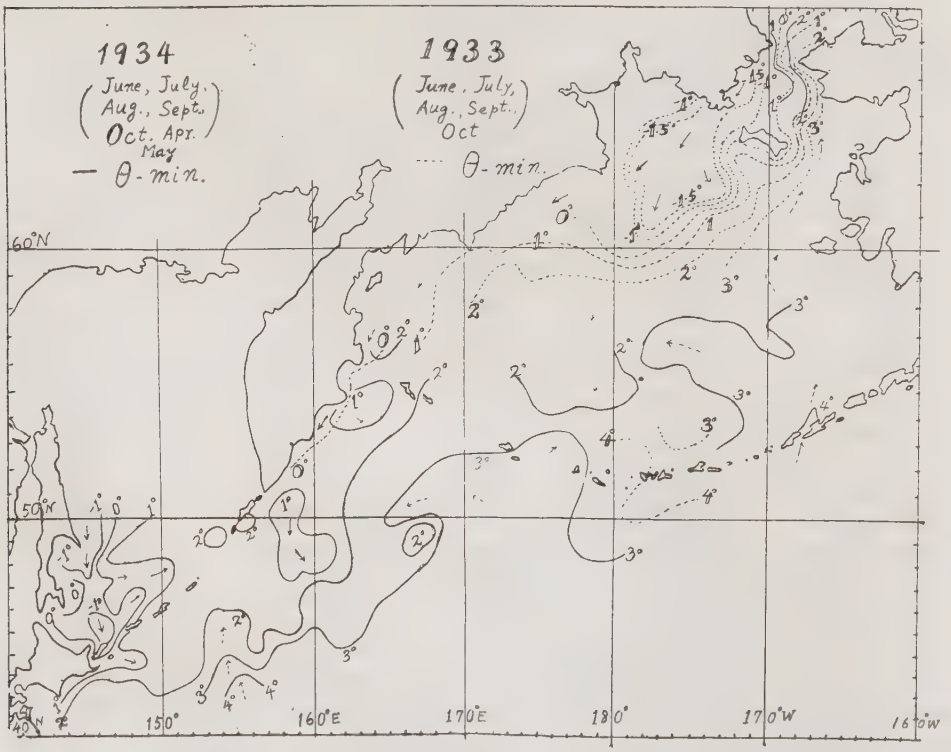

Fig. 2 The Isolines of θ-min. (Dichothermal Water) and the Estimated Movement in the Years of 1933 and 1934.

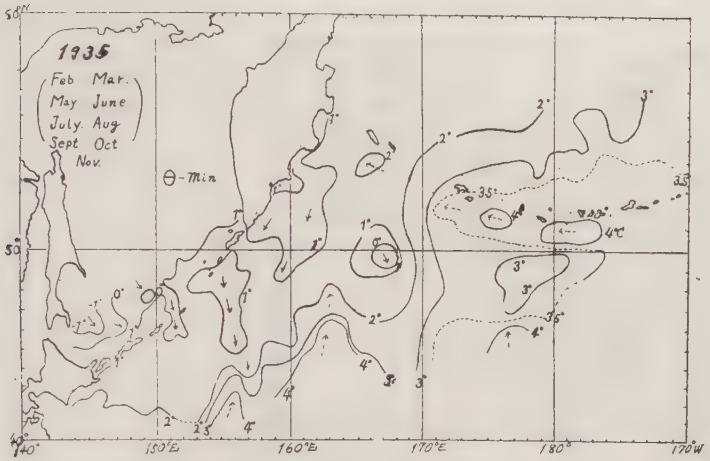

Fig. 3 The Isolines of θ-min. (Dichothermal Water) and the Estimated Movement in the Year 1935.

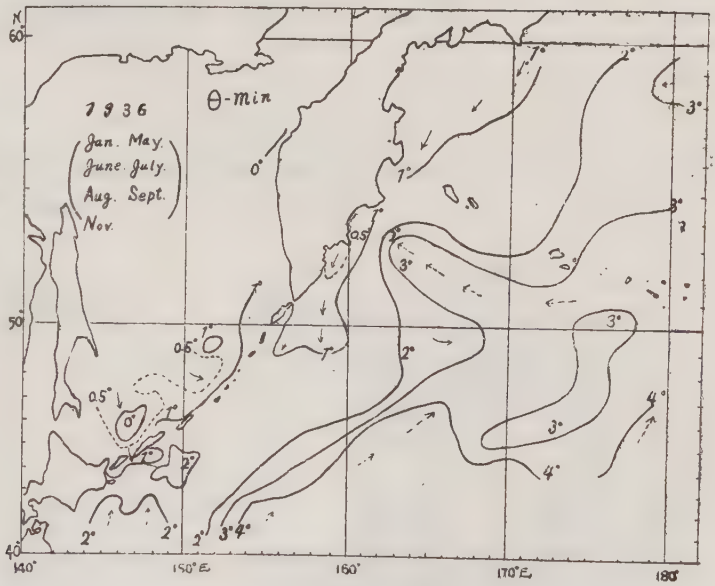

Fig. 4 The Isolines of θ-min. (Dichothermal Water) and the Estimated Movement in the Year 1936.

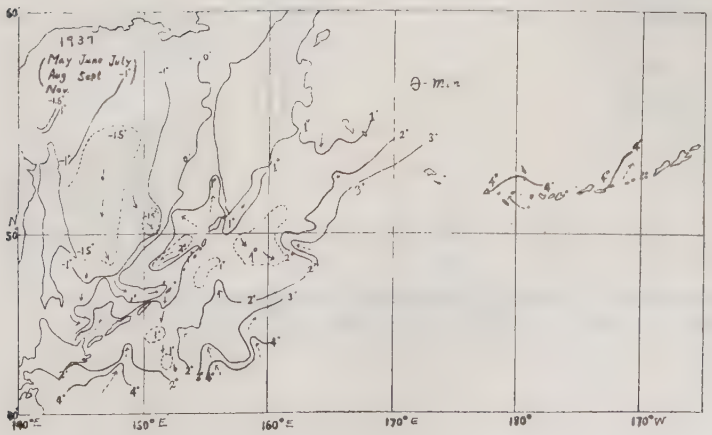

Fig. 5 Distribution of θ-min. (Dichothermal Water) and the Estimated Movement in the Year 1937.

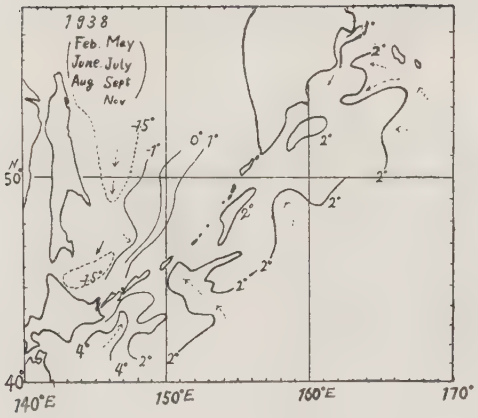

Fig. 6 Distribution of θ-min. (Dichothermal Water) and the Estimated Movement in the Year 1938.

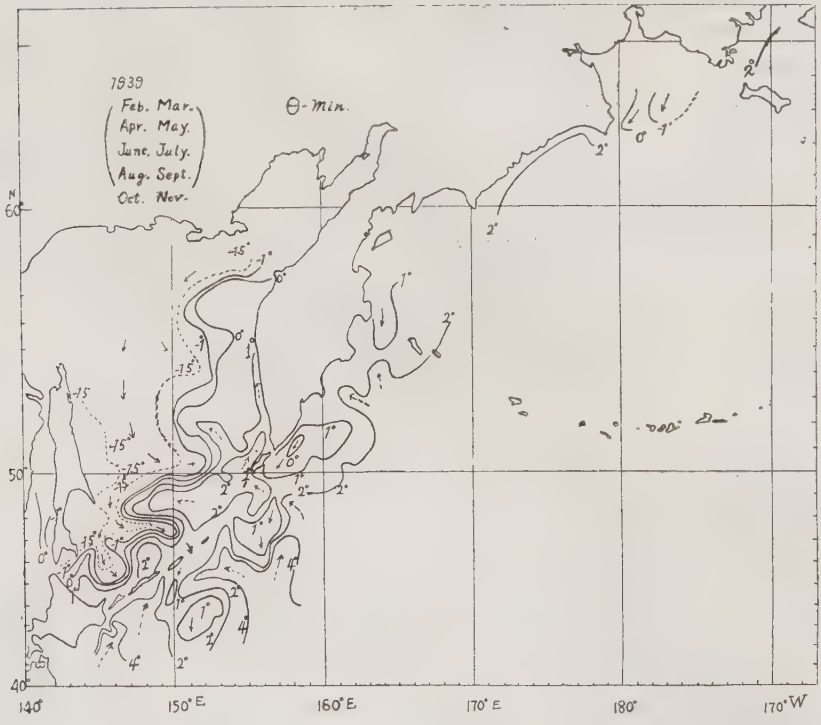

Fig. 7 Distribution of θ-min. (Dichothermal Water) and the Estimated Movement in the Year 1939.

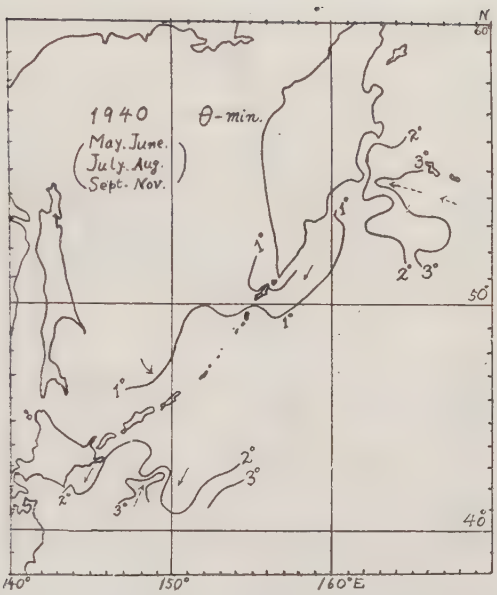

Fig. 8 Distribution of θ-min. (Dichothermal Water) and the Estimated Movement in the Year 1940.

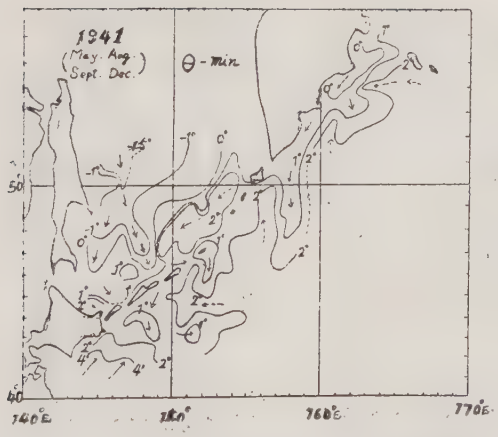

Fig. 9 Distribution of θ-min. (Dichothermal Water) and the Estimated Movement in the Year 1941.

Fig. 10 Distribution of θ-min. (Dichothermal Water) and the Estimated Movement in the Year 1942.

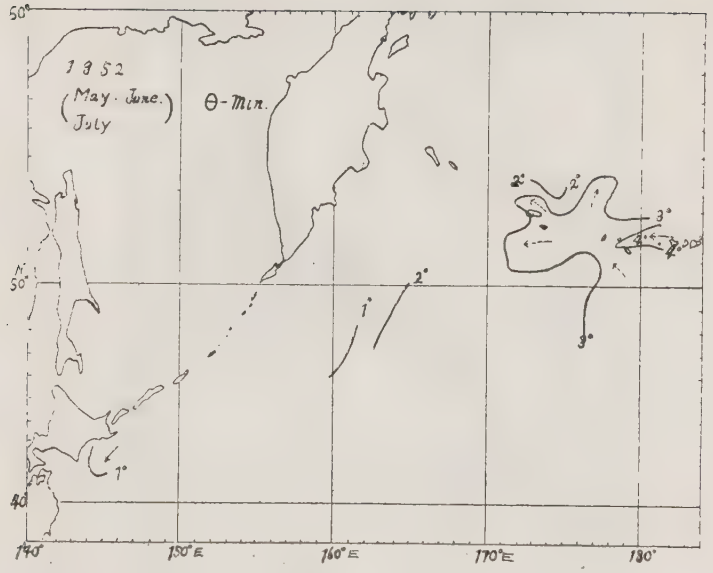

Fig. 11 Distribution of θ-min. (Dichothermal Water) and the Estimated Movement in the Year 1952.

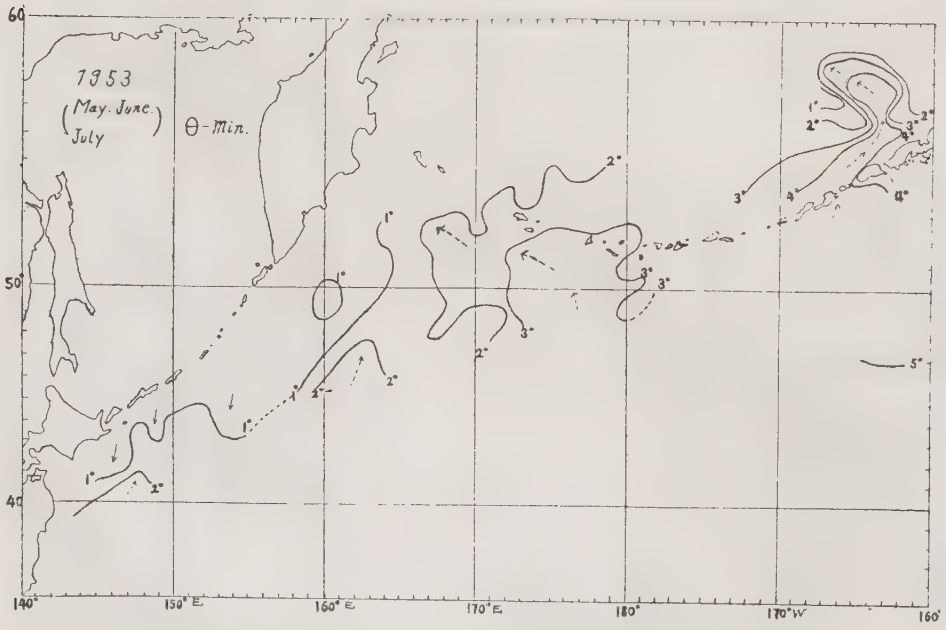

Fig. 12 Distribution of θ-min. (Dichothermal Water) and the Estimated Movement in the Year 1953.

For the purpose of prediction the author plotted the distribution maps of the dichothermal waters (isolines of θ-min. and its layer depth) in every year during the period from 1885 to 1953 basing on the data published by the Assoc. of the Agricultural Technology of Japan (1954) (see Fig. 2-12) and also plotted seasonal maps in Fig. 13, and the vertical distribution of water temperature and salinity in Fig. 14.

Inspecting them we have the following results;

(1) The dichothermal water has shown once temporary southward extension in the years of 1934 and 1935, following northward shrinkage during 1936-1938, again extended southward year by year from 1939 to 1942 (lacking our data during 1943—51), and coming in 1952 and 1953 it holds yet a considerable southward extension. (Refer to the area of the water temperature less than 0°C—1°C, −1.5°C, see Fig. 15).

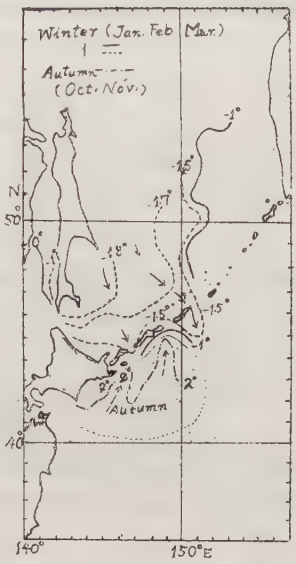

Fig. 13a. Distribution of θ-min. (Dichothermal Water) in Winter and Autumn. (1937—1953).

(2) According to the sea-districts the values of θ-min. and its layer depths of the core water indicate some great characteristic differences.

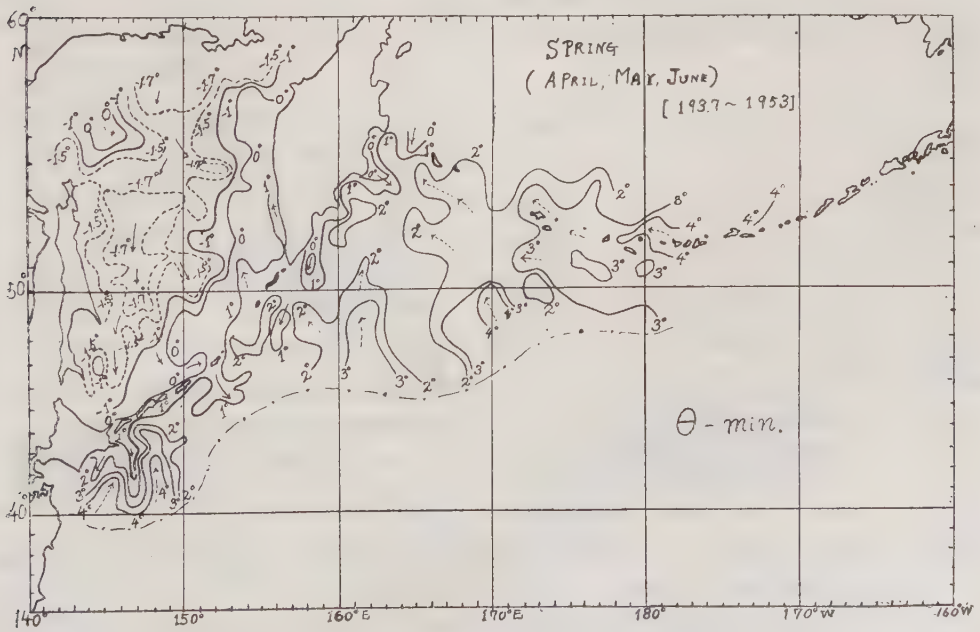

Fig. 13b. Distribution of θ-min. (Dichothermal Water) in Spring. (1937—1953).

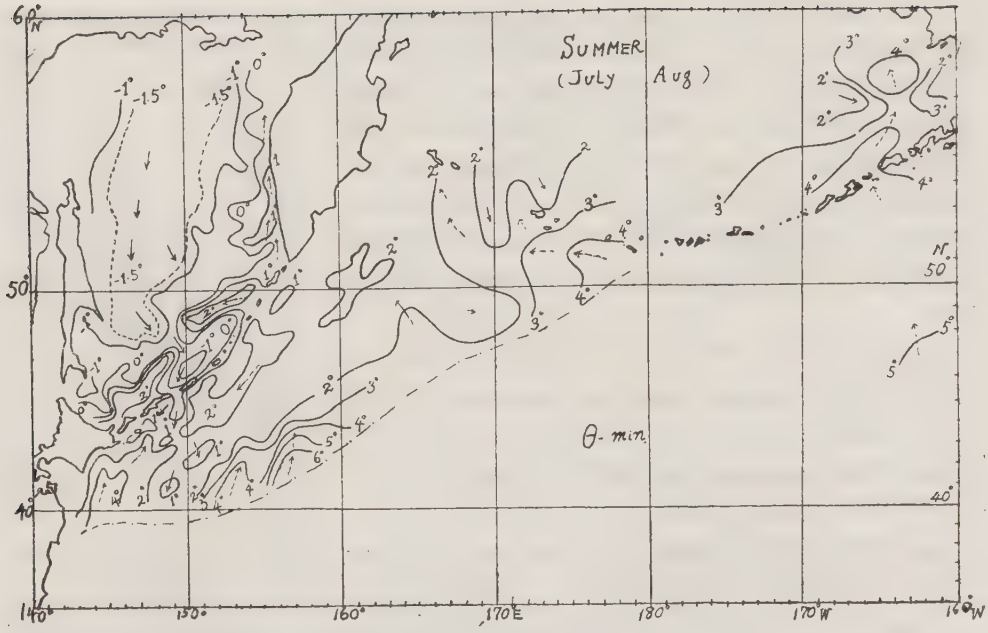

Fig. 13c. Distribution of θ-min. (Dichothermal Water) in Summer. (1937—1953).

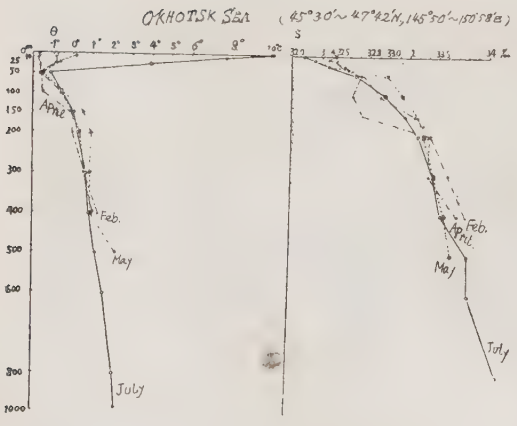

Fig. 14. Vertical Distribution of Water Temperature and Salinity in the Okhotsk Sea.

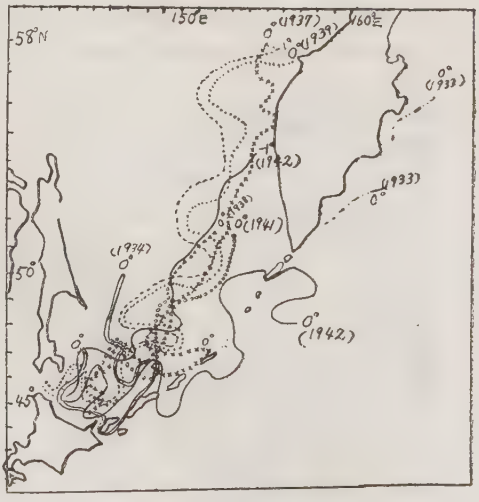

Fig. 15. Distribution of Isotherms of θ-min. 0°C (and −1°C) in Respective Years (1933∼42).

(i) In the Okhotsk Sea, −1°∼−1.8°C (most frequently about −1.5°C) in the layer of the 25m.∼50m. (central) ∼75m. depth.

(ii) On the Pacific side, in the waters south off Kurile Islands, 1°∼2°C, in the layers of 50m∼100m. (central) ∼125m.∼150m., and likely them in the waters off and along the East Coast of Kamchatka.

(iii) In the waters adjacent to the Aleutian Islands 2°∽4°C (eastern warmer) in the layer of 75m.∽100m. (central) ∽150m. depth. (Fig. 16).

(3) In the western half of the Okhotsk Sea there is a semi-permanent cold water area (θ-min. less than-1.5°C) and comparatively warmer in the eastern region of the sea. The head of the dichothermal water in the Okhotsk Sea extends to south in the Pacfic Ocean after passing through the straits of Middle Kurile Is. (the channels near the Uruppu Is.∽Sinsiru Is.) Or in other words we can see the conspicuous advection of the ice-melted cold water of the Okhotsk Sea into the Pacific Ocean as the core water of Oyasiwo. From the sea of pacific side off the North Kurile Is. (Paramusiru to Onnekotan Is.) the relatively warmer water of θ-min. higher than 2°C enters into the eastern part of the Okhotstk Sea and another branches off southwest to North Kurile.

(4) In the sea south off Kamchatka Penn. and in the waters adjacent to Ka mchatka Bay there lies the dichothermal water of θ-min less than 0°C or 1°C which is independent one from the Okhotsk Sea origin and seems to be originated from the ice-melted cold water of the Western Bering Sea.

(5) A belt of comparatively warm water θ-min. higher than 3°C along the south of the middle Aleutian Islands corresponds to the west going warm current branched from the Pacific Current or the West Drift Current, which developes in summer season from June to August in accord with the movement of the favourable salmon fishing grounds and approaches finally near the Kamchatka Penn. In the Eastern Bering Sea the warmer water (θ-min. higher than 3°C) extends to north, passing through the straits of the eastern Aleutian Islands from the eastern Pacific Ocean.

(6) As we see in Fig. 13, the value of θ-min. is lowest in winter and the dichothermal water less than 0°C extending to the waters adjacent to South Kurile. show the outflow the Okhotsk Sea into the Pacific Ocean. The area of dichothermal water shrinks somewhat northward in spring, and shows remarkable shrinkage with the rise of θ-min. in summer, however, the pattern of the persistemt outflow through the straits of middle Kuril of the dichothermal water maintained.

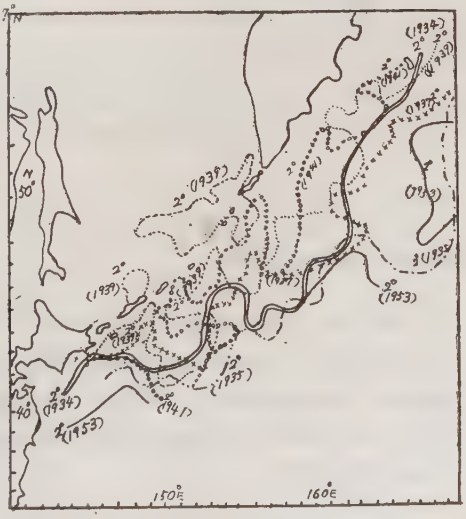

Fig. 16 Distribution of Isotherms of θ-min. 2°C in Respective Years (1934∽1953).

(7) In order to illustrate the matter in (6) more clearly we can see the vert-

ical distribution of water temperature and salinity (Fig. 14) the main variation represented in the upper layer above the 100m. depth, especally remarkable summer warming in the surface layer less than the 25~50m depths.

(8) Comparing the distribution and abundance of sea-ice with the area of the dichothermal water, we have a fairly good coincidence of the years of prevalent dichothermal water with the years of abundant sea ice e.g. 1934, 1935, 1953).[13] (See Fig. 15, 16).

(9) The area of the pure subarctic water mass is almost limited by the southern boundary line of the dichothermal water. (See Fig. 17). In the years of 1934, 1935, 1941 1952, and 1953 the area extended to south and retarded to North in 1937~1939. (See Fig. 15, 16, 17).

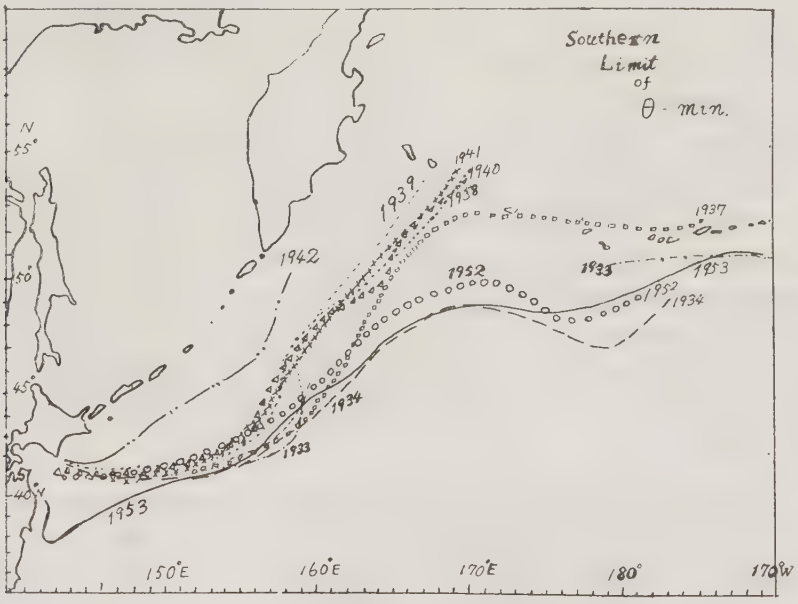

Fig. 17. Southern Limit of θ-min. (1933~1953).

Concluding Remarks

(1) The rôle of the Aleutian Low (P_A) in the North Pacific circulation is very important as a controling factor of the development of Oyasiwo Cold Current and of the production of the cold water masses in the northern seas in cooperation of the Siberian High by the prevalence of the winter monsoon W ($\propto\sqrt{(P_s-P_A)}$).

(2) The distribution of the dichothermal water in the North Pacific appears to be a good indicator of the secular and yearly hydrographical fluctuation, especially for the Oyasiwo Current.

(3) The advection of the dichothermal water from the Okhotsk Sea into the Pacific Ocean through the straits to Middle Kurile is very remarkable and that along the East coast of Kamchatka is recognized comparatively feeble.

(4) The recent strong southward extension to the dichothermal water from the year 1940 may be remarked in comparison with the similar prosperity to the lower water in the Japan Sea in the same period.

(5) The mechanism to the movement, mixing, eddies, upwelling and the fine structure at the head of the frontal dichothermal water-mass are demanded to study in fisheries more precisely.

(6) The secular variation of the dichothermal water correlated with the climatic change and its prediction should be studied more closely in future.

Acknowledgement : The author wishes to state his thanks for the assistance of Mr. Hisayasu Ōtubo and Miss. Kōko Namegaya in preparing this paper.

Reference

1) KŌTARO ANDŌ: Special Report No. 30 of the Agricultural Experimental Station. (1915).
2a) TAKEMATU OKADA: Some Reasearches in the Far Eastern Seasonal Correlations. J. Met. Soc. Japan. 1917.
2b) SAKUHEI FUJIWHARA: "Story to enhance Cloud". P. 157—161. 1950. (Iwanami).
3) KANJI SUDA: Tenki to Kikō. (Weather and Climate) **5**. 1. 1938
4) M. UDA: Hydr. Fluctuation in the NE-Sea region of Japan. J. Imp. Fish. Expt. St. No. 9. 1938.
5) MASAO HANZAWA and TAMIO INOUE: Oceanogr, Report of CMO, **2**, 3, 1952.
6) NOBUO WATANABE: SUISANKAI. (J. of the Fisheries Assoc. of Japan) 1953. Oct.
7) Barometric Table in the Northern Hemisphere. (1931—34) CMO. 1954.
8) M. UDA: "Umi to Sora" (SEA and Sky). **15**. 12. 1935.
9) YUKIMASA SAITŌ: On the Oyashio Curr. J. of Inst. Polytechnics, Osaka City Univ. **3**. 2. 1952.
10) 11) 12) Not Yet Published.
13) KOJI FUKUTOMI et al: Study of Sea ice. Report 4, Inst of Low Temp. Sc. 1950.

Records of Oceanographic Works
in Japan, Vol. 2, No. 2,
October 1955

On the Theorem of Helland-Hansen and Ekman and Some of Its Applications

By
Shoitiro Hayami, Hideo Kawai and Masao Ouchi
(Geophysical Institute, Kyoto University)

Abstract

The theorem of Helland-Hansen and Ekman which is also known as the law of parallel solenoids laid a corner stone in physical oceanography. In this paper the theorem is explained mathematically in a form suitable for its practical application and further development. As an application of the theorem a method of calculating the absolute velocity of a current without any knowledge of zero surface is developed. Using this method, a volume transport of the Kuroshio above the 1000 decibar level was calculated and was estimated to be about 6.5×10^7 (m^3/sec) for the summer of 1938. Finally, an important role of this theorem in the practical analysis of the internal dynamics of an oceanic current was suggested.

1. Introduction

Basing their work on an extensive hydrographic survey in the North Atlantic, Helland-Hansen and Ekman discovered an important law governing the distribution of temperature and salinity in an open ocean (Ekman, 1923). This law was explained by Ekman in terms of physics and to-day it is referred to as the theorem of Helland-Hansen and Ekman or as the law of parallel solenoids. This theorem laid a corner stone in physical oceanography, but the value of the theorem, it seemed to us, has so far not been too widely appreciated. This situation was probably due to the fact that the representation of the theorem was somewhat obscure. The proof of the theorem given by Ekman was merely qualitative and his mode of demonstration was followed by standard text books of physical oceanography (Thorade, 1928; Defant, 1929), which hindered its wider applications and further development. In the present paper the authors wish to explain the theorem quantitatively in mathematical language and to show some of its practical applications.

2. Theorem of Helland-Hansen and Ekman

2.1 The essential contents of the theorem of Helland-Hansen and Ekman are as follows;

(1) If the physical state of an oceanic water is stationary, and

(2) the conservative quantities such as heat, salinity and momentum contained in a volume of water are conserved during its motion, and

(3) that volume of water always flows along a same isobaric (or equipotential) surface,

then,

(a) isotherms, isohalines, isotaches (equal velocity curves) and dynamic isobaths (or isobars) lying on an isobaric (or equipotential) surface are all parallel to each other and also to the stream lines on the same isobaric (or equipotential) surface.

(b) If we project orthogonally these iso-lines lying on an isobaric (or equipotential) surface upon any other isobaric (or equipotential) surfaces, then the projections coincide with iso-lines on the latter surfaces.

(c) In the region of an open sea where no discontinuity in the distribution of conservative quantities occur, the above mentioned conditions are generally established, except near the surface and the bottom of the sea.

2.2 In physical oceanography two systems of reference coordinates are in general use. The one is the system of isobaric surfaces and their orthogonals, the other is the system of equipotential surfaces and their orthogonals. As the processes of treatment in both systems are quite similar, we adopt, in the following, the former system in which the curvature of the isobaric surfaces are neglected.

We assume a sea surface as a standard isobaric surface of zero pressure and take x_1 and x_2 as rectangular coordinate axes on the same surface, with x_3 axis as its orthogonals in pressure units, positive downward.

We denote further :

s_i unit velocity vector

r_i unit vector lying on the same isobaric surface with s_i and perpendicular, positive clock-wise, to s_i

v absolute value of velocity

δs line element of a stream line

θ temperature or salinity

λ Coriolian parameter

R radius of curvature of a stream line on an isobaric surface

D dynamic depth below an assumed equipotential surface above the sea

D_0 value of D of the sea surface

η_{ii} Austausch tensor

α specific volume

t time

where $i=1, 2, 3$.

As the specific heat of sea water is nearly constant, heat quantity is proportional to temperature, so that we treat the temperature of sea water as a conser-

vative quantity. The general equation of conservation of salinity and temperature is given by

$$\frac{D\theta}{Dt}=\Sigma\frac{\partial}{\partial x_i}\left(\eta_{ii}\frac{\partial\theta}{\partial x_i}\right) \tag{1}$$

with

$$\frac{D\theta}{Dt}=\frac{\partial\theta}{\partial t}+s_i v\,\mathrm{grad}\,\theta \tag{2}$$

where grad is taken along an isobaric surface. Assumption (2) implies

$$\frac{D\theta}{Dt}=0 \tag{3}.$$

As the state is stationary by assumption (1), we get from eqs. (1) and (2),

$$\Sigma\frac{\partial}{\partial x_i}\left(\eta_{ii}\frac{\partial\theta}{\partial x_i}\right)=0 \tag{4}$$

and

$$s_i v\,\mathrm{grad}\,\theta=0 \tag{5}.$$

From eq. (5) we know that

$$s_i\perp\mathrm{grad}\,\theta \tag{6},$$

that is, isotherms and isohalines are parallel to stream lines. Eq. (4) requires that

$$\eta_{ii}=0 \tag{7},$$

because θ may take any value, so long as it satisfies eq. (5).

As the mass of a volume of water does not change during its motion, the general equation of conservation of momentum is given by

$$\frac{D(s_i v)}{Dt}=r_i\lambda v+\mathrm{grad}\,D+\Sigma\frac{\partial}{\partial x_j}\left(\eta_{jj}\frac{\partial(s_i v)}{\partial x_j}\right) \tag{8}$$

$$j=1,\ 2,\ 3$$

and

$$\frac{D(s_i v)}{Dt}=\frac{\partial(s_i v)}{\partial t}+(s_i v\nabla)s_i v=\frac{\partial(s_i v)}{\partial t}\pm r_i\frac{v^2}{R}+s_i v\frac{\partial v}{\partial s} \tag{9},$$

upper sign: anticyclonic motion,
lower sign: cyclonic motion.

By assumptions (1) and (2), we get from eqs. (7), (8) and (9)

$$\pm r_i\frac{v^2}{R}+s_i v\frac{\partial v}{\partial s}=0 \tag{10}$$

and

$$r_i\lambda v+\mathrm{grad}\,D=0 \tag{11}.$$

Eq. (10) requires that

$$\frac{v^2}{R}=0 \tag{12}$$

and

$$\frac{\partial v}{\partial s}=0 \tag{13},$$

that is, the radius of curvature of a stream line must be very large and the speed of current does not change along a stream line. By assumption (3) vertical velocity does not exist, so that horizontal divergence must vanish which, in combination with eq. (13), requires that stream lines must be parallel to each other. On the other hand, multiplying s_i into the left hand side of eq. (11), we get

$$s_i\,\mathrm{grad}\,D=0 \tag{14},$$

that is

$$s_i \perp \operatorname{grad} D$$

which indicates that dynamic isobaths are parallel to stream lines. This conclusion is also established in case of a special accelerated motion where eq. (12) does not obtain. In this case, we get, instead of eq. (11),

$$r_i\left(\lambda v \mp \frac{v^2}{R}\right) + \operatorname{grad} D = 0 \qquad (11'),$$

which also leads to eq. (14).

Now, differentiating eq. (14) with respect to x_3, we get

$$\frac{\partial s_i}{\partial x_3} \operatorname{grad} D + s_i \frac{\partial}{\partial x_3} \operatorname{grad} D = 0 \qquad (15).$$

By the definition of dynamic depth,

$$\operatorname{grad} D = \operatorname{grad} D_0 + \int_0^{x_3} \operatorname{grad} \alpha \, dx_3 \qquad (16),$$

hence

$$\frac{\partial \operatorname{grad} D}{\partial x_3} = \operatorname{grad} \alpha \qquad (17).$$

Putting eq. (17) into eq. (15), we get

$$\frac{\partial s_i}{\partial x_3} \cdot \operatorname{grad} D + s_i \operatorname{grad} \alpha = 0 \qquad (18).$$

By eq. (5), this becomes

$$\frac{\partial s_i}{\partial x_3} \cdot \operatorname{grad} D = 0 \qquad (19)$$

which requires that

$$\frac{\partial s_i}{\partial x_3} = 0 \quad \text{or} \quad \frac{\partial s_i}{\partial x_3} \perp \operatorname{grad} D$$

Owing to eq. (14), the latter case must be excluded, hence

$$\frac{\partial s_i}{\partial x_3} = 0 \qquad (20).$$

In other words, the direction of velocity vector at any points does not change along the orthogonals passing through the points. In the above treatment, the continuity of the conservative quantities has been assumed, so that the relations thus obtained are only valid in a region where such an assumption may be made. Eqs. (5), (13), (14) and (20) correspond with (a), (b) of the theorem and the assumptions (1), (2) and (3) are necessary and sufficient for these relations.

3. Computation of Absolute Velocity

3.1 In practical oceanography, the velocity of a current is usually computed from data of observed salinity and temperature by the aid of eqs. (11) and (16). Although in recent years, the direct recording of velocity in superficial layers by G. E. K. is rapidly developing, the computation of velocities at relatively deep layers still depends solely upon dynamic calculations. In order to calculate a current velocity by eq. (11), we must know the value of grad D. This is,

however, impossible, so long as its value of the sea surface-grad D_0 in eq. (16) is unknown. As is well known, the only reliable method of obtaining the value of grad D_0 so far used is to extend an observation deep enough until velocity vanishes. As grad D vanishes with the velocity at this depth, we get from eq. (16)

$$\text{grad}\, D_0 = -\int_0^{x_{30}} \text{grad}\, \alpha dx_3$$

where x_{30} is the depth of the zero layer.

The practical use of this method is quite limited, because it can not be applied when observations do not reach a no current level or a certain discontinuity occurs in the vertical distribution of velocity. The theorem of Helland-Hansen and Ekman, however, permits the calculation of an absolute velocity in more general cases. As was explained in 2.2, eq. (11) is satisfied only in a parallel solenoids field, so that eqs. (5), (14) and (20) must be satisfied simultaneouly. If this is not the case, eq. (11) can not be applied. In a parallel solenoids field, we may put

$$\text{grad}\, D = -A\, \text{grad}\, \alpha,\ \text{grad} D \neq 0,\ \text{grad}\, \alpha \neq 0 \qquad (21),$$

where A is a certain positive function of x_3.
Putting eq. (21) into eq. (16), we get

$$A\, \text{grad}\, \alpha = A_0\, \text{grad}\, \alpha_0 - \int_0^{x_3} \text{grad}\, \alpha dx_3 \qquad (22),$$

where A_0 and α_0 express respective values on the sea surface.
Differentiating eq. (21) with respect to x_3, we get

$$\frac{d(A\, \text{grad}\, \alpha)}{dx_3} = -\text{grad}\, \alpha \qquad (23).$$

The direction of grad α does not change with x_3, hence

$$A\frac{d\, \text{grad}\, \alpha}{dx_3} = -\left(1+\frac{dA}{dx_3}\right)\text{grad}\, \alpha \qquad (24).$$

Integration of eq. (24) gives

$$\text{grad}\, \alpha = \text{grad}\, \alpha_0 \exp\left\{-\int_0^{x_3} \frac{1+\frac{dA}{dx_3}}{A} dx_3\right\} \qquad (25).$$

If A does not change with x_3, which is possible only in the case when grad α decreases with depth, eq. (25) becomes

$$\text{grad}\, \alpha = \text{grad}\, \alpha_0 \exp\left(-\frac{x_3}{A}\right)$$

or

$$lg(\text{grad}\, \alpha) = lg(\text{grad}\, \alpha_0) - \frac{x_3}{A} \qquad (26).$$

From this equation the value of A is easily obtained, so that the value of grad D are known at every point by eq. (21). In this case the current velocity decreases exponentially with the depth. The behavior of grad α relative to the depth is easily seen by plotting the values of grad α or lg (grad α) against x_3. In a strong current like the Kuroshio, at least some part of the curve (grad α ~

x_3) or (lg (grad α)$-x_3$) becomes decreasing downward and straight below several hundred decibars as is shown in the following examples.

(a) If the curve (lg (grad α)$-x_3$) is decreasing and linear from x_{31} to x_{32}, we get from eq. (25)

$$(\text{grad}\,\alpha)_{x_{32}}=(\text{grad}\,\alpha)_{x_{31}}\exp\left(\frac{x_{31}-x_{32}}{A}\right) \tag{27}$$

then the value of A is given by

$$A=\frac{lg(\text{grad}\,\alpha)_{x_{31}}-lg(\text{grad}\,\alpha)_{x_{32}}}{x_{32}-x_{31}} \tag{28}$$

The value of grad D is then obtained at the depth $x_{31}\leq x_3\leq x_{32}$. Starting from this value the values of grad D at other points may easily be calculated by eq. (16).

(b) If the curve (grad $\alpha-x_3$) is decreasing and linear from x_{31} to x_{32}, and is expressed by

$$\text{grad}\,\alpha=(\text{grad}\,\alpha)_{x_{31}}-b(x_3-x_{31}) \tag{29}$$

then A will be also assumed to be linear in this interval, so that

$$A=(A)_{x_{31}}+a(x_3-x_{31}) \tag{30}$$

Putting eqs. (29), (30) into eq. (24), we get

$$(A)_{x_{31}}=\frac{(\text{grad}\,\alpha)_{x_{31}}}{2b} \tag{31}$$

The value of grad D at the depth $x=x_{31}$ is thus easily obtained.

3.2 In an example of the Kuroshio observed during August, 1938 off the southern coast of Japan and shown in the next paragraph, a parallel solenoids field is beautifully formed in a strong current area. On the left side of the strong current, grad α seems to change with depth generally in the fashion shown in Fig. 1 (a), while on the right side it usually changes in the manner shown in Fig. 1 (b). The former corresponds to case (a) in 2.2 and the latter to case (b) in 2.2.

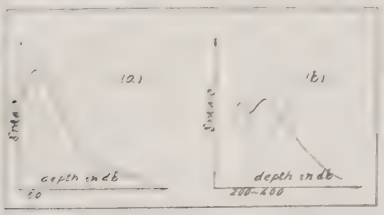

Fig 1. Types of the change of grad α with depth.

In Fig. 2 examples of type (a) and type (b) are given. From the linear portion of

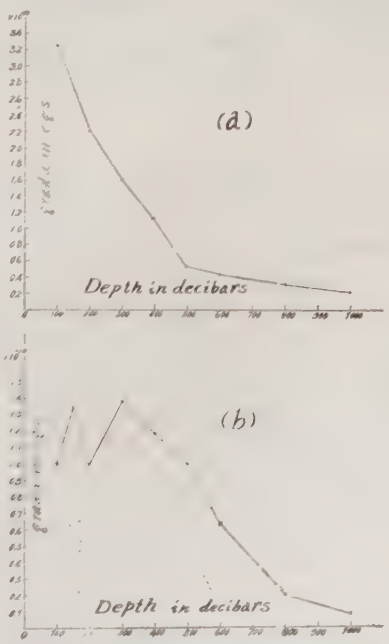

Fig 2. Examples of the change of grad α with depth.

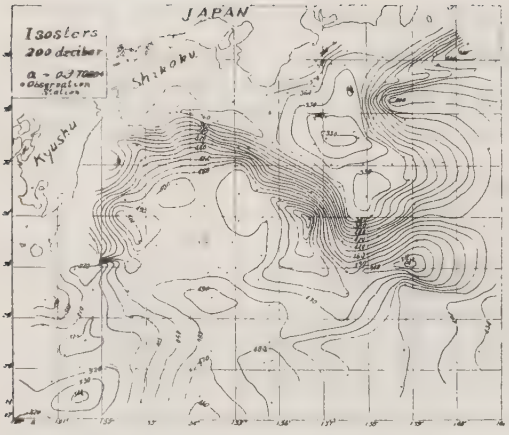

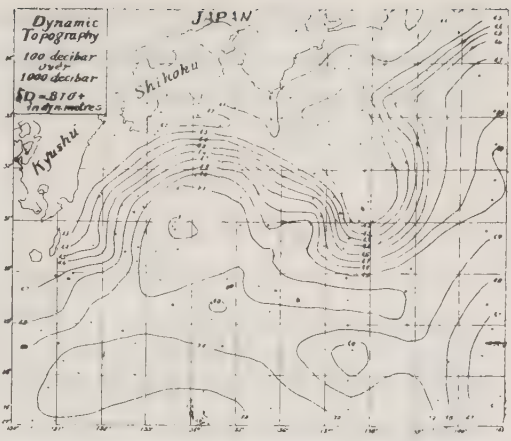

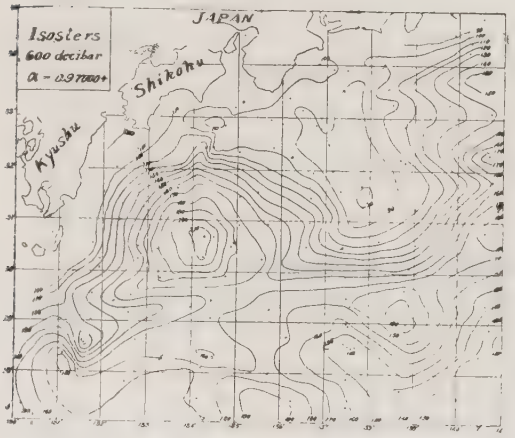

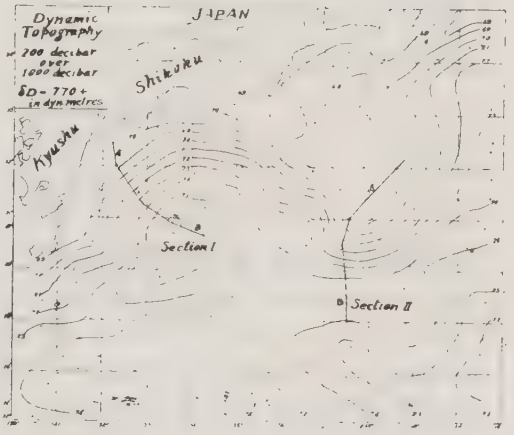

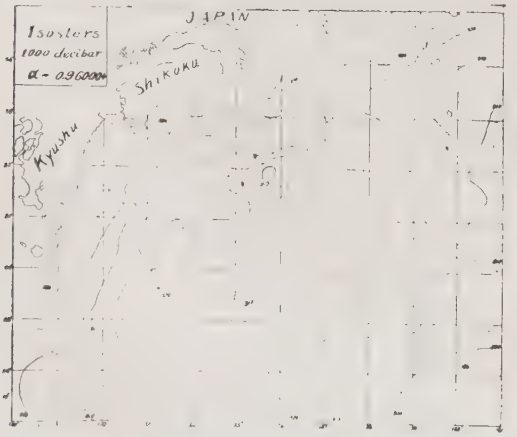

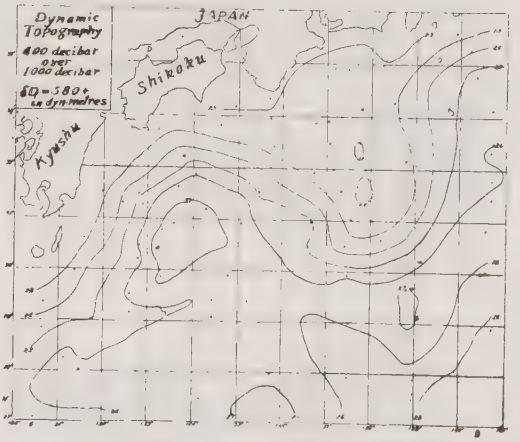

Fig 3. Isosteric lines on isobaric surfaces.

Fig 4. Relative dynamic topography of isobaric surfaces referred to the 1000 decibar surface.

these curves, the values of A were calculated by the procedure mentioned in 2.2 at the respective depths and, based on these values, grad D and the absolute velocity v at the 1000 decibar isobaric surface which was the deepest observation level were obtained. The result is shown in Table 1.

Table 1. Values of A

Type	A	Depth (db) for A	Grad D (dyn. m/m) $\times 10^{-5}$ (1000 db surface)	Absolute velocity (cm/sec) (1000 db surface)
a	607	600	0.1346	18.1
b	357	300	0.0771	10.1

In the 1000 decibar layer, the velocity attains the value of about 10cm/sec in spite of very weak solenoids.

4. Volume Transport of the Kuroshio

4.1 As an example of the practical application of the preceeding method, the volume transport of the Kuroshio was estimated. The materials used were those collected from August 2 to August 21, 1938 in the Kuroshio region off the soushern coast of Japan by five survey ships of the Hydrographic Bureau of Japan. The total number of observation stations was 133 and the observation depths were 0, 25, 50, 100, 150, 200, 300, 400, 500, 600, 800, and 1000 decibars. From these data isotherms, isohalines, isosters and relative dynamic isobaths were drawn on various isobaric surfaces. Some of them are reproduced in Figs. 3 and 4. As is seen from these figures, a parallel solenoids field develops well, especially in

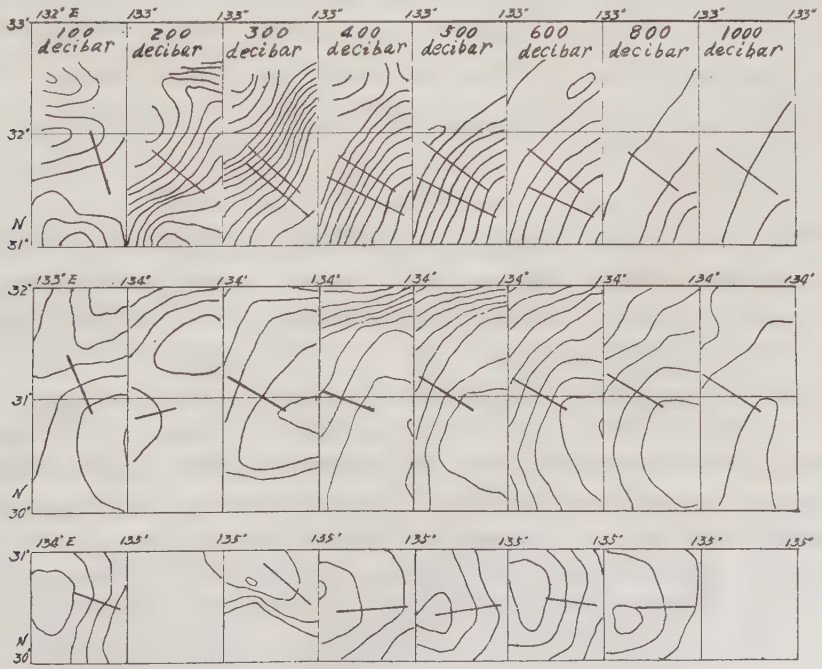

Fig 5. Isosteric lines on isobaric surfaces in the neighbourhood of the section I.

the region of a strong current.

Two sections (I, II) were chosen in the western and eastern parts of the main current as shown in Fig. 4 and the absolute current velocities were calculated by the method mentioned in the preceeding paragraph; the volume transport of the main current was also calculated. To verify the parallelism of the iso-lines more closely, isosteric lines were drawn on different isobaric surfaces in the neighbourhood of these sections as shown in Figs. 5 and 6. These figures vouch for the present method.

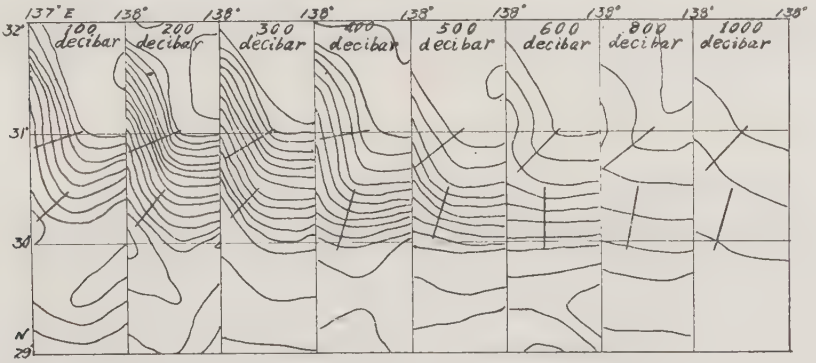

Fig 6. Isosteric lines on isobaric surfaces in the neighbourhood of the section II.

4.2 Isotaches in the sections derived from these calculations are shown in Figs. 7 and 8. On both sides of the main current, counter currents are inferred from the dynamic topography, but in these regions the parallel solenoids fields do not develop so well, so that the method can not be applied directly in these regions. In these figures, therefore, only the boundaries of the main current are indicated by dotted lines of zero velocity. The volume transport calculated from these figures is shown in Table 2.

Table 2.

Volume transport of the Kuroshio above the 1000 decibar surface in $(m^3/sec) \times 10^6$

Section	0 — 200db	200 — 400db	400 — 600db	600 — 800db	800 — 1000db	Total	Relative volume ttransport referredt o he 1000dbsurface
I	21.5	18.6	13.1	7.6	4.2	65.0	49.5
II	27.3	18.9	12.8	8.0	4.6	71.6	55.7
	(24.4)	(17.4)	(12.1)	(7.7)	(4.5)	(66.1)	(50.2)

Remarks. The curvature of the stream lines through the section II is not negligible, the radius of curvature being about 120km in the central portion of the strong current. Hence, for the computation of the volume transport through the section II, the effect of centrifugal force must be taken into acount. The distribution of velocity in Fig. 8 was calculated by eq. (11), from which the values of transport in this table were estimated. For the sake of comparison, the values in the brackets were calculated by eq. (11)′. The corrected transport agree well with that of the section I.

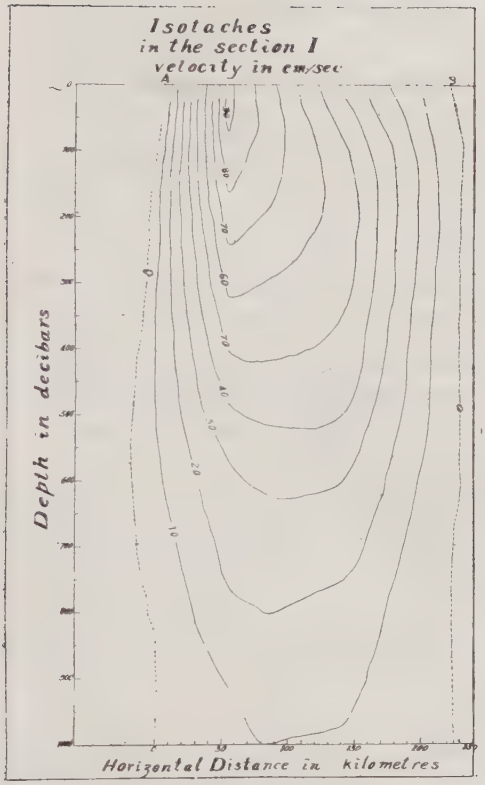

Fig. 7. Distribution of the absolute velocity in the section I.

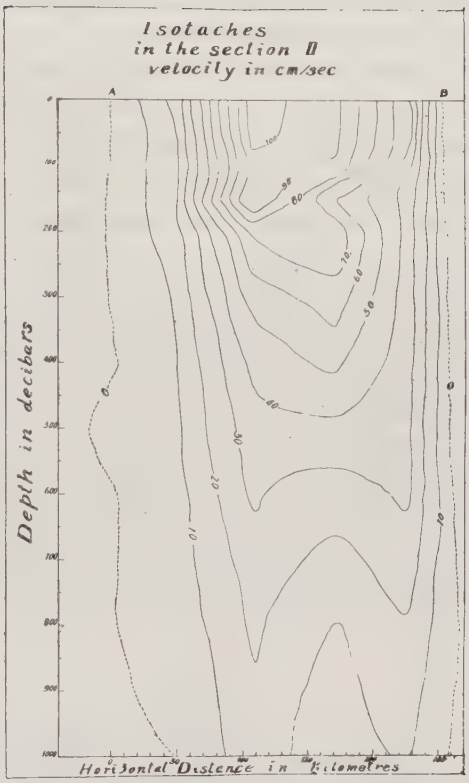

Fig. 8. Distribution of the absolute velocity in the section II.

As the velocity does not vanish at the 1000 decibar level, total volume transport will be somewhat greater than the value obtained above, but this value agrees with the recent estimates obtained from various sources (Sverdrup et al, 1952).

4.3 As will be seen from Figs. 5 and 6 the Kuroshio winds remarkably in its course from long. 134°E to long. 139°E. This course is not permanent. The Kuroshio took this course about eleven years (1934-1945) and changed its course. When the Kuroshio takes this course, a cold water upwells in the region of a large cyclonic whirl which causes severe damage to the fisheries of the region. The cause of this winding has been a matter of much debate among Japanese oceanographers (Uda, 1949). This course seems to have some connection with the bottom topography of the region which is shown in Fig. 9. It has many features in common with the remarkable winding of the Gulf stream off the Grand Bank of Newfoundland and will be explained in a similar fashion. It is worthy to note that in our case the velocity of the main current is appreciable at the 1000 decibar level (about 10cm/sec), while grad α is very small on the same level. If we assume grad α vanish below this surface, then we get from eq. (16)

$$\text{grad}\, D = (\text{grad}\, D)_{1000}, \quad x_3 > 1000$$

where $(\text{grad}\, D)_{1000}$ is the value of grad D of the 1000 decibar surface. In the deep layer, therefore, the velocity does not change with depth (Ekman's deep current). If the deep current in our case was of such a character, it would extend to a considerable depth right down to the bottom. Then, when it approached a shallower sea or deeper sea, it would be deflected toward right or left and gradually flow along the bottom contours (Ekman, 1923). The remarkable bending of stream lines over areas located around (long. 134°. 5E, lat. 33°N), (long. 137°E, lat. 31°N) and (long. 139°E, lat. 31°N) seems to indicate such an effect. In the period when the Kuroshio does not take such a winding course, the main current seems to be restricted to a relatively shallow layer.

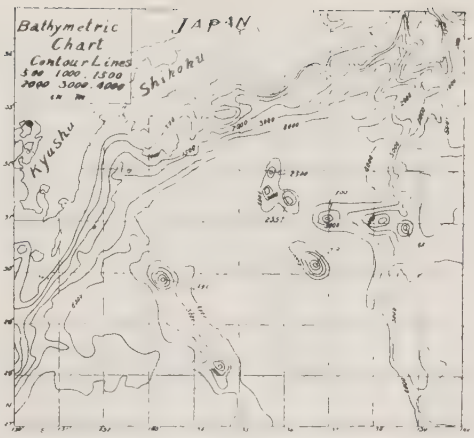

Fig 9. Bathymetric chart of the ocean bottom off the southern coast of Japan

5. Internal Dynamics of an Oceanic Current

The item (c) of the theorem of Helland-Hansen and Ekman, which was thereafter supported by many observations, indicated that in an open sea the water moves as if no external action affected it. The energy of an oceanic current is supplied mainly by the wind stress acting upon its surface and for long time it is stored in the form of solenoids until a stationary state is reached when external actions balance each other. This balancing is usually expressed by a vorticity equation, that is a balance between wind stress curl, lateral stress curl and planetary vorticity including occasionally bottom stress curl, and the water moves as if under no external action. But this is a mere abstraction. The actual states are ever changing and practical oceanographers must deal with these changing states. Moreover, oceanographical observations are fragmental in time and space. The physical image based on these data are subjected to the worker's personal opinion and it is not unusual to arrive at many contradictory conclusions derived from the same data (Fuglister, 1955). The theorem of Helland-Hansen and Ekman seems to offer a solid alternative to this chaotic state of affairs.

The climate of the earth did not change so much since the last glaciation. So, there is no doubt that a parallel solenoids field forms the basic structure of an oceanic current on which such ever changing actions as vertical motion, acceleration, mixing process, wind stress, bottom stress, boundary constraint, evaporation, precipitation and radiation overlap. If we divide θ and $(s_i v)$ into two parts respectively such as

$$\theta=\theta_0+\delta\theta,\quad s_iv=(s_iv)_0+\delta(s_iv) \tag{32}$$

where $\theta_0,(s_iv)_0$ represent parallel solenoids field and $\delta\theta,\delta(s_iv)$ disturbing field, then the general equations of conservation (eqs. (1), (8)) will be split into two parts respectively, one for $\theta_0,(s_iv)_0$ and the other for $\delta\theta,\delta(s_iv)$. A parallel solenoids field may persist for a much longer time than a variable field, so in the integral form of eq. (32), e.g.

$$\int_0^{x_3}\alpha dx_3=\int_0^{x_3}\alpha_0 dx_3+\int_0^{x_3}\delta\alpha dx_3$$

the second term of the right hand side will be much smaller than the first term. As the term of the left hand side is nothing but a dynamic depth, a parallel solenoids field will be approximately revealed in a relative dynamic topography of a deep isobaric surface referring to the sea surface. In practice, the relative dynamic topography of the 300-400 decibar surfaces in reference to the deepest observation level will be conveniently used. Taking this topography as the topography of the iso-lines of a parallel solenoids field, we may obtain θ_0 and $\delta\theta$ from the actual data and consequently $(s_iv)_0$ will be calculated by the method already described. Then, by using these data we may derive usefull knowledge of the disturbing field from the equations of this field. Further considerations along this line will be reported elswhere.

Acknowledgment

The authors wish to express, belatedly, their gratitude and indebtedness to the late Mr. Mitsutoshi Nakamiya, ex-chief of the hydrographic division, Japanese Hydrographic Bureau, who kindly offered them many observational materials on the Kuroshio obtained by the bureau, and express their heartfelt loss on his unfortunate death.

References

Hayami, S. and Kawai, H. (1950) On the Theorem of Helland-Hansen and Ekman. Read before the annual meeting of the Oceanograph. Soc. Japan.

Hayami, S. and Ouchi, M. (1955) On Mass Transport of the Kuroshio. Read before the annual meeting of the Oceanograph. Soc. Japan.

Ekman, V. W. (1923) Über Horizontalzirkulation bei winderzeugten Meeresströmungen. Ark. f. Math., Astr. o. Fys., Bd. 17, No. 26.

Thorade, H. (1928) Physik des Meeres. Müller-Pouillets, Lehrbuch der Physik, Bd. 5.

Defant, A. (1929) Dynamische Ozeanographie.

Sverdrup, H. U., Johnson, M. W. and Fleming, R. H. (1952) The oceans.

Uda, M. (1949) On the Correlated Fluctuation of the Kuroshio Current and the Cold Water Mass. Oceanograph. Mag., Vol. 1, No. 1.

Fuglister, F. G. (1955) Alternative Analysis of Current Surveys. Deep-Sea Research, Vol. 2, No. 3.

Records of Oceanographic Works
in Japan, Vol. 2, No. 2.
October 1955

On a Problem Concerning the Vertical Circulation of Sea Water Produced by Winds, with Special Reference to Its Bearing on Submarine Geology and Submarine Topography.

By

Masito Nakano

(Meteorological Research Institute)

§ 1. Introduction. It is a well-established fact that when winds blow from the offing towards the coast or from the coast out to the offing, an elevation or depression of sea level is produced in the vicinity of the coast, resulting in vertical circulations of sea water. In the former case, viz. in case of landward wind, a descending current occurs near the coast, while in the latter case, viz. in case of seaward wind, an ascending current or upwelling occurs near the coast. Thus, in the sea around the Galapagos Islands, for instance, owing to the impelling action of a regular wind, vertical circulations of water are produced in the sea on the windward and leeward sides of the islands, respectively, and consequently the water temperature at the sea surface sometimes shows a difference as much as 10°C between those on both sides of the islands. The vertical circulation of sea water is a cause of changes in the vertical distributions of various nutritious salts and plankton organisms as well as of temperature and salinity, and a great deal of discussion has already been made by many authors on these subjects. As another natural consequence of the vertical circulation of sea water due to wind, it can be considered that the depth of shallow seas or bays may change due to the transport of loose deposit along the sea bed. As regards this subject the present author has once made a detailed discussion[1], but here he intends to summarize his conclusions and make some additional remarks.

About thirty years ago, the construction of Isohama Harbour on the Pacific coast of our Mainland (Honshu) was frustrated by the introduction of sand and grit which filled up at last the greater part of the harbour in a comparatively short time. The cause of this remarkable event was investigated by the late Prof. T. Terada, who, on drawing a curve representing the area of the region of the bay filled up by sand and grit against the time as abscissa, found that, although the area in question went on increasing generally, it somewhat decreased, or at least the rate of increase fell off during summer, while it always increased during winter, and the maximum and minimum of the curve corresponded to the turning points

of monsoon in spring and autumn, respectively. Thus, he could ascertain that this event was caused by the transport of sand and grit into the bay from outside, owing to the vertical circulation of water produced by winds.[2]

Similar events are occurring at various places, though with less impetuosity. For example, the construction of Nobiru Harbour (Miyagi Prefecture) also met with the same fate as Isohama Harbour. It is also known that, at Taito-Misaki situated near the south end of Kujukuri-Hama (Chiba Prefecture), the depth of the sea frequently increases and decreases by more than one metre in a day in monsoon season[3]. Again, it is known that there is a bay of about 6-m depth on the Chilian coast, the depth of which, in monsoon season, frequently decreases to about 3 m owing to the introduction of sand and grit, and increases again to the original depth, 6m, when the wind direction turns.[4]

The actual examples mentioned above will be sufficient to show that the transport of loose deposit along the sea bed due to the vertical circulation of water produced by winds becomes a cause of change in the depth of seas and bays, together with the vertical movement of submarine ground, erosion of the bed by tidal or oceanic currents, transport of sand and mud by rivers, etc.

§ 2. Vertical circulation of sea water due to wind, and the movement of sand and clay on sea bed. As regards the vertical circulation of sea water due to wind, a great deal of investigation has been made by many authors such as V. W. Ekman[5], K. Hidaka[6], T. Nomitsu[7], T. Takegami[8], etc.

The present author has once discussed the vertical distribution of velocity of the current produced by wind in an enclosed sea and in a sea with a straight coast, for the cases where "slips" occur in various degrees at the bottom as well as for the case of no "slip". He has also made some model experiments in order to verify his theoretical results.[9] It is the current near the sea bottom that affects the movement of the bed load, and according to the result of calculation made by the present author, based on W. Ekman's theory of drift current, for the case of an enclosed sea of uniform depth d (in the Northern Hemisphere), the angle α between the direction in which the wind blows and that of the bottom current, measured clockwise starting from the former to the latter, is as shown in Table 1,

Table 1. The values of α and α_1 for various values of d/D'.

d/D'	0.1	0.2	0.3	0.4	0.5	0.6	0.7	0.8	0.9	1.0
α	180°.6	182°.3	185°.1	188°.9	193°.9	199°.3	205°.7	212°.0	218°.1	223°.6
α_1 $(=\alpha-180°)$	0.°6	2°.3	5°.1	8°.9	13°.9	19°.3	25°.7	32°.0	38°.1	43°.6

where D' denotes the "depth of frictional influence". As seen from this table, if the the depth d is less than 1/10~2/10 of the depth of frictional influence D', the value of the angle α_1 $(=\alpha-180°)$ is negligibly small; in other words, the bottom current lies nearly in the vertical plane containing the direction of wind. Again, in a sea of uniform depth d with a straight coast (in the Northern Hemisphere),

the angle β between the direction in which the wind blows and that of the bottom current, measured ***counterclockwise*** starting from the former to the latter, is as shown in Table 2, where θ and θ_0 denote the angles which the normal drawn to the coast line (directed from land to sea) and the direction in which the wind blows make with the North, respectively, both θ and θ_0 being measured ***counterclockwise*** from the North. As seen from this table, when $\theta-\theta_0=0$ or 180°, viz. when the wind blows in the direction perpendicular to the coast line either from the coast out to the offing or from the offing towards the coast, β is always equal to 180° for all values of d/D', or in other words, the bottom current lies in the vertical plane containing the direction of wind.

Table 2. The values of β for various values of d/D' and $\theta-\theta_0$.

$\theta-\theta_0$ \ d/D'	0.1	0.2	0.3	0.4	0.5	0.6	0.7	0.8	0.9	1.0
0°	180°	180°	180°	180°	180°	180°	180°	180°	180°	180°
45°	289°.6	293°.2	299°.8	309°.8	322°.5	335°.2	345°.9	353°.2	357°.6	360°
90°	1°.4	5°.6	12°.4	20°.8	29°.5	36°.8	42°.1	45°.3	46°.9	47°.4
135°	72°.7	75°.8	80°.4	85°.4	90°	93°.4	95°.3	95°.9	95°.5	94°.5
180°	180°	180°	180°	180°	180°	180°	180°	180°	180°	180°
225°	289°.6	293°.2	299°.8	309°.8	322°.5	335°.2	345°.9	353°.2	357°.6	360°
270°	1°.4	5°.6	12°.4	20°.8	29°.5	36°.8	42°.1	45°.3	46°.9	47°.4
315°	72°.7	75°.8	80°.4	85°.4	90°	93°.4	95°.3	95°.9	95°.5	94°.5

In the cases of actual seas or bays, circumstances are very much complicated, but judging from the result of investigation for the two extreme cases mentioned above, we shall be justified in regarding that in shallow seas or bays, at large, in the regions near the coast where wind blows in the direction perpendicular to the coast line (except the region of seas or bays in the immediate vicinity of the seashore where the depth is too shallow to produce the vertical circulation of water), the bottom current nearly lies in the vertical plane containing the direction of wind and is opposite in sense to that of wind.

Now, consider a sand particle at the bottom of a sea or bay stirred up by wind waves and suspended in water. If there were no general current in the water, the sand particle would execute a periodic motion in an elliptic orbit. But, if a general current exists in the water, the suspended particle must be thereby subject to a displacement in the direction of the current on an average. Though the displacement to which the particle is subject during one complete period of wave motion may be very small in amount, such a displacement occurring successively is of a ***cumulative*** nature. Hence it is certain that the result of these minute displacements gives rise to a finite cumulative effect. Again, even if the direction of the current may sometimes turn, the integral effect with respect to time will reveal itself in the direction of the prevailing current. Thus, it appears that, in case the winds which blow over a bay, for instance, have a so-called prevailing direction, owing to the vertical circulation of the bay water induced thereby, the sand particles at the bottom of the bay disturbed by wind waves will be moved in the direction nearly opposite to that of the prevailing winds,

resulting in the change of depth of the bay. In this case, it is to be remarked that the properties of the bed load under consideration, especially its grain size, play an important role in our subject. This will be understood from the result of the following experiments made by the present author. (10)

Experiment 1. A rectangular vessel made of galvanized-iron plate 1.3mm thick, whose longitudinal vertical cross section is as shown schematically in Fig. 1 was used as a model of sea. The length and the breadth of the basin are 48 and 15 cm, respectively, and the depth at the middle of it 2.5 cm ; thus the slope of the bed against the horizontal plane is about 6°. To the margin of the basin is attached a horizontal brim whose breadth is 5 cm on two sides and 3cm on the other two sides, and the surface of the vessel is coated white.
This vessel was filled with water up to the depth of 1.5cm at the middle of the basin, and was fitted into a rectangular hole pierced in the bottom wall of a wind tunnel.

Fig. 1. A schematical view of the vertical circulation of water produced by wind in a sea model.

Now, grains of coal prepared in the following process were employed as the bed load. Namely, a piece of coal (density : 1.42gr/cc) was crushed to grains ; larger grains were removed by sieving with a wire-netting of 25 meshes for 10cm, and the finest ones were then removed by sieving again with a wire-gauze of 75 meshes for 10cm. The average diameter of the grains thus obtained was 1~2mm approximately, though not quite regular in shape. About 12 grammes of these coal grains were put into a lidded beaker filled with water, concussed for some time, and then left for about 5 hours. The coal grains thus prepared were distributed on the bed of the basin on the lee side (right-hand side in Fig. 1), and wind (velocity : about 7 m/sec) was made to blow in the direction shown by the arrow in the figure. It was observed that most of the coal grains, except a part situated in the immediate vicinity of the water's edge on the lee side, were transported little by little along the bed toward the windward side, showing that a vertical convection of water was produced in the basin, as shown schematically in Fig. 1. After 10 minutes since the wind was made to blow, we saw that the majority of the coal grains had already moved to the windward half of the basin. In fact, a part of them has been transported up to the immediate vicinity of the water's edge on the windward side, opposing against the very slope of the bed. When this state was once attained, the distribution of the coal grains was hardly altered by making wind blow further.

The result of the above experiment may be explained as follows :
As the bed load employed is comparatively coarse, it is always distributed in the vicinity of the bed of the basin, where the bottom current prevails. Consider the

flux of particles through the cross section *pq* (Fig. 1). The bottom current will transport the bed load into the region *Apq* from right to left through the lower part of the cross section. When the particles approach the water's edge on the windward side, they will be subject to a strong upward force, but as they are sufficiently heavy, when they have once been transported up to the region near the water's edge, most of them remain there, instead of being stirred up further. Finer particles may indeed be stirred up and somewhat carried away off the water's edge by the surface current, but they are still heavy enough, they will sink down again before they are carried away. Thus they are again transported toward the water's edge on the windward side by the bottom current. It follows then that, when the particles have once been brought up to the region near the water's edge on the windward side, they cannot leave there. Thus deposition occurs on the windward side. In the same way we see that erosion occurs on the lee side, except in the region immediately near the water's edge where the depth is too small to produce a vertical convection of water.

Experiment 2. Another vessel made of galvanized-iron plate 1.3mm thick and of similar shape as that in Experiment 1 was employed as a model of sea, the length and the breadth of the basin being 50 and 15 cm, respectively, and the depth at the middle of it 1.5cm; thus the slope of the bed against the horizontal plane is about 3.4°. To the margin of the basin is attached a horizontal brim whose breadth is 5cm on two sides and 3cm on the other two sides, and the inside of the basin is coated black, whereas the surface of the brim is white.

In the present experiment, chalk powder was employed as the bed load. Two pieces of chalk, each of which is of 5.3 gr weight and 7.8 cc volume, were ground down to powder against a wire-gauze of 125 meshes for 10 cm. Under a microscope, it was found that the average grain size of the powder was 0.02~0.08mm in diameter, though not uniform in size as well as in shape. This chalk powder was put into a lidded beaker filled with water of 400 cc volume, and was violently concussed for several minutes.

Now, the basin was fitted into the said hole pierced in the bottom wall of the wind tunnel, and the water mixed with chalk powder prepared as above was transfused from the beaker into the basin as soon as the mixture was violently concussed. The depth of water was 1.3 cm at the middle of the basin. After one minute since the above mixture was poured into the basin, wind (velocity : about 5 m/sec) was made to blow. On gazing at the basin, we saw that the bed of it near the water's edge on the windward side began to be gradually eroded. At first, it was thought that the vertical convection of water could not be produced in the region near the water's edge on the windward side, where the said erosion occurred. However, on gazing at the movement of the bed load, it was found, contrary to expectation, that on the windward side of the basin, the general vertical convection developed almost up to the water's edge itself as in the case of experiment 1. In other words,

in the present case erosion occurred in the very region where deposition must occur if the bed load were coarse. On the lee side of the basin, the front of the general convection was about 15 cm distant from the water's edge. In the region nearer to the water's edge than this front, the movement of the bed load was very haphazard compared with that on the opposite (windward) side. Thus, when wind was made to blow for about 20 minutes, an apparent change began to be seen in the distribution of the bed load in the basin. Namely, it became recognizable that on the windward side of the basin, the region within the distance of 5~6 cm or more from the water's edge has been conspicuously eroded, while on the lee side, deposition of the bed load has sensibly occurred. Wind was made to blow further for 20 minutes, but any sensible change did not occur after the above state was once attained.

The result of the above experiment may possibly be explained as follows : The bed load employed in the present experiment is very fine, so that it is not only easily stirred up by the disturbance of wind, but also when once stirred up it is suspended for a long time. Conceive a vertical cross section pq. The bottom current will transport the bed load into the region Apq from right to left through the lower part of the cross section. When the bed load approaches the water's edge on the windward side, it will be stirred up, instead of depositing, until it enters the upper layers where the surface current prevails. The surface current is much stronger than the bottom current. Thus, the bed load which has once entered the surface layers will be transported out of the region Apq (through the upper part of the cross section pq), and will be carried far away off the water's edge on the windward side before it settles down. (In fact, some particles are carried as far as the water's edge on the lee side.) Therefore, it will naturally happen such a case that some of the particles never come back to the region Apq. If such process be repeated, the bed of the basin on the windward side must be gradually eroded.

Again, conceive a vertical cross section rs situated at such a point as shown in Fig. 1 on the lee side. The bottom current will transport the bed load out of the region Crs from right to left through the lower part of the cross section. On the other hand, the surface current will transport the bed load into this region from left to right through the upper part of the cross section. But in the present case as the bed load is very fine, the concentration of particles does not much differ for different heights. Moreover, among the particles which have been stirred up on the windward side and carried by the surface current, there will be some particles which enter the region Crs from left to right through the upper part of the cross section. In other words, the flux of particles through the cross section rs from right to left is always compensated by the contrary flux in some measure. Thus, in the present case no sensible change of depth may not occur in the very region where the general convection prevails.

Again, consider the region immediately near the water's edge on the lee side. In this region, water moves rather in the same direction from the surface to the bottom, as the depth is too small to produce the vertical convection. If particles which have been brought by the strong surface current have once entered this region by some chance, it is difficult for them to get out of this region. Thus, deposition occurs in the region near the water's edge on the lee side.

From the results of the above experiments as well as the preceding discussions, we may conclude as follows :

(1) In case the prevailing winds blow from the offing toward the coast, the region of a sea or bay near the coast is deepened along the direction of wind, while on the contrary, when the prevailing winds blow from the coast out to the offing, the region near the coast becomes shallower and shallower along the direction of wind, provided that the bed load is ***coarse***. The case of Isohama Harbour mentioned before is really a remarkable example belonging to such a case.

(2) On the other hand, in case the bed load is very fine, especially when the sea or bay is shallow off the shore, mostly in the case of inland seas, when the prevailing winds blow from the coast out to the offing, the region of the sea or bay is deepened along the direction of wind, while if the prevailing winds blow from the offing toward the coast, the region of the sea or bay near the coast becomes shallower and shallower along the direction of wind. As for the actual examples which seem to justify this conclusion, we may mention the fact which has been pointed out by Dr. T. Okada[11], viz. the fact that on the eastern side of Tokyo Bay, Osaka Bay, Ise Bay, etc. it is decidedly shallower than on the opposite (western) side, where prevailing winds are westerly (or northwesterly).

§ 3. A mathematical expression which represents the effect of prevailing winds. For simplicity's sake, we shall consider a bay whose depth is so small that the effect of the deflecting force of the earth's rotation is negligible. Further, consider the case where the bed load is ***coarse***. (Analogous treatment can be made also for the case where the bed load is very fine.)

Now, let s be the length along the coast line, measured from a certain fixed point such as, for example, one of the end points of the mouth of the bay, to any point P on the coast. The sense in which s is measured may be either such that the land is always seen on the left-hand side or always on the right-hand side. Let PW be the direction in which the prevailing winds blow, and θ_0 be the angle which PW makes with the direction of the North, measured counterclockwise. Again, let PL be the normal drawn to the coast line, directed from land to sea, and θ be the angle which this normal makes with the direction of the North, measured counterclockwise, too.

Now, according to the results of the foregoing discussions, in the case where the prevailing winds blow from land to sea at right angles to the coast line, viz.

when $\theta-\theta_0=0$, the region near the coast is to become shallower and shallower along the normal PL, while on the contrary, in the case where the prevailing winds blow from sea to land at right angles to the coast line, viz. when $\theta-\theta_0=\pi$, the region near the coast is to become deeper and deeper along the normal PL. Therefore, we may take $\Phi(s)=F(r)\cos(\theta-\theta_0)$ as a mathematical expression which roughly represents the effect of prevailing winds, where r denotes the "fetch" for the point P, viz. the distance measured along the normal PL from the point P to the opposite coast. $F(r)$ is an increasing function of r such as, for example, $Ar/(B+r)$, and we may assume that $F(r)\propto r$ for the values of r less than several kilonometers, say, and $F(r)=const.$ for the values of r exceeding several dozen kilometers, say. The reason why the function contains the increasing function $F(r)$ will be obvious if we consider that the circulation of bay water in the vertical plane containing the normal PL produced by winds will be more intense as r becomes larger.

Now, let P_1 and P_2 be the two points on the normal PL such that $PP_1=\delta_0$, $P_1P_2=\delta$, and let D be the mean depth along P_1P_2, then if δ_0 and δ be kept constant, $D(s)$ is a function of s. Next, let $\bar{D}$ be the mean value of D with respect to s, that is, the mean depth of the belt-shaped region of constant breadth bounded by two curves parallel to the coast line, and further let $\bar{D}-D=\Delta$, then Δ is naturally a function of s. If the effect of prevailing winds predominates, while the other effects are slight, then D will be small when Φ is large and *vice versa*. But, since $D(s)+\Delta(s)=\bar{D}=const.$, it appears that Δ is large when Φ is large, and small when Φ is small. Thus, the above arguments can be summarized as follows; viz. both Δ and Φ are functions of the curvilinear co-ordinate s, and their phases of change are expected to coincide with each other to some extent. Hence, in order to see if there exists any correlation between the depth distribution of a bay and the effect of prevailing winds, we have only to draw the two curves, $\Delta(s)$ and $\Phi(s)$, and see if there exists any parallelism between them.

§4. Application to some actual cases. The above method of treatment was applied to some actual cases. In the following, I shall give the results obtained for two cases, both belonging to the case where the bed load is coarse.

(A) Suttsu Bay. Suttsu Bay is a small bay situated on the western coast of Hokkaido. According to the sea chart published by the Hydrographic Office of Japan, the greater part of the bay consists of sand, gravel and shells. The chief reasons why this bay was chosen for our investigation are as follows : (i) As it is situated on the coast of Japan Sea where the tidal range is very small (spring range : 1/2 ft, neap range : 1/4 ft), it is conjectured that the effect of tidal or oceanic currents is not large. (ii) The shape of the bay is simple and also its size is small, the length of the mouth-line being about 9km (large bays are rather unsuitable for the present investigation, for in large bays there frequently exist tidal currents particular to each of them, and the effect of prevailing winds in

question is apt to be obliterated). (iii) No large river does not flow into it. (iv) Wind is high at large and also the direction of prevailing winds is sharply defined.

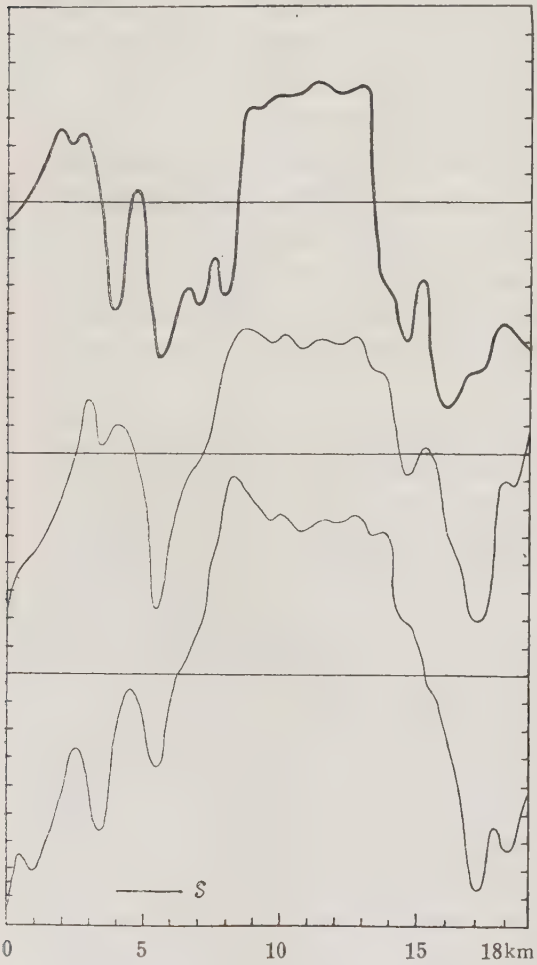

Fig. 2 The effect of prevailing winds as appeared in the depth distribution of Suttsu Bay. Three horizontal lines in the middle correspond to the mean height of each of the three curves, respectively. The scale on the ordinate axis is such that one division is 1m for $\Delta(s)$ curve ; the scale is arbitrary for $\Phi(s)$ curve.

Fig. 2 shows the result of application of the above method of treatment, wher δ_0 is taken as zero in the present example. In this figure, the uppermost curve shows the $\Phi(s)$ curve, and the middle and the lowest ones show the $\Delta(s)$ curve for $\delta=500$m and $\delta=1000$ m, respectively. Glancing at the figure it is obvious that there does exist a parallelism as a whole between the curves $\Phi(s)$ and $\Delta(s)$. It must be especially remarked that the parallelism reveals itself even as regards the minute fluctuations in the two curves in some measure. This cannot be a mere accidental coincidence, but it seems more plausible to consider that the depth distribution of this bay is really influenced by the effect of prevailing winds in such a way as explained in the preceding section. In the present example, the prevailing wind blows from the coast out to the offing, and it is seen from Fig. 2 that the bay has become shallow as a whole along the direction of the prevailing wind.

The depths of bays are naturally affected to some extent by general features of topography of bays and their neighbourhood. For example, if there is a precipitous cliff along some part of the coast of a bay, the bay is usually deep in the region adjacent to the cliff, and on the contrary, if there is a plain of gentle slope along some part of the coast, it is usually shallow in the region adjacent to the plain, and this is really the case to some extent in the present case. This does not, however, lead to a conclusion that the parallelism appearing in Fig. 2 is by no means due to the effect of prevailing winds, but is merely due to the effect of topography. If the depth of the bay in question had

not been influenced by the effect of prevailing winds, such a close parallelism as shown in Fig. 2 would not exist between the two curves $\Phi(s)$ and $\Delta(s)$ which are physically independent *a priori*. Besides, as T. Terada has pointed out, the fact that the region of a bay which is adjacent to a precipitous cliff is usually deep and the region adjacent to a plain is usually shallow, is not necessarily contradictory to our theory, but viewed in some aspect, it seems rather favourable for us. That is to say, consider, for example, a deep bay surrounded by cliffs and precipices. If sand and mud were strongly transported into the bay from outside, even if the bay were deep at the very outset, it would become shallow, being filled up by sand and mud after many years. In order that the bay remains deep for ever, it is necessary that some special reason exists. The effect of prevailing winds under consideration will be regarded as this reason. That is, on account of such a feature of topography, when the wind blows from the offing towards the coat, the action of bringing out sand and mud produced thereby is rather promoted, while the action of carrying sand and mud from outside by the effect of wind blowing from the coast out to the offing will be weakened compared with the case

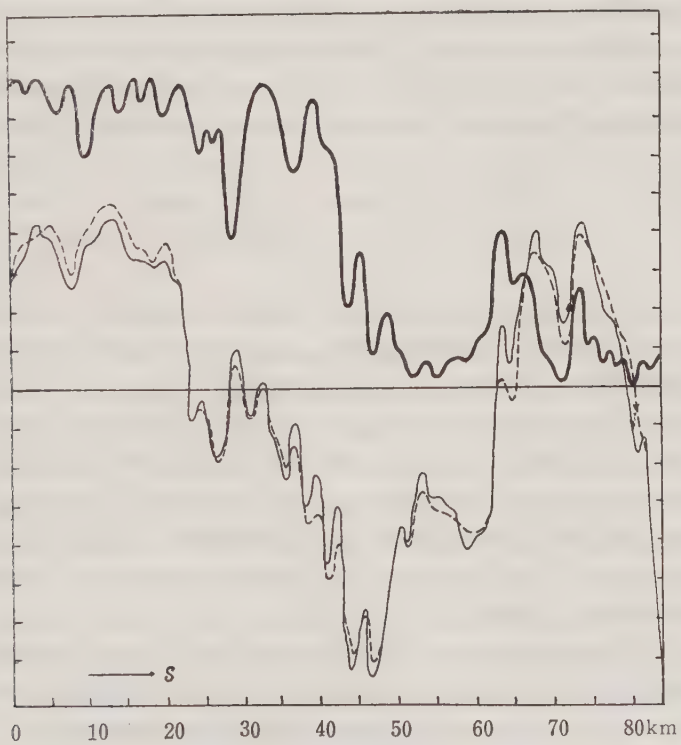

Fig. 3. The effect of prevailing winds as appeared in the depth distribution of Beppu Bay. A horizontal line in the middle corresponds to the mean height of each of the $\Delta(s)$ curves. The scale on the ordinate axis is such that one division is 5m for $\Delta(s)$ curve ; the scale is arbitrary for $\Phi(s)$ curve.

in which the bay is surrounded by plains. Thus, by recognizing the very existence of the said action of wind we are really convinced of the reason why bays surrounded by cliffs and precipices usually remain deep for ever.

(B) Beppu Bay. This bay is situated on the northeastern coast of Kyushu, and it is fairly larger than the preceding example, the length of the mouth-line being about 20 km. According to the sea chart published by the Hydrographic Office of Japan, the greater part of the bay consists of sand, mud and shells. Moreover, in the present case a small inlet named Kitsuki-wan is situated in one part of the bay, and the coast line is sharply bent there. Hence, the contour-line of 3 fathoms (5.4m), instead of the coast line itself, was adopted for the axis of s, the small unevenness in it being smoothed. Fig. 3 shows the result of application of the above method of treatment, where δ_0 is taken as zero as in the prceding example. Moreover, in the present case, since the size of the bay or the value of r is fairly large, the function $F(r)$ was taken as constant from the reason stated before.

In Fig. 3, the curve shown in thick full line (——) shows the $\Phi(s)$ curve, and those in thin full line (——) and broken line (- - - -) show the $\Delta(s)$ curves for $\delta=1500$m and $\delta=2500$m, respectively. Glancing at the figure, we can see that there exists a parallelism as a whole between the curves $\Phi(s)$ and $\Delta(s)$, except a part near the right end of the figure, viz. the part $s=60\sim80$ km, showing that the depth distribution of this bay has really been influenced by the effect of prevailing winds in such a manner as we consider. The anomaly in $\Delta(s)$ curve for the part $s=60\sim80$ km seems to have been caused by the transport of sand and mud by a somewhat large river named Ono-gawa whose mouth is situated in the vicinity of $s=60$ km.

Further, looking at the figure we can see that the phase of undulation of $\Delta(s)$ curve is somewhat different from that of $\Phi(s)$, viz. if we consider that the depressions in $\Phi(s)$ curve at the points $s=10.0$ km; 28.5km; 37.5km; 44.0 km and 47.0 km correspond to those in $\Delta(s)$ curve at $s=8.0$ km; 27.0 km; 36.0 km; 41.0 km and 44.5 km, and that the elevations in $\Phi(s)$ curve at $s=39.0$ km; 45.0 km and 48.5 km correspond to those in $\Delta(s)$ curve at $s=37.0$ km; 42.5 km and 46.0 km, then we may say that $\Delta(s)$ curve is displaced towards the left end of s by 2.2km on an average against $\Phi(s)$ curve. This displacement in s corresponds to $15°\sim20°$ or thereabouts in angle.

It is somewhat interesting to note that the phase difference between each of these corresponding pairs of depressions or elevations is not only always of the ***same sign***, but also it is always of the ***same order of magnitude***.

As for the physical meaning of the phase difference mentioned above, a possible explanation will be given as follows: As stated before (§2), in the case of an enclosed sea of uniform depth d (in the Northern Hemisphere), the angle between the direction in which the wind blows and that of the bottom current, measured clockwise starting from the former to the latter, is given by α in Table 1. In

other words, the direction of the bottom current is not coincident with that of the vertical plane containing the wind, but is deflected from the latter by α_1 (in Table 1) in clockwise direction. But, the direction of the bottom current is none other than that in which the sand particles on the bottom of the sea are displaced. Thus, we may say that, owing to the earth's rotation, the sand particles on the bottom of the sea are to be displaced in the direction deflected by angle α_1 from the vertical plane containing the wind in the ***clockwise*** direction. The deflecting angle of the bottom current last-mentioned is insensibly small in case the depth of the sea, d, is decidedly less than $0.5D'$, as in the case of Suttsu Bay,* but it becomes larger and larger as d increases. For example, in case $d=D'$, this deflecting angle is nearly 44° (See Table 1). Applying the above theory to the present case, it follows that the phase of undulation of the curve representing the actual depth distribution produced by the action of prevailing winds under the influence of the earth's rotation is to be displaced in the ***clockwise*** direction in comparison with the case in which the effect of the earth's rotation is not utterly taken into consideration. In other words, the phase of the undulation of $\Delta(s)$ curve is to be displaced ***towards*** the origin of s against that of $\Phi(s)$ curve. (In the present case, s was measured along the 3-fathom contour-line starting from a point near the north end of the mouth of the bay in ***counterclockwise*** direction)

Now, the mathematical expression for the "depth of frictional influence", D', is as follows :

$$D' = \pi \sqrt{\frac{\mu}{\rho\omega\sin\varphi}},$$

where μ is the coefficient of eddy viscosity, ρ the density of sea water, ω the angular velocity of the earth's rotation, and φ the latitude of the place under consideration. If we take $\mu=100$, $\rho=1.025$, then D' is 52m and 46m for $\varphi=30°$ and 40°, respectively. Further, the mean values of D taken along the axis of s, for the cases of $\delta=1500$m and $\delta=2500$m, are about 22m and 24m, respectively. These values may be regarded approximately as the mean depths of the belt-shaped region bounded by the 3-fathom contour-line and the parallels 1.5 km and 2.5 km respectively distant from it. If we regard the mean values of D mentioned above as the value of d, then we see that the deflecting angle α_1 of the bottom current from the vertical plane containing the prevailing wind is approximately 15°, which agrees in the order of magnitude with the above-obtained actual result. Thus, the said phase difference between the curves $\Phi(s)$ and $\Delta(s)$ can be explained not only in its ***sense***, but also in its ***magnitude***.

§5. Concluding remarks. In the present paper some discussions were made

---

* In the case of Suttsu Bay, the mean depth of the belt-shaped region bounded by the coast line and the curve parallel to it and distant therefrom by δ is about 10m and 15m corresponding to $\delta=500$m and $\delta=1000$m, respectively.

on a problem concerning the vertical circulation of sea water produced by winds, especially on the change of depth in shallow seas and bays which is produced by the circulation. It was found that the grain size of the bed load plays an important rôle in this subject. The conclusions obtained are summarized as follows :

(1) In case the prevailing winds blow from the offing toward the coast, the region of a sea or bay near the coast is deepened along the direction of wind, while on the contrary, when the prevailing winds blow from the coast out to the offing, the region near the coast becomes shallower and shallower along the direction of wind, provided that the bed load is ***coarse***. The result of investigations for some actual cases, viz. the fact that the depth distribution of Suttsu Bay, etc. is in accord with that which is expected from the theory, seems to justify the above conclusion.

(2) On the other hand, in case the bed load is ***very fine***, especially when the sea or bay is shallow off the shore, mostly in the case of inland seas, when the prevailing winds blow from the coast out to the offing, the region of the sea or bay near the coast is deepened along the direction of wind, while, if the prevailing winds blow from the offing toward the coast, the region of the sea or bay near the coast becomes shallower and shallower along the direction of wind. As for the actual examples which seem to justify this conclusion, we may mention the fact which has been pointed out by T. Okada, viz. the fact that on the eastern side of Tokyo Bay, Osaka Bay, Ise Bay, or other bays, it is decidedly shallower than on the opposite (western) side, where prevailing winds are directed from west (or northwest) to east (or southeast) approximately.

The change of depth of sea sand bays due to the effect of prevailing winds bears upon harbour engineering, shallow sea product industry, etc. It sometimes controls the growth of ports, as exemplified by the cases of Isohama Harbour, Nobiru Harbour, etc. Again, as has been pointed out by T. Okada, on the Pacific coast of our Mainland (Honshu), there is a tendency such that good harbours do not grow on the eastern coast of a bay at large, and one of its causes is frequently the decrease of depth of water due to the said effect of prevailing winds, though the leading one of the causes is the difficulty in loading and unloading ships. It will be superfluous to say that the culture of shellfish, lavers, etc. is affected by the change of depth of water.

In conclusion, the present author wishes to express his sincerest thanks to the Special Committee on Marine Resources, Japanese National Commission for UNESCO for financial aids.

References

(1) M. Nakano : An investigation on the effect of prevailing winds upon the depth of bays(I-VII). *Geophys. Mag.*, Vol. 9, Nos. 1~2 (1935) ; Vol. 10, No. 1 & Nos. 3~4(1936);

Vol. 14, Nos. 2~4 (1947)

(2) T. Terada : On the movement of sand and clay on sea bed (in Japanese). *Toyo-Gakugeizasshi*, Vol. 38, No. 475 (1921)

(3) I. Hiroi : ***Construction of Harbours*** (in Iapanese), Vol. 1, p. 39, Tokyo (1924)

(4) I. Hiroi : ditto.

(5) V. W. Ekman : On the influence of the earth's rotation on ocean-currents. ***Arkiv för Mathem., Astr. och Fysik***, Vol. 2, No. 11 (1905)

(6) K. Hidaka : An investigation on wind-driven ocean circulation (I-III)(in Japanese). *Umi-to-Sora*, Vol. 17, No. 10 (1937) ; Vol. 18, Nos. 1 & 9 (1938)

(7) T. Nomitsu and T. Takegami : Coast effect upon the ocean current and the sea level. ***Memoirs of the College of Science, Kyoto Imp. Univ.***, Ser. A, Vol. 17, No. 3 (1934)

(8) T. Takegami : The boundary value problem of the wind current in a lake or a sea. ***Memoirs of the College of Science, Kyoto Imp. Univ.***, Ser. A, Vol. 17, No. 5 (1934)

(9) M. Nakano : Some experiments on the effect of prevailing winds upon the depth of bays. ***Journ. Oceanogr. Soc. Japan***, Vol. 3, No. 2 (1943)

(10) As for the details of these experiments, see the paper (9).

(11) T. Okada : On the relation between the situation of ports and the direction of prevailing winds (in Japanese). ***Journ. Meteorol. Soc. Japan***, Vol. 41, No. 10(1922)

Records of Oceanographic Works
in Japan, Vol. 2, No. 2,
October 1955

On the Possible Origin of the Intermediate Water in the Kuroshio

(Central Meteorological Observatory)

By

Takashi Ichiye

§ 1. Introduction. It has been generally observed that the water with low chlorinity exists widely at the depth of about 300~1000 m under the haline water within the Kuroshio and forms the minimum chlorinity layer, which is called the intermediate water.(1) Some authors considered that it was originated from the Oyashio water which sank under the Kuroshio Current at the so-called polar front and was transported by the counter current below the eastward Kuroshio Current(2). However, we cannot find such counter current at the depth of intermediate water at least within the region of the Kuroshio, and thus the customary conception that the intermediate water is transported directly from the Oyashio region should be revised. On the other hand, when such water is transported by the current, which is slight in its velocity but flows to the same direction as the upper strong Kuroshio Current, then the vertical diffusion should mix it with upper and lower waters with higher chlorinity, since there is no supply of the water with low chlorinity, or there is no source region of such water in the southern sea, whereas in the practical case the intermediate water is traced everywhere within the Kuroshio region. Therefore, some mechanism of supply is necessary to maintain such water. In the present paper, the relation between the depth of intermediate water and the current velocity there is determined from the observed data and some theoretical considerations for the origin are proposed.

§ 2. The current velocity at the layer of the intermediate water.

First, we define the intermediate water as the water with chlorinity less than 19.0 ‰ and from the observations along the G-line (south off Shionomisaki, along the meridian of about E 135°50′) the mean depths of the upper and lower boundary of this water (h_1, h_2) are determined for each station, where the data used are of about 36 sections from Aug. 1951 to Nov. 1953(3). Further, the mean values of surface velocity (v_1) and mean velocity within the layer of the intermediate water above defined (v_2) are computed by the dynamic calculation taking 1000 m as the reference level. These mean values are tabulated in Table 1, with the confidence limits of 95% reliability for each case. The values of $\bar{v}_2$ indicate clearly that there is no counter current within the layer under consideration and generally the current in the layer of the intermediate water flows to the same

Table 1

St.	G_1	G_2	G_3	G_4	G_5	G_6	G_7	G_8
lat. (*N*)	33°10′	32°55′	32°40′	32°20′	32°00′	31°30′	31°00′	32°20′
$\bar{h}_1(m)$	383	443	512	574	629	680	680	670
$\delta h_1(m)$	31	30	37	40	37	31	30	32
$\bar{h}_2(m)$	725	769	841	901	980	1051	1097	1004
$\delta h_2(m)$	33	35	34	36	49	40	43	46
$\bar{v}_1$(cm/sec)	92.3	58.4	64.2	55.3	17.2	2.4	−11.3	
δv_1(cm/sec)	20.4	15.4	12.6	13.7	8.1	11.6	6.7	
$\bar{v}_2$(cm/sec)	16.9	15.5	14.7	9.5	4.5	1.5	− 1.9	
δv_2(cm/sec)	5.2	4.9	2.8	3.4	2.0	1.6	1.3	

$\bar{h}_1$, $\bar{h}_2$ Mean depth of upper and lower limit for chlorinity of 19.0‰
$\bar{v}_1$, Mean surface velocity computed by dynamic calculation with level depth of 1000m.
$\bar{v}_2$, Mean velocity within the layer of chlorinity less than 19.0‰.
$\bar{h}\pm\delta h, \bar{v}\pm\delta v$, Confidence limits with 95% confidence coefficient.
Positive values in $\bar{v}_1$, $\bar{v}_2$ mean the eastward current.

direction as the upper current, even when we take account of the confidence limits. In fact, the counter current exists at the intermediate layer with the relatively strong eastward surface current only in two cases, *t. i.* Jun. 16, 1953, Sec. $G_4\sim G_5$, $v_1=24$, $v_2=-1.1$ and Jul. 3, 1953, Sec. $G_5\sim G_6$, $v_1=82$, $v_2=-1.2$ (cm/sec). Further, the values $\bar{h}_1$ and $\bar{h}_2$ increase towards off-shore and reach maximum at G_7, which corresponds to the boundary of the mean eastward current, and such condition suggests that the isohaline curves correspond closely to isotherms and iso-oxygen curves, even at the layer of the intermediate water. The fact that v_1 and v_2 have the same sign on the average is more clearly demonstrated by classifying the values of v_1 in several ranges and taking the averages of v_1 and v_2 belonging to the same group, the results of which are shown in Table 2, with similar symbols as in Table 1. They indicate more definitely the above conclusion as to the denial of the existence of the counter current.

Table 2

Range of v_1	>100	50∼100	25∼50	0∼25	−25∼0	−50∼−25
$\bar{v}_1$	128.2	69.6	36.8	12.5	−11.0	−31.4
δv_1	10.2	3.9	2.7	2.4	2.4	4.0
$\bar{v}_2$	26.3	13.6	10.1	4.2	−0.4	−4.8
δv_2	4.9	2.4	2.9	2.0	1.8	2.3

$\bar{v}_1$, $\bar{v}_2$, Mean values of v_1 and v_2 for several ranges of v_1. (cm/sec)
$\bar{v}\pm\delta v$, Confidence limits with 95% confidence coefficient.

§ 3. The horizontal distribution of the intermediate water.

In order to obtain the general view of the water, we discuss the results of synoptic observation in Aug. 1954 carried out by C.M.O. and its subordinate marine observatories.[4] In fig. 1, the surface dynamic topography referred to 1000-decibar level is shown, the details of which will be discussed in another places, but here the characteristic features are shortly stated. First, the Kuroshio Current flows eastward, making détour around the cold water region at about 137°∼139°E,

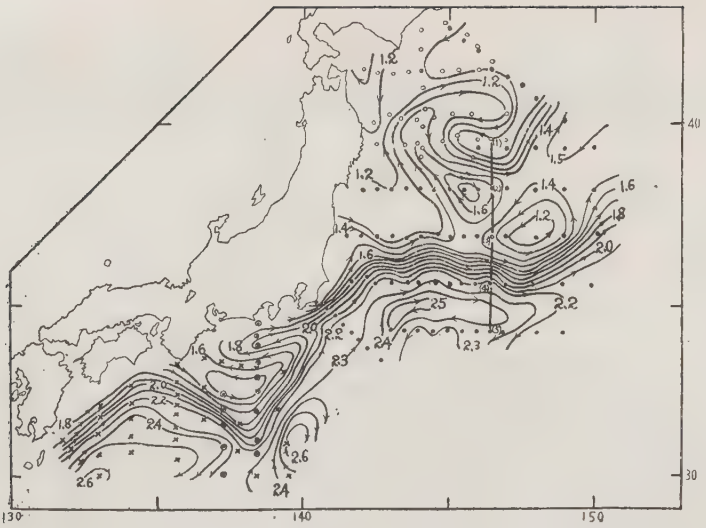

Fig. 1. Surface dynamic Topography referred to 1000-decibar level in Aug., 1954.
∘—∘ Yushio Maru, Hakodate M. O.
·—· Ryofu Maru, C. M. O.
×—× Sympu Maru, Kobe M. O.
◉—◉ Ozika and Tsugaru, C. M. O.

and then leaves the coast at 142°E, with one branch flowing further north, which forms the anti-cyclonic vortex, contacting with the southward flowing Oyashio. On the northern edge of the Kuroshio Main Current, the cyclonic vortex due to the inflow of the Oyashio is seen, forming somewhat complicated current pattern, together with the cyclonic vortex above stated. All along the off-shore bounbary region of the Kuroshio, the isolated anti-cyclonic vortices exist at three

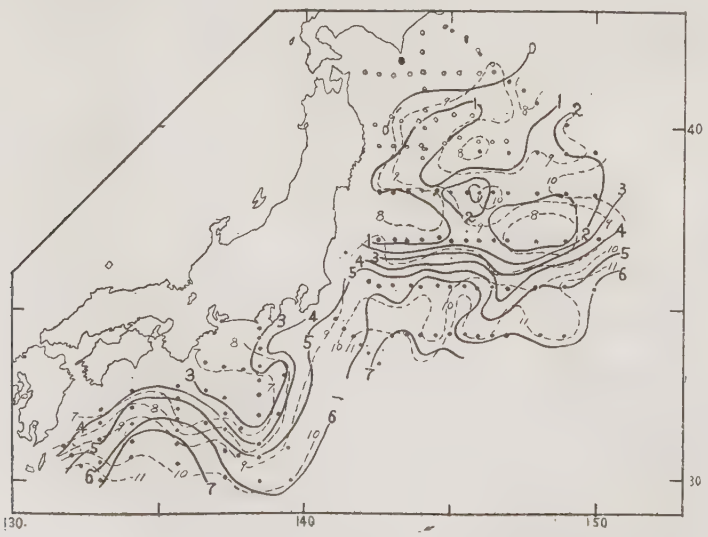

Fig. 2. Distributions of h_1 (full line, the depth of the upper layer of chlorinity 19.0‰) and h_2 (broken line, the depth of lower layer.) (Figures mean the depth in 100m.)

places, which induces the counter current, though this does not form the continuous movement from north, at least within the area occupied by the present observation. Next, we plot the distributions of h_1 (full lines) and h_2 (broken lines) in fig. 2, corresponbing to such current pattern. Generally speaking, isobaths of h_1 and h_2 are closely correlated with the stream lines in fig. 1, making the similar détour in the southern section and forming the deeper and more shallow region corresponding to the anti-cyclonic and cyclonic vortex, respectively, in the northern section. Especially, the horizontal gradient of h_1 is conspicuous on the northern bounbary of the Kuroshio Main Current east of 140°E, and thus the depths of upper boundary of the intermediate water are less than 200m in the area north to 37°N, where zero for h_1 means that the upper boundary vanishes. The general tendency that these isobaths are similar to the surface topography suggests that the intermediate water is transported by the current with almost same direction as the surface current.

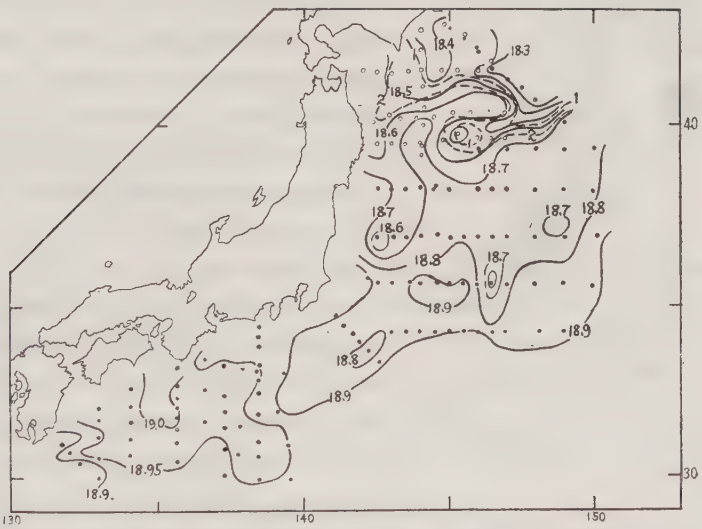

Fig. 3. The distribution of the minimum chlorinity (‰) at each station. (The broken lines are the isobaths of the minimum chlorinity layer in the area with no upper boundary of 19.0‰)

In fig. 3, the distribution of the minimum chlorinity at each station is shown, with the depths of its occurrence (broken lines) in the northern section, where the upper boundary of the intermediate water vanishes. This figure indicates somewhat different pattern to the above charts, and the values are higher in the southern sea between 132° and 139°E with chlorinity more than 18.95‰. Further, the thickness of the intermediate water also decreases in this region, indicating that the supply of this water is poor, and that the vertical mixing diffuses the minimum chlorinity, which is also confirmed by the existence of relatively lower values west of 132°E. Along the Kuroshio Main Current east of 142°E, the decreasement of the minimum values is not so conspicuous as those of h_1, h_2 and

only the isolated low value regions are found at some places near the northern edge. On the other hand, the horizontal gradient is marked further north of about 40°–41° N, where the Oyashio Current contacts with the branch of the Kuroshio. Therefore, we can consider that the supply of the intermediate water occurs in this region by the effect of lateral mixing, because no advective current so as to transport it southward is seen and the lateral mixing is most efficient in the region with the strong horizontal gradient. The isolated low value areas also contribute to such supply, and they seem to be discharged spontaneously from the source region further north. In other words, large scale lateral mixing occurs all along the frontal region of the Oyashio, which produces the intermediate water extensively all over the Western North Pacific[5], and thus the water is not transported southward by the advection, which is also ascertained by the fact that the counter current at the southern edge of the Kuroshio shown in fig. 1 does not correspond to the lower minimum zone in fig. 3. The frequent appearance of the isolated low chlorinity water has been reported in other papers, both in the Kuroshio[6] and the Gulf Stream[7], and thus here only the vertical section of chlorinity and velocity is shown in fig. 4, the location of which is indicated in fig. 1. In this case, the low chlorinity water is found even below the Kuroshio Main Current, and formerly some authors considered that it was transported by the southward flowing current, but in realty it is discharged spontaneously as stated above since there is no such steady southward current, though the detailed mechanism of discharge is still unknown.

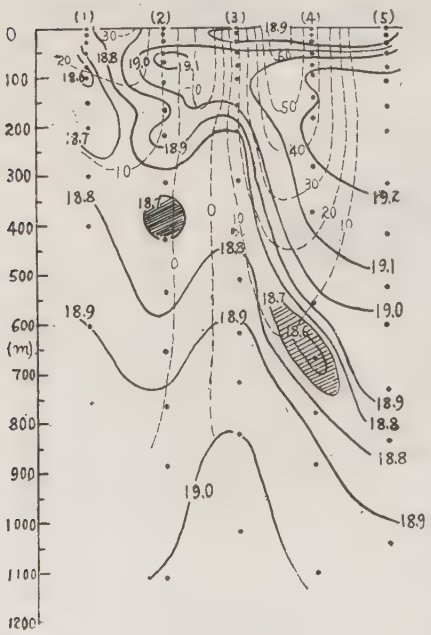

Fig. 4. Vertical section for illustrating the isolated low chlorinity water (shaded portion). The location of the section is shown in fig. 1 and the full lines indicate chlorinity, the broken line the velocity in cm/sec. (positive values mean the eastward current).

§ 4. The effect of lateral mixing

The intermediate water in the southern section of the Kuroshio is also influenced by the lateral mixing, since it should lose its characteristics by the vertical mixing with the upper and lower waters of more haline property, if there is no supply from the outer region, as stated in § 1. In fact, the minimum chlorinity increases in the southern area as shown in fig. 3, and thus the estimation for the interaction between the vertical and lateral mixing is necessary. Anyhow, the necessary supply for the maintenance of the intermediate water is expected from the right side boundary in the southern section of the Kuroshio, which forms the extensive source region of such water produced by

the lateral mixing further north. This conception is also consistent with the theory of C-G. Rossby[8], who stated that the water is absorbed from the oceanic areas to the right of the current and discharged into the counter current to the left, though the counter current to the coastal side is not so obvious in the Kuroshio, especially south of 35° N, as in the Gulf Stream.

Here, only the formal treatment is given[9], starting from the diffusion equation such as

$$u\frac{\partial S}{\partial x}=A\frac{\partial^2 S}{\partial y^2}+K\frac{\partial^2 S}{\partial z^2} \tag{1}$$

As for the boundary conditions, we should take into account of the actual state that the eastward current at the intermediate depth is found only within the Kuroshio region, to the right of which the counter current at the deep layer is almost negligible, and there is a coast to the left in the southern sea, which prevent the lateral mixing. Further, in the present case the intermediate water is defined as having chlorinity less than 19,0‰, and thus we should consider that the upper and the lower boundary of this water is kept at the constant chlorinity of 19,0‰. Therefore, the boundary conditions become

at $x=0$, (initial point), $S=S_0-p(y,z)$,
at $z=0, h$ (h=thickness of the intermediate water, 0=the lower boundary) $S=S_0$ ($=19.0$‰),
at $y=0$ (coastal side), $\partial S/\partial y=0$;
at $y=a$ (off shore boundary), $S=S_0-q(y,z)$

In practise, u, h are not constant and the levels of the intermediate water are also not horizontal, but the lateral mixing should occur on the isentropic surface, and thus we may assume that the depth z is taken as referred to this surface. Then the solution of (1) under above boundary conditions is given by

$$S_0-S=\frac{2}{a}\sum_{m=1}^{\infty}\sum_{n=0}^{\infty}e^{-(\nu_m+\text{æ}\beta_n^2)x}\cos\beta_n y\Big\{(-1)^n\text{æ}\beta_n\int_0^y e^{(\nu+\text{æ}\beta_n^2)\lambda}q_m(\lambda)\,d\lambda$$
$$+\int_0^a p_m(\lambda)\cos\beta_n\lambda\,d\lambda\Big\}\sin\frac{m\pi z}{h} \tag{2}$$

where

$$\text{æ}=A/u,\quad \nu_m=K(m\pi/h)^2/u,\quad \beta_n=(2n+1)\pi/2a,$$
$$p_m(y)=\frac{2}{h}\int_0^h p(y,z)\sin\frac{m\pi z}{h}dz,\qquad q_m(y)=\frac{2}{h}\int_0^h q(y,z)\sin\frac{m\pi z}{h}dz$$

When $p_m(y)$, $q_m(y)$ are independent with y,

$$S_0-S=\sum_{m=1}^{\infty}q_m\frac{\cosh\alpha_m y}{\cosh\alpha_m a}\sin\frac{m\pi z}{h}+\frac{2}{a}\sum_{m=1}^{\infty}\sum_{n=0}^{\infty}e^{-(\nu_m+\text{æ}\beta_n^2)x}\cos\beta_n y\Big\{(-1)^n p_m/\beta_n$$
$$+(-1)^{n+1}\text{æ}\beta_n q_m/(\text{æ}\beta_n^2+\nu_m)\Big\}\sin\frac{m\pi}{h}z \tag{2'}$$

where $\alpha_m^2=K(m\pi/h)^2/A$

For numerical computation, we obtain the physical constants by taking the average of observed values in Table 1 from G_1 to G_7, such as

$u=8.9$ (cm/sec), $h=344$(m), $a=240$(km)

From these values we have A and K by the 4/3 power law of the eddy viscosity[10] as $A=5.96\times10^7$, $K=1.12\times10^2$ (cm²/sec). With these constants, we compute the equation(2′) for the case that $p_1=q_1=p$, $p_i=q_i=0$ $(i\neq1)$ and the change of $(S_0-S)/p$ with x at the central point $(z=h/2,\ y=a/2)$ is shown in fig. 5 (A), (curve II), where that of the case of no lateral mixing is also indicated (curve I), for comparison. When the lateral mixing works, the decreasement of S_0-S (or increase of chlorinity) is more rapid than the curve I near the initial point, but it increases again to the limiting value. Further, the lateral distributions of $(S-S_0)/p$ for $z=h/2$ are shown in fig. 5 (B) at several distances from the source, which also indicates the values of S_0-S at the midway becomes less then the limiting values. Such condition seems to correspond to the increase of the minimum chlorinity in the southern section of the Kuroshio as indicated in fig . 3. In the present model, the mixing coefficients seems to be somewhat larger than those corresponding to the actual state, since the values of $(S_0-S)/p$ in the region between 132°E and 136°E computed by the same data as in fig. 3 are also plotted in fig. 5 (A), which show the similar tendency as Curve II, but their change with x is more gradual. Anyhow, the qualitative agreement proves the model to be not so unreasonable.

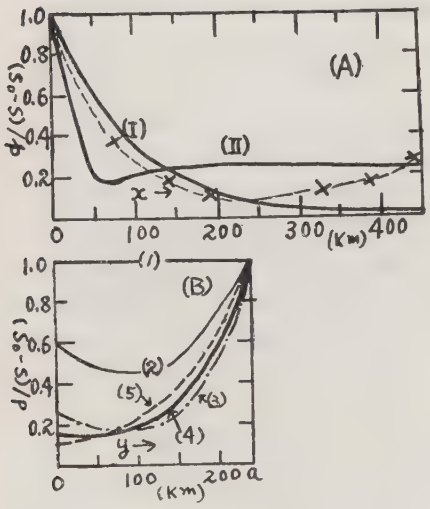

Fig. 5. (A)
(I) The curve for no lateral mixing.
(II) The curve for the eq. (2′)
×···× The values determined from the data in fig. 3.
Fig. 5. (B)
(1) for $x=0$, (2) for $x=25$(km)
(3) for $x=50$(km), (4) for $x=100$(km)
(5) for $x=\infty$

§ 5. Conclusion. It is demonstrated statistically from the observeddata that no counter current flows at the depths of the intermediate water, and the production of this water is made on the boundary of the Oyashio further north to the edge of the Kuroshio. The transport of this water to the south is proved to be due to the lateral mixing, not to the direct advection from the source region, whereas the mixing is made sometimes as a discharge of the isolated low chlorinity water. Further, for the maintenance of this water in the southern section of the Kuroshio, also the lateral mixing has an important rôle, though it occurs at the oceanic side of the current there.

In the last, the author expresses his hearty thanks to Mr. Y, Fujii and Mr. J. Masuzawa for their useful advices and also to Dr. M. Nakano for his kind encouragements.

Literatures

(1) K. Koenuma, On the hydrography of the south-western part of the North Pacific. Part. I, Mem. of Imp. Mar. Obs. Vol. VI, No. 3, 1936.

(2) M. Uda, The result of simultaneous oceanographical investigations in the North Pacific in 1933. Journ. Imp. Fish. Exp. Station. No. 6, 1935.

(3) The auther is indebted to Mr. T. Yasui for use of the unpublished data.

(4) Results of Oceanographic Observations. No. 14. C. M. O. (to be published)

(5) K. Koenuma, ibid. Part III.

(6) J. Masuzawa, On the hydrography of the Kuroshio System (VI) (To be published in Oceano. Mag. Vol. 7. No. 1)

(7) W. F. Ford, J. R. Longard and R. E. Banks, On the nature, occurrence and origin of cold low salinity water along the edge of the Gulf Stream. Journ. Mar. Res. Vol. XI, No. 3, 1952.

(8) C-G. Rossby, Dynamics of the steady ocean currents in the light of experimental fluid mechanics. Pap. in phys. Oceano. and Met. Vol. V. No. 1, 1936.

(9) T. IChiye, On the distributions of oxygen and their seasonal variations in the adjacent sea of Japan (I). Oceano. Mag. C. M. O., Vol. 6, No. 2, 1954.

(10) E. Inoue, On the turbulent diffusion phenomena in the ocean. Journ. Oceano. Soc. Japan. Vol. 7, No. 1, 1951.

Records of Oceanographic Works
in Japan, Vol. 2, No. 2,
October 1955

On the rapid determination of the dynamic depth anomaly in the Kuroshio Area

By

Masashi Yasui

(Central Meteorological Observatory)

1. *Preface*

The geostrophic current is computed by Bjerknes-Sandstrom's method[1] from the temperature and chlorinity measured by serial oceanographical observations. But this method needs the titlation of the chlorinity, so it takes a pretty long time to obtain the dynamic topography. Several authors developed some methods to obtain the dynamic depth rapidly. K. Yamashita (1941)[2] introduced the mean temperature $\frac{1}{h}\int_0^h t dz$ and advocated a method to use this mean temperature distribution in place of dynamic topography. H. Stommel (1947)[3] published an approximate method to compute the dynamic depth anomaly using the known standard T-S diagram in the particular sea area composed of the same water mass, and discussed the accuracy of the computation.

In Japan, the sectional observation line, the "G-line", south off Shionomisaki, was occupied continuously by the marine research ships of the Central Meteorological Observatory 45 times from July 1951 to November 1953 (Fig. 1), and the number of the stations of serial observation amounts to 310. In these data, we obtained 282 pairs of satisfactory data of the mean temperature and dynamic depth anomaly above 1000 decibars.

Using these data, the author obtains the relation between these two values and gives a method of rapid estimation of dynamic depth anomaly on board.

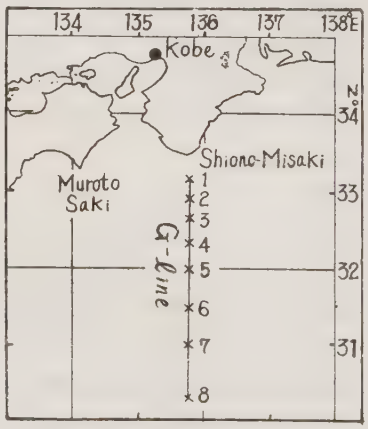

Fig 1. Location of stations along the "G-line".

2. *The relation between the dynamic depth anomaly and vertical distribution of the temperature.*

The anomaly of the dynamic depth can be computed by using the standard tables of Bjerknes and Sandstrom (1910)[1], from the formula $\Delta D=\delta_s+\delta_t+\delta_{s,t}+\delta_{s,p}+\delta_{t,p}$ and summing them up from surface to 1000 meters of depth.

In not so wide range of chlorinity value, σ_t may be represented approximately by the formula: $\sigma_t=a+bT+cT^2+dCl$. Now, in the Kuroshio Area, the ranges

of the temperature and chlorinity are as follows, T ; 3°~30°C, Cl ; 18.80~19.35‰. In such ranges, the above relation for σ_t is given by

$$\sigma_t = 1.2327 - 0.080016T - 0.004509T^2 + 1.39214Cl, \quad \cdots\cdots(1)$$

as determined by the method of least squares from Kalle and Thorade Table[4]. In this formula, if we can obtain the relation between T and Cl, we can compute σ_t by the temperature distribution only.

To investigate the relation between T and Cl in the Kuroshio Area, we plot all data of the 282 stations on a T-Cl diagram (Fig. 2). In this figure, it is

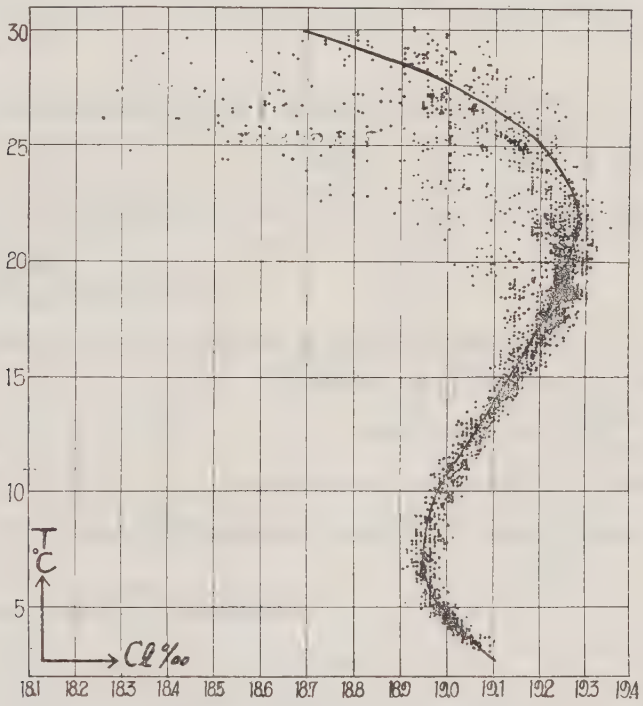

Fig 2. Temperature and chlorinity relationship obtained by all observational data of the "G-line".

immediately apparent that the synthetic T-Cl diagram may be divided into two temperature intervals from scattering of each T-Cl points. In the first interval, below 18°C, the scattering of points is relatively slight, while in the second interval, above 18°C, Cl-values against the same temperature value are broadly scattered about the mean value. On the other hand, this scattering almost reduces, in the cold seasons from autumn to spring and the depth of 18°C-isotherm is about 200m at most even in summer, therefore the contributions from this part to the total dynamic depth anomaly are almost negligible through the year. Thus, we can express Cl by the relation without serious error,

$$Cl = a + bT + cT^2 + dT^3.$$

In order to determine the constants a, b, c and d, the method of least squares may be applicable usually, but for simplicity we make fit the cubic equation for

T-Cl points especially in the first interval such as

$$Cl=19.378-0.1255T+0.0112273T^2-0.000258674T^3, \quad \cdots\cdots(2)$$

by trial and error, and the computed T-Cl curve from this equation is also drawn in Fig. 2, which seems to correspond reasonably to the observed data.

Substituting (2) in (1), we get,

$$\sigma_t=28.2065-0.254799T+0.0111209T^2-0.00036011T^3 \cdots\cdots(3)$$

Now the dynamic depth anomaly $\underset{1000}{\Delta D}$ above the 1000 meter layer is computed from Sverdrup's formula[1] as follows,

$$\underset{1000}{\Delta D}=\int_0^{1000}\Delta_{st}dz+\int_0^{1000}(\delta_{t,p}+\delta_{s,p})dz. \quad \cdots\cdots(4)$$

Since

$$\Delta_{st}=0.02736-\frac{\sigma_t\times10^{-3}}{1+\sigma_t\times10^{-3}}\fallingdotseq0.02736-\sigma_t\times10^{-3}(1-\sigma_t\times10^{-3}+\sigma_t^2\times10^{-6}-\cdots\cdots)$$

we obtain for the first term in the formula (4)

$$\int_0^{1000}\Delta_{st}dz=-0.073-0.000241033\int_0^{1000}Tdz-0.000010461\int_0^{1000}T^2dz$$
$$-0.00000033426\int_0^{1000}T^3dz.$$

And, assuming the 1000-decibar-layer as a reference level, we obtain the mean value of the second term of (4) as follows;

$$\int_0^{1000}(\delta_{t,p}+\delta_{s,p})dz\fallingdotseq0.089.$$

Then the fomula (4) is reduced to the following,

$$\Delta D=0.016-0.000241033\int_0^{1000}Tdz+0.000010461\int_0^{1000}T^2dz$$
$$-0.00000033426\int_0^{1000}T^3dz. \quad \cdots\cdots(5)$$

Table I

The anomaly of the dynamic depth		
Computed by the stand. method	Computed by the formula (5)	Computed by the formula (7)
dyn. m.	dyn. m.	dyn. m.
1.680	1.672	1.683
1.683	1.659	1.666
1.755	1.781	1.814
1.818	1.797	1.802
1.943	1.999	2.172
2.048	2.025	1.953
2.090	2.065	2.101
2.100	2.107	2.179
2.135	2.039	2.220
2.179	2.161	2,234
2.197	2.130	2.257
2.212	2.282	2.282
2.243	2.242	2.216
2.367	2.383	2.356
2.389	2.423	2.345
2.494	2.478	2.439
Standard deviation	0.0484	0.0772

The maximum error due to uncertainty of chlorinity against temperature in this formula is 0.162 and 0.047 when the surface temperature is 30°C and 19°C respectively, according to Stommel's method and table[3].

In Table I, several examples of $\underset{1000}{\Delta D}$ computed by the above formula (5) are shown with those obtained by the standard method for comparison.

3. *Simplification of the formula.*

We can compute the dynamic depth anomaly in any depth by use of (5) with a vertical temperature distribution only, but it takes much trouble for an observer on board to calculate $\int T^2dz$ and $\int T^3dz$, so it is desirable to simplify the formula at least for the surface dynamic depth anomaly.

In practice, as seen in Fig. 3 the terms containing $\int T^2dz$ and $\int T^3dz$ in (5) are so closely related to the term containing $\int Tdz$ that we may assume the following formula for (5),

$$\underset{1000}{\Delta D}=a+b\int_0^{1000}Tdz. \quad \cdots\cdots(6)$$

Determine the constants a and b by the method of least squares from the data of $\underset{1000}{\Delta D}$ and $\int_0^{1000}Tdz$ available, we obtain the following formula

$$\underset{1000}{\Delta D}=(0.2637\pm0.0182)+(0.0001543\pm0.0000015)\int_0^{1000}Tdz. \quad \cdots\cdots(7)$$

$$r=0.045$$

where r is the probable error of $\underset{1000}{\Delta D}$.

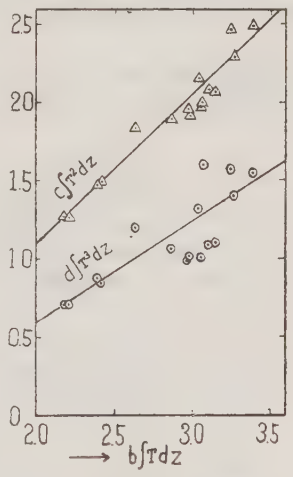

Fig 3. Relation between the term containing $\int T^2dz$ & $\int T^3dz$ of (5) and that of $\int Tdz$

By this formula, we calculate the same examples as those obtained by (5) and insert them also in Table 1, and further we calculate the standard deviation of $\underset{1000}{\Delta D}$ for the same examples to compare the accuracy of (5) and of (7), which indicates that the result given by (7) has the sufficient accuracy for practical use.

4. *The formula applicable to bathythermograph records.*

Recently the development of the bathythermograph is making possible to survey easily a vertical thermal structure of the ocean from a ship underway, but even by the newest type of the bathythermograph we can obtain a record in the upper 600 meter only, and to estimate surface ocean current with bathythermograph records it is convenient to introduce the formula to calculate the dynamic depth anomaly from the mean temperature in the layer from surface to 600 meter depth or less.

For this purpose, we classify all data into nine groups according to the location and season, and decide the constants of (6) by means of least squares in each group, but we can not recognize any seasonal and local differences between them, so we combine the formulae of nine groups into one as follows?

$$\Delta D_{1000} = (-0.0159 \pm 0.0242) + (0.0002237 \pm 0.0000025) \int_0^{600} T dz \; ; r = 0.048, \cdots\cdots (8)$$

$$\Delta D_{1000} = (-0.2022 \pm 0.0261) + (0.0002722 \pm 0.0000030) \int_0^{500} T dz \; ; r = 0.051, \cdots\cdots (9)$$

$$\Delta D_{1000} = (-4277 \pm 0.0483) + (0.0003543 \pm 0.0000066) \int_0^{400} T dz \; ; r = 0.081, \cdots\cdots\cdots (10)$$

$$\Delta D_{1000} = (0.2742 \pm 0.0732) + (0.0003175 \pm 0.0000124) \int_0^{300} T dz \; ; r = 0.129. \cdots\cdots\cdots (11)$$

The probable errors of the formulae (7), (8) and (9) are comparatively small and almost of the same order, but rapidly increases with the decreasing thickness of the layer less than 500m. So it is needed to know the thermal distribution at least down to the 500m layer to make comparatively accurate estimation.

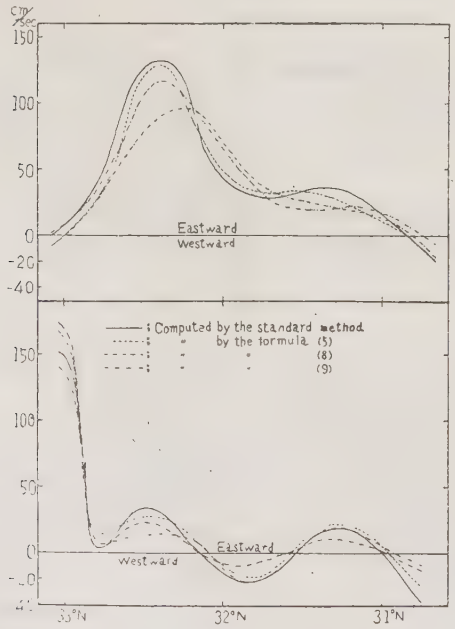

Fig 4. E-W component distribution of the surface current along the *"G*-line" on Sept. 3. 4. 1951 (upper), and on April 16. 17. 1954 (lower)

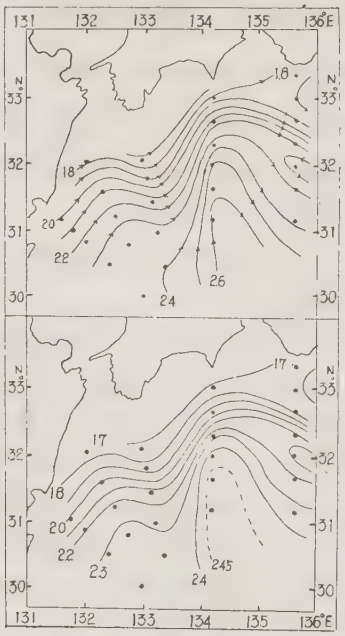

Fig 5. Dynamic topography of the sea surface in dynamic meters referred to the 1000-decibar surface according to observations south off Honshu on Oct. 19. 31. 1954, computed by the standard technique (upper) and by the formula (8) (lower).

For example we show in Fig. 4 the E-W component distribution of surface current along the *"G*-line" on September 3. ~4. 1951 and April 16. ~17. 1953, according to each formula. And for another example, we show in Fig. 5 the dynamic topography of the sea area south off Honshyu in October 1954, computed

by the standard method and the formula (7).

5. *Acknowledegment.*

The author wishes to express his sincere thanks to Mr. J. masuzawa who mentioned the original idea and has encouraged him during this work, and also to Dr. Y. Fujii and Dr. T. Ichiye for his kind advices.

References

1) Sverdrup, H., M. Johnson and R. Fleming, 1949.
The oceans, third printing, pp 402—416.

2) Yamashita, K., 1941.
Introduction of the mean temperature and its application. *Hydrographic Bulletin* (Suiro Yoho), **20** (2). (in japanese)

3) Stommel, H., 1947.
Note on the use of T-S correlation for dynamic height anomaly computations. *Journ. Mar. Res.* **6** (2),

4) Kalle, K. und H. Thorade, 1940.
Tabellen und Tafeln für die Dichte des Seewassers. *Der Archiv der deutschen Seewarte and des Marineobservateriums,* **60** (2).

5) The results of marine meteorological and oceanographical observations. C. M. O. No. 9 —No. 14. 1951—1953.

6) 〃 No. 14, part 1. 1954 (in printing)

Records of Oceanographic Works
in Japan, Vol. 2, No. 2,
October 1955

Notes on the Cross-current Structure of the Kuroshio

(Currents and Water Masses of the Kuroshio System V)

By

Jotaro Masuzawa and Toshisuke Nakai

(Central Meteorological Observatory)

In the Gulf Stream have been found such caracteristic phenomena as the "cold wall", "warm core" or "ribbon of hot water" (DIETRICH 1937, FUGLISTER & WORTHINGTON 1951) and the "cold low salinity water" (FORD and others 1952) etc. Furthermore recently, the detailed current observations reveal an asymmetry in the cross-current distribution of the current-velocity, the narrowness of the strongest current and sometimes a multiple current system (von ARX 1952, NEUMANN 1952, WORTHINGTON 1954).

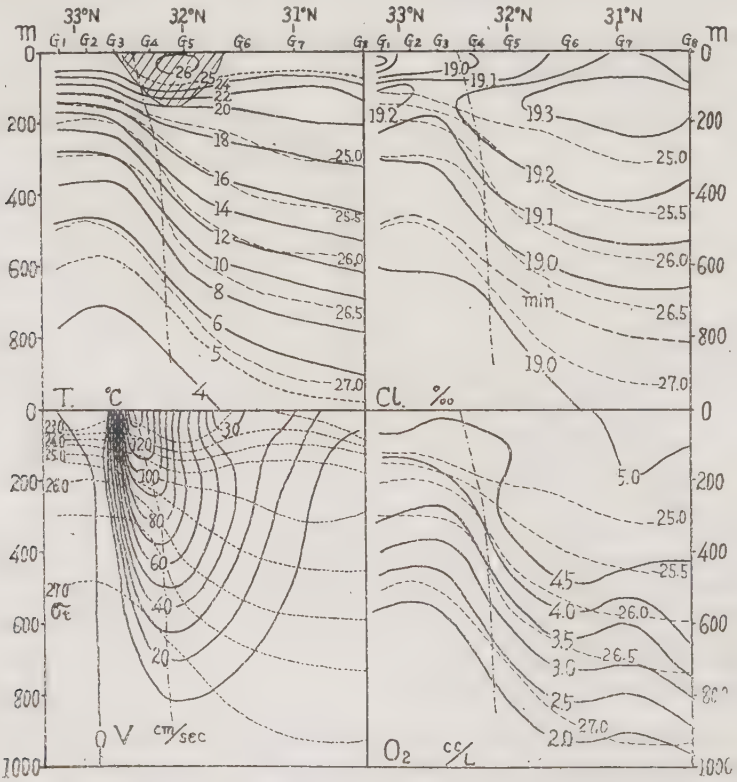

Fig. 1 Vertical distributions of temperature, chlorinity, oxygen and calculated velocity (relative to 1000m) in the section south off Cape Shiono-misaki in October, 1953. broken line : iso-σ_t line, chain line : calculated stream-axis.

Most of those features have been actually detected in the Kuroshio in the southern sea of Japan as well as in the Gulf Stream (Uda 1943, Masuzawa 1954). It is shown from recent cross-current observations on board the *Ryofu-Maru* that the Kuroshio in the eastern sea of Japan which leaves the coast of Japan presents similar characteristic features to those of the Gulf Stream east off Cape Hatteras (Masuzawa 1955 a, b).

In this paper, we wish to describe general structures of the Kuroshio from many available cross sections in the southern and eastern sea of Japan.

A typical section of the Kuroshio south off Japan

In Fig. 1 is shown an example of sectional distributions of water masses when the main stream-axis of the Kuroshio is relatively far off the coast at Cape Shionomisaki. On the north side of the calculated stream-axis exists the colder, salinity-lower and oxygen-poorer water in the mid-depth, but on the south side, the same water mass is found in the deeper layer. The layer between $\sigma_t=26.0$ and 27.0 shows the difference in depth more than 400 meters between both sides of the stream axis and the sharpest inclination as much as about 1 : 200 at the stream axis. The upper water above $\sigma_t=25.5$ on the north side of the stream-axis

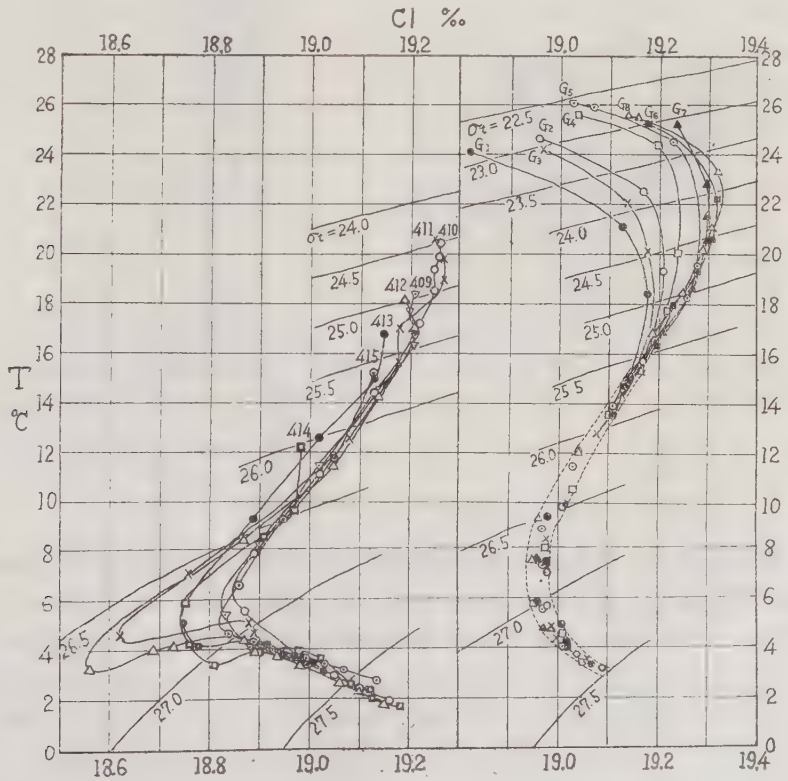

Fig. 2. Temperature-Chlorinity relationship (except the upper 50m layer) of all stations in two sections, shown in Fig. 1 (right) and Fig. 7 (left).

is lower in salinity, which may de diluted by the coastal fresh water. In the lower layer below σ_t=25.5, however, T-Cl curves at all stations of this section shows no significant differences. In other words, the Kuroshio in this sea region consists of the water mass with the almost same T-Cl relationship except the upper layer and it may de regarded as a geostrophic current adjusted to the inclined stratification of the water mass.

Warm core

Fig. 3 shows the profiles of warm core in the upper layer according to the observations carried out south off Cape Shiono-misaki during 1952—1953. The width of the warm core at the surface and its maximum depth are on the average about 40 miles and 200 meters respectively. As the origin (0) of the abscissa in Fig. 3 is the centre of the warm core at the sea surface, the bottom of warm core may be expected to be rather south from the position of its centre

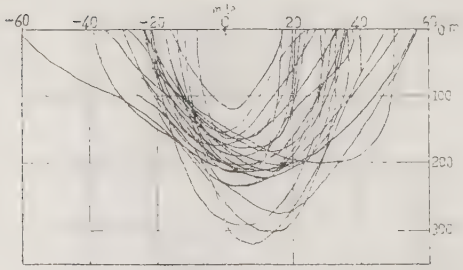

Fig. 3. Profiles of warm core in the section south off Cape Shiono-misaki in 1952-1953.

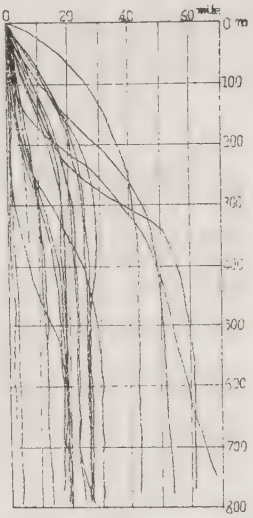

Fig. 4. Vertical distribution of calculated stream-axises in the section south off Cape Shiono-misaki in 1952-1953.

at the surface. This is correspondent to the fact that the calculated stream-axis in the upper layer is displaced southwards with depth and its slope is on the average about 1:130 (Fig. 4). The relative location of the warm core, the calculated stream-axis and the maximum zone of the horizontal temperature gradient is shown in Fig. 5 from the same data as in Fig. 1. Namely, the warm core can be detected most characteristic by the temperature distribution at 100m depth. For instance, Fig. 6 shows a continuous band of the warm core observed in May of 1955 by the ***Syunpu-Maru*** of the Kobe Marine Observatory, the

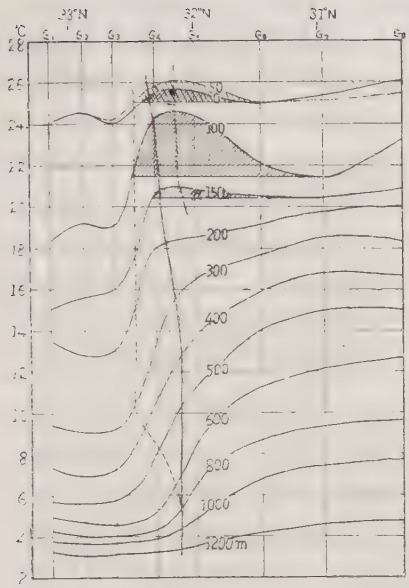

Fig. 5. Sectional distribution of temperatures at each depth in the section south off Cape Shionomisaki in October, 1953. full line: calculated stream-axis, chain line: centre of warm core, broken line: centre of maximum horizontal temperature gradient. Hatched area : warm core.

Ryofu-Maru of the Central Meteorological Observatory and the *Kaiyo-Maru* No. IV and *Meiyo-Maru* of the Hydrographic Office. The maximum temperature of the warm core at 100m depth is more than 22° in the southern sea of Honshu, but it decreases to about 20.5° in the east side of the Izu Submarine Ridge. In the eastern sea of Honshu, it seems to become lower in flowing eastwards, though it is not so decidely.

Whether the fluctuation of the width, thickness and temperature etc. of the warm core are related to the fluctuation of the strength of the Kuroshio Current or not, has not been known for the scarcity of suitable observations.

Also, the calculated stream-axis of the Kuroshio seems to coincide generally with the observed one at the sea surface according to recent G.E.K. observations, and so we can infer the position of actual stream-axis from the upper temperature observations only.

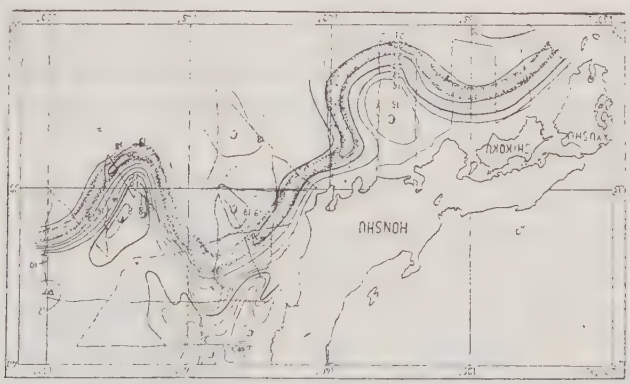

Fig, 6. Distribution of water temperature at 100m depth in May, 1955. Hatched band : warm core

A characteristic section east off Japan

Though only a few cross-current observations have been carried out in the eastern sea of Japan, the Kuroshio Current is also a well-defined narrow current with various meandering courses. The most remarkable feature on the sectional structure at this sea region is, as already suggested (Masuzawa 1955 a, b), that there exists the salinity-lower and oxygen-richer intermediate water (the Oyashio

Undercurrent water) in the Kuroshio Current System. This low salinity water is situated in the intermediate layer between σ_t=26.5 and 27.0, (Fig. 2 and 7), the inclination of which gives a most important contribution to the strength of geostrophic current. (Fig. 7)

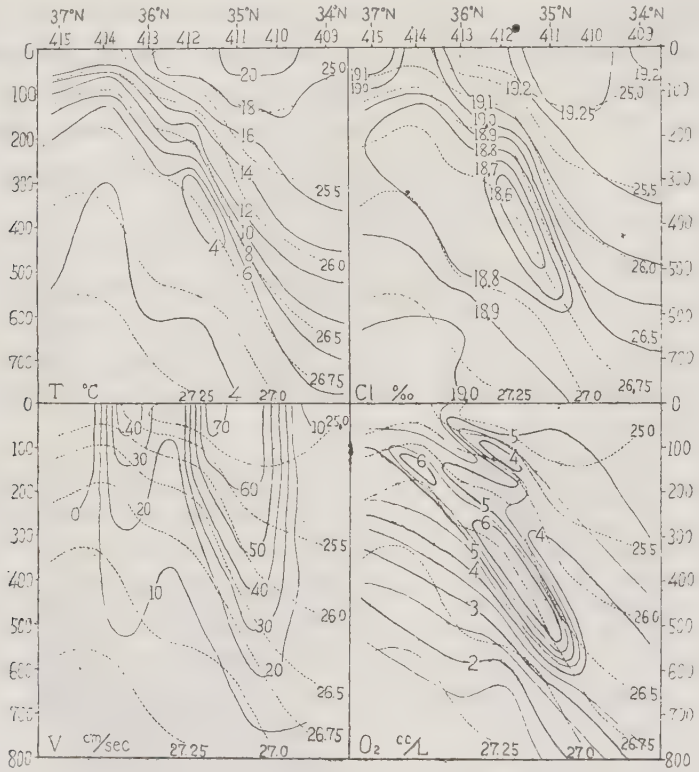

Fig. 7 Vertical distributions of temperature, chlorinity, oxygen and calculated velocity (relative to 1000m) in the section along the meridian of 148° E in May, 1955. broken line : iso-σ_t line.

This cold intermediate water originates from the Oyashio Water (the subarctic water) and flows down southwards on the isentropic surfaces of σ_t=26.5−27.0

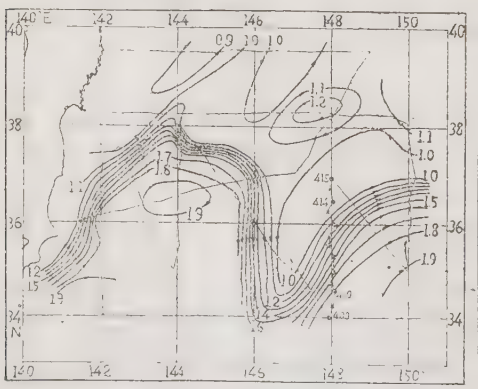

Fig. 8a Surface anomaly of dynamic depth (relative to 800 d. b. layer) in May 1955.

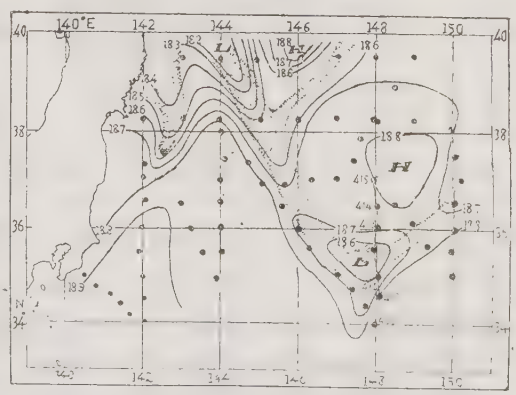

Fig. 8b Minimum chlorinity distribution in May, 1955.

and then as it contacts with the Kuroshio, it is included in the Kuroshio Current System. Therefore, as shown in Fig. 8 a, b, the extremely salinity-low intermediate water (below Cl=18.75‰ or S=33.9‰) has not been found on the southern side of the Kuroshio Current. The growth and history of the cold low salinity water pointed out by FORD and others (1952) in the Gulf Stream is may be applicable similarly to the Oyashio undercurrent water. But, though the water mass in the Gulf Stream has the density almost equal to one of the Oyashio Undercurrent Water, for the sake of the generally larger density in the Atlantic Ocean than in the Pacific Ocean, in the Atlantic it does not sink to the mid-depth but is limited to the subsurface layer.

Acknowlegements

The authors wish to express their hearty thanks to Mr. Y. Fujii, the chief of Oceanographical Section, Central Meterological Observatory for his encouragement and kind advices.

References

DIETRICH, G. (1937): Über Bewegung und Herkunft des Golfstrom Wassers. *Veroeff. Inst. Meereskunde Univ. Berlin.* N.F.A. **33.**

FORD, W.L., J.R. LONGARD and R.E. BANKS (1952) : On the Naure, Occurrence and Origin of Cold Low Salinity Water Along the Edge of the Gulf Stream. *Jour. Mar. Res.* **11** (3).

FUGLISTER, F.C. & L.V. WORTHINGTON (1951) : Some Results of a Multiple Ship Survey of the Gulf Stream. *Tellus* **3** (1).

MASUZAWA, J. (1954) : On the Kuroshio South Off Shiono-misaki of Japan. *Oceanogr. Mag.* **6** (1).

MASUZAWA, J. (1955a) : Preliminary Report on the Kuroshio in the Eastern Sea of Japan. *Records Oceanogr. Works in Japan* N.S. **2** (1).

MASUZAWA J. (1955b) : An Outline of the Kuroshio in the Eastern Sea of Japan. *Oceanogr. Mag.* **7** (1)

NEUMANN, G. (1952) : Some Problems Concerning the Dynamics of the Gulf Stream. *Trans. of New York Academy of Sci.* Ser. II, **14** (7).

UDA, M. (1934) : On the Structure of the Boundary Zone of Different Water Masses (in Japanese) *Jour. Oceanogr. Soc. Japan* **2** (4).

von, ARX (1952) : Notes on the Surface Velocity Profile and Horizontal Shear Across the Width of the Gulf Stream. *Tellus* **4** (3).

WORTHINGTON, L.V. (1954) ; Three Detailed Cross-sections of the Gulf Stream. *Tellus* **6** (2).

Records of Oceanographic Works
in Japan, Vol. 2, No. 2,
October 1952

Oceanic Condition in the North-western Pacific Ocean

(Preliminary Report)

Jiro Fukuoka
(Central Meteorological Observatory)

§ *Preface*

The oceanic data from 1936 to 1940 have been recently published by the Hydrographic Department and the Imprerial Fisheries Experimental Station in Japan. The writer summarized these data and drew the isotherms maps on the 100m, 200m, 400m, 600m and 800m. But these oceangraphical observations have a tendency to practise in summer and in other seasons data are a few.

In both summers, 1938 and 1939, oceanographical observations were carried out in the wide area, especially in 1939 the area from 6°N to 45°N and from 120°E to 160°E were covered by the research ships in Japan. Now the writer

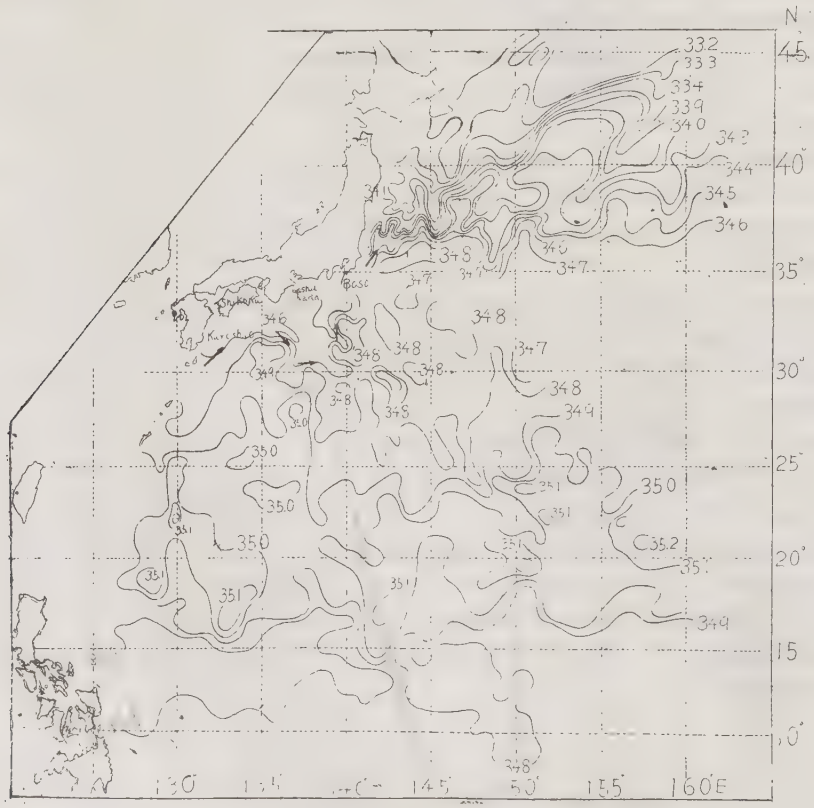

Fig 1. Isohaline map on the 100m layer in Aug. 1939

intend to chiefly study the oceanic condition in summer based on data of the temeperature and salinity, and to publish the report of the outline of the oceanic conditons in the North-western Pacific Ocean.

§ *Ocean Condition near the Kuroshio system area*

In 1939 the large cold water mass occupied the Enshu Nada, and the Kuroshio run through the each points, 31°N 132°N, 31°N 138°E, 34°N 140°E and 37.5°N 145°E. (fig. 1) (Uda, 1949) The Oyashio flew from the sea adjacent Hokkaido along 145°E and reached at 36°N 145°E. The another Oyashio branch run to south along 148°E from the sea near Hokkaido. The extension of these Oyashio branches might get to 34.5°N 143°E. (fig. 2)

At the outside of the Kuroshio, the warm water masses occupied in the area off Shikoku, near Hachijojima and east off Boso Peninsula. These water masses appear often at the same area in every year and may be constructed by descending motion. (fig. 2) (Uda, 1949) The writer is interested in the oceanographical observations in summer 1939 for plentiful data by the Hydrographic Department. As these data are very valuable for the study of the oceanic conditions in the low latitude district, many oceanographers utilized the data in order to study the

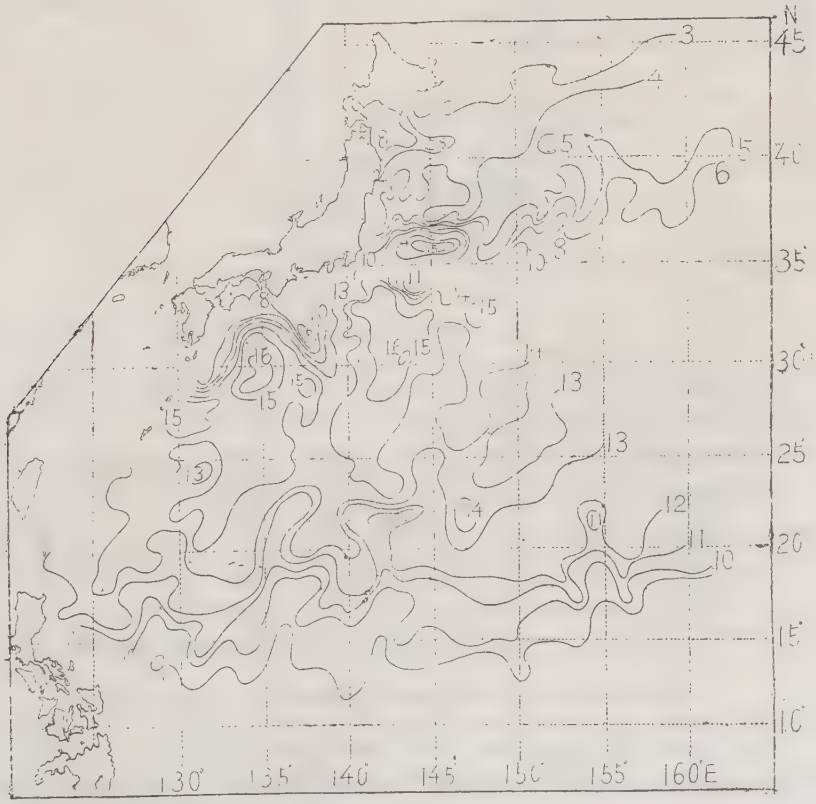

Fig 2. Isotherms map on the 400m layer in Aug. 1939 (°C)

oceanic conditions. (Yoshida and Mao, 1954, Uda 1955) So writer made the iso thermal and isohaline maps on the selected depth to analize the oceanic conditions. Referenced these maps, various characteristics are shown in water mass.

§ *Oceanic Condition in the low latitude district*

From 30°N to 20°N water temperature distributions are monotone and is not noticed the difference depending on the area. But the line of the steepest temperature gradient on the 100m layer appears along 20°N. This line may be shown the subtropical convergence. In the distribution of the salinity on the 100m layer, the highest value appears along 20°N–25°N and in area north or south than this area, salinity is lower. (fig. 1) So referencing the distributions of temperature and salinity, it is seen that the convergence line occupy near 20°N. Below the 400m layer, the distribution of the temperature is different from the distribution on the upper layer (above 200m).

The area of the warmest temperature on the 400m occupy in the area south off Shikoku, near Hachijojima and east off Boso Peninsula. (fig 2) The water temerature is lowering in company to southward from these area. (fig. 2)

The temperature gradient on this layer is steepest along 20°N, besides the direction of temperature gradient is opposite to direction of temperature gradient on the upper layer above 200m.

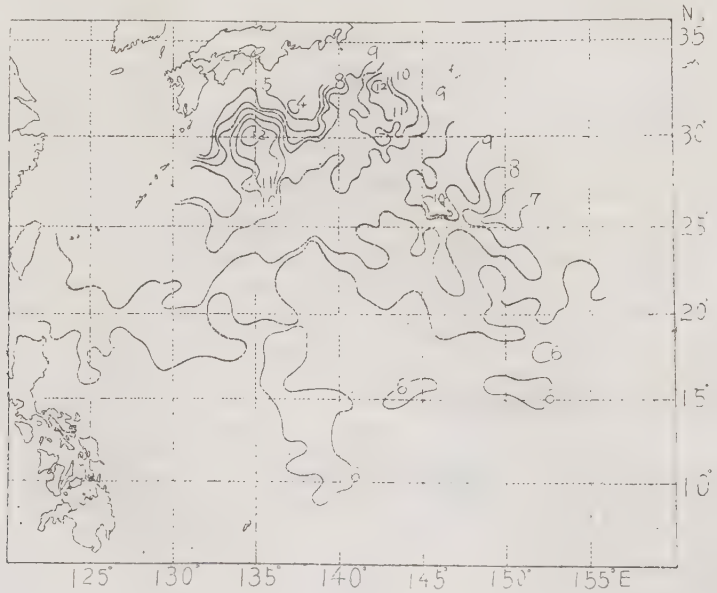

Fig 3. Isotherms map on the 600m layer in Aug. 1939

The cold waters on the 400m, 600m, and 800m layers may appear from 25°N to 5°N and extend from east to west, (fig. 3) according to the theory which the intermediate water in the Pacifc Ocean flows to west in the low latitude

from 20°N 180°. (Sverdrup and others, 1949) The writer studied the vertical section in order to research the current motion and the structure of water mass.

The distribution of temperature and salinity on the section is monotone from 25°N to 20°N and shown by the simple water mass. But to southward from 20°N, the distribution of temperature and salinity have a trend of different type. The depth of thermocline is 100m in 10°N and deeper than the depth of it in 25°N. Below the thermocline the clold and low salinity water is ascending to south. (fig. 4) The ascending motion of the cold water mass is similar to the motion in the Atlantic Ocean. (Iselin 1936)

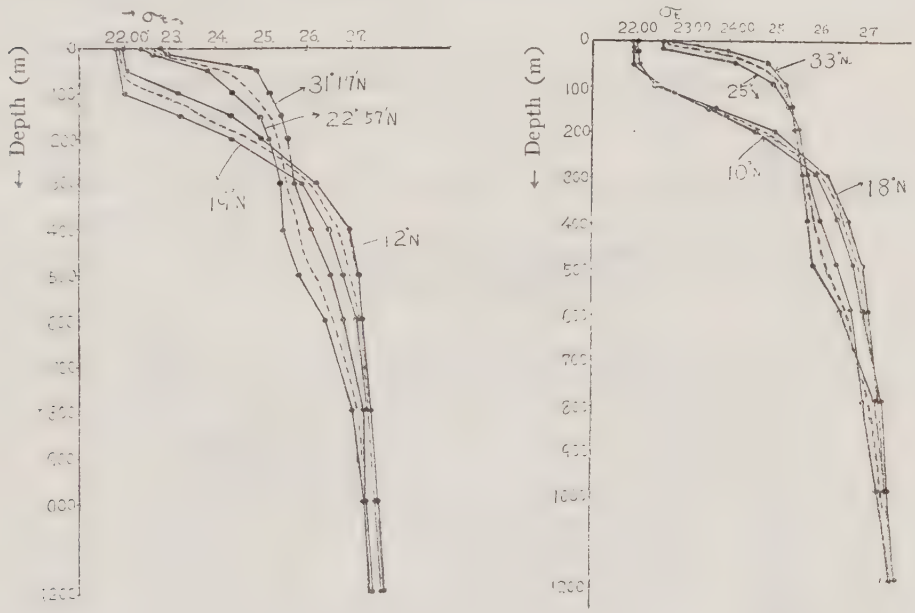

Fig 5. Vertical distribution of Sigma-t ·····mean value

§ *The vertical distribution of Sigma-t*

By researching the above distribution of water temperature and salinity, it is seen that the distribution of sigm-t may be different depending on the observing area. The distribution of sigm-t to notrthward from 20°N is shown a few difference from upper layer to lower layer. (below the depth of thermocline) In the area, southward from 20°N, the difference of sigma-t between the upper layer and lower layer is much and water stratum is stable. (fig. 5)

The boundary between the north water and south water may be along 20°N based on the data of sigm-t.

§ *Conclusion*

The writer researched the water masses in the wide area, and described the warm water mass in the Kuroshio system, the monotone water mass from 25°N

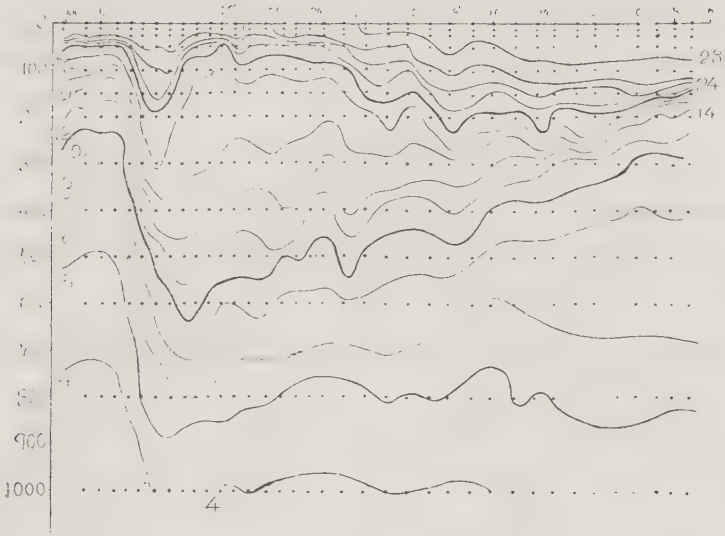

Fig 4. Sectional distribution of water temperature (°C)
(34°N137°37′E-6°55′N, 144°35′E)

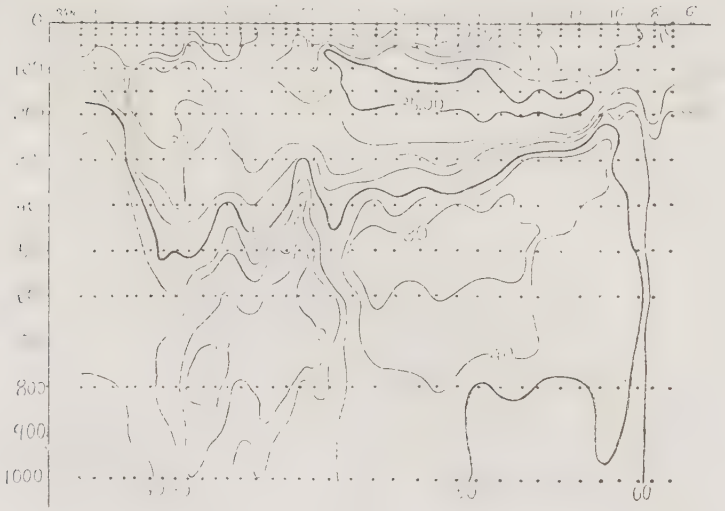

Fig 4. Sectional distribution of salinity (‰)
(34°N137°37′E-6°55′N, 144°35′E)

the subtropical convergence line and the water mass in the low latitude District (from 5°N to 15°N). In the near furture the motion of the water mass and the variation of the subtropical convergence should be studied.

§ *Acknowledgements*

The writer wishes to thanks Dr. Y. Fujii, chief of Oceanographical Section for many helpful comments.

References

Iselin, COD 1936
A study of the circulation of the western North Atlantic. Papers in Phys. *Oceanogr. and Meteor.* Vol. 4 No. 4 pp 101

Sverdrup, H. U. and others 1949
The Oceans pp 727 Prentice Hall Inc

Uda, M. 1949
On the correlated fluctuation of the Kuroshio current and the cold water mass. *Oceanogr. Mag.* Vol. 1 No. 1 p 1

Uda, M. 1955
On the subtropical convergence and the currents in the North Pacific *Records of Oceanogr. Works in Japan* Vol. 2 No. 1 pp 141

Yoshida, K and Mao H. 1955
Physical oceanography in the Marshall Islands area, *Geological Survey Professional Paper.* c60-R.

Records of Oceanographic Works
in Japan, Vol. 2, No. 2,
October 1955

THE RADIOCHEMICAL ANALYSIS OF RADIO-NUCLIDES IN SEA WATER COLLECTED NEAR BIKINI ATOLL

By

Y. Miyake and Y. Sugiura

(Meteorological Research Institute)

Introduction

As a result of the large-scale scattering of fission materials by H-bomb tests at Bikini Atoll carried out during the period from March to May, 1954, the radioactive contamination around the atoll was brought about. By the observation accomplished by Japanese oceanographers aboard the "Shunkotsu-maru" considerably higher level of activity was detected even in the area as far as several thousand miles from Bikini, mainly flowing on the direction of North Equatorial Current. As to the distribution of the radioactivity, another paper was written by the present authors[1]. In this paper, the present authors intend to report the results of radiochemical analysis of radioactive constituents in sea water. The sample which was used for the analysis had been collected at 12°-18′N, 161°-03′.5 E on 20th June, 1954, situated at about 450 km northeast from Bikini Atoll.

Sea water of 16.5 l was used for analysis, while the precipitate adhered to the inner wall of a glass container was washed with hydrochloric acid (1:1) and subjected to the analysis too. The total activity of sea water was 1830cpm/l measured aboard the "Shunkotsu-maru" immediately after sampling. Later, by 12th Aug. in 1954, it decayed to 320 cpm/l. It was found that the decay rate of radioactivities of sea waters collected near Bikini Atoll is approximately expressed by the next formula. $A(t)=ct^{-1.5}$ where A(t) is the activity, c, a constant and t, time elapsed since the date of detonation. Assuming that the last experiment at Bikini was carried out on 5th May, the activity on lst December on which the analysis was started should be about 190 cpm/l. Therefore, the total activity of sea water used for the analysis might be about 3100 cpm.

The method of analysis

In the analysis of radioactive materials in sea water, they must be first separated from a larger amount of salt. As shown in Table 1, most of radioactive materials were collected in precipitates of hydroxide and oxalate by coprecipitation with carriers, leaving the main part of salt in filtrates.

At first, sea water of about 1 l was boiled with hydrochloric acid to drive off the dissolved carbonate. Then, iron and lanthanum salts (respectively, each 5 mg as Fe and La) were added. They were precipitated by adding ammonium

Table 1

The scheme of the radiochemical analysis of sea water

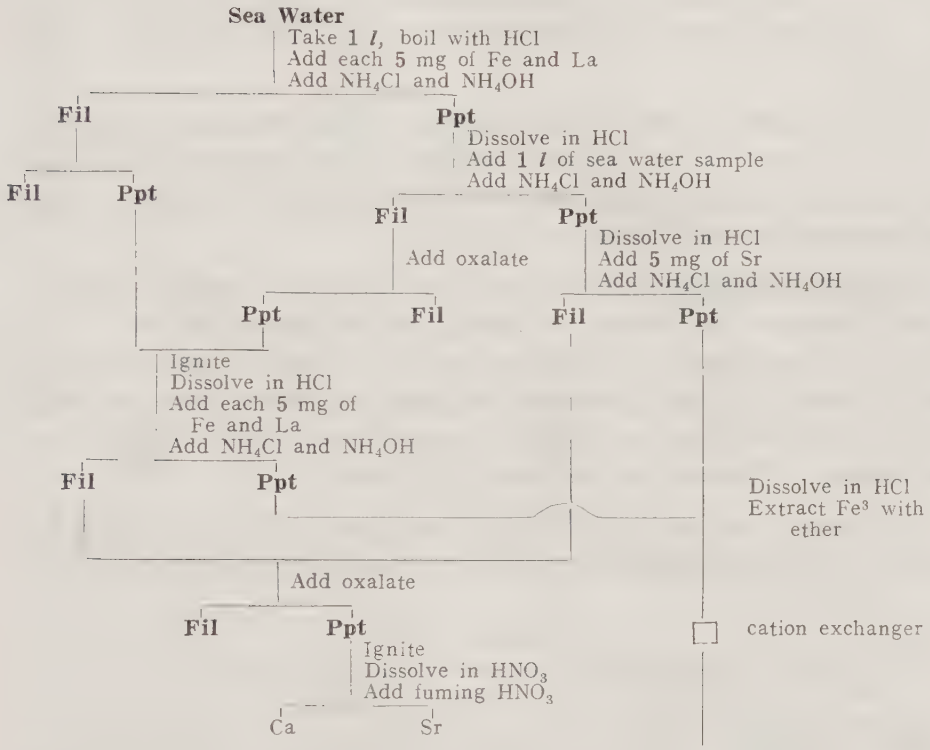

chloride and ammonium hydroxide solution. The precipitate was dissolved again in hydrochloric acid. In the latter solution another sample of sea water of 1 *l* was poured and boiled again. Then, ammonium chloride and ammonium hydroxide solution were added. Such a procedure was repeated until all of samples were used. The precipitate containing iron and lanthanum hydroxide was dissolved in hydrochloric acid, to which the strontium salt (equivalent to 5mg Sr) was added as a hold back carrier. The precipitate was obtained by adding ammonium hydroxide solution and dissolved again in hydrochloric acid. Then, ferric chloride was extracted from the acidic solution using ether. The remaining acidic solution was evaporated nearly to dryness and the residue was dissolved in 0.2 *N* hydrochloric acid and poured into a cation exchanger column. Thereafter, the group analysis was made by the ordinary process.

On the other hand, to the filtrate already separated from the precipitate containing iron and lanthanum was added ammonium oxalate to obtain the precipitate of alkaline earths. After igniting the precipitate it was dissolved in hydrochloric acid to which iron and lanthanum salts were added as scavengers and precipitated with ammonium hydroxide solution. After filtering out the latter precipitate, oxalate was changed into oxide by ignition and dissolved in a concen-

trated nitric acid. Then, a fuming nitric acid was dropped in. Thus, strontium nitrate was obtained as precipitate while calcium nitrate remained in a solution. Strontium nitrate was dissolved on a glass filter pad in warm diluted nitric acid and transfered into a planchet for the measurement of radioactivity by a G-M counter.

Next, the analysis of the precipitate adhered on the glass wall of the original container was made. In this case there was only a little amount of salt matter, therefore, the solution in hydrochloric acid was directly passed through a cation exchanger column to make the group separation.

As the cation exchanger, Amberlite IR-120 was used under following conditions. (1) Inner diameter of the column was about 20 mm and height, 50 mm. The grain size was between 100 to 150 meshes. The flow rate of effluent was about 0.8 cc/min. (2) Inner diameter of the column was about 7 mm and height 560 mm. particles of grain size 100 to 150 meshes and of about 50 meshes were mixed together. The flow rate was about 0.3 cc/min.

The ordinary group analysis were carried out under the first condition and for the seperation of yttrium and cerium the second condition was employed.

Table 2

The results of radiochemical analysis of the sea water near Bikini.

Nuclide	1* Activity cpm	%	Date of measurement	2** Activity cpm	%	Date of measurement	210 day activity (%) in fission materials (U-235, slow neutron)
Y-91	750	37	Dec. 22, 1954	850	93	Mar. 29	10
Ce-141, 144	1100	55	Dec. 22				15.0
Ru-103, 106 Rh-106	75	3.8	Dec. 1	34	3.7	Mar. 28	8.2
Zr-95 (Nb-95)	45	2.2	Des. 3	30.5	3.3	Mar. 28	39
Sr-89 (90)	40	2.0	Dec. 20	-	-	Mar. 29	7.5

* The sea water.

** The precipitate which adhered on the glass wall of the container.

Results of radiochemical analysis

In Table 2 the results of analysis are shown. Each nuclide was identified by the shape in elution curves and the β ray energy absorption curves with aluminum. Fig. 1 shows the elution curves obtained for the supernatant sea water sample. The first peak of activity appeared in the effluent from 0.2 N hydrochloric acid. It is considered to be attributed to Ru-103 and Rh-106 (a daughter of Ru-106) according to the β ray energy absorption curves shown in Fig. 2. The second peak appeared in effluent from 0.5% oxalic acid. This may be attributed to Zr-95 estimating from the β ray energy absorption curves shown in Fig. 3.

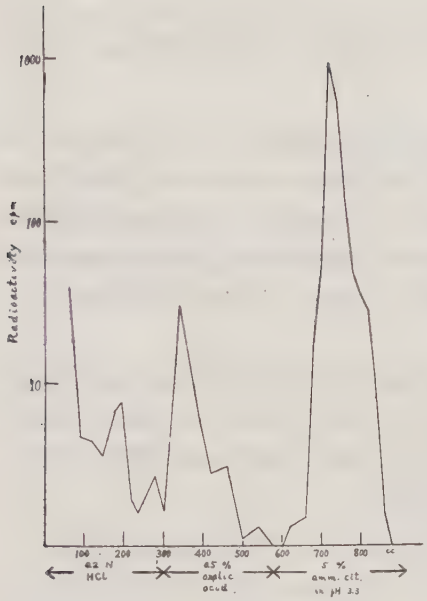

Fig. 1 The elution curves for the sea water sample

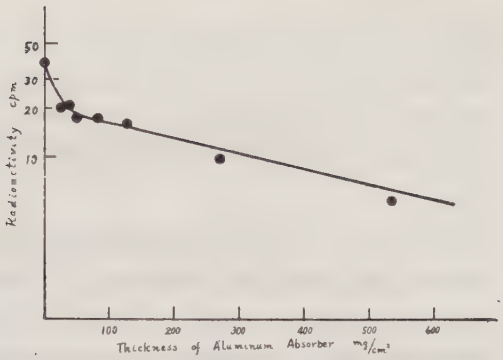

Fig. 2 The β ray energy absorption curves in the effluent from 0.2 N HCl

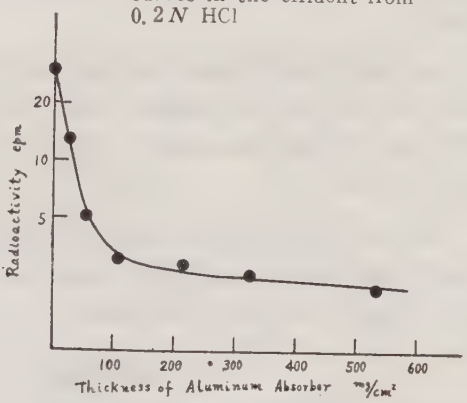

Fig. 3 The β ray energy absorption curves in the effluent from 0.5 % oxalic acid

Though Nb-95 was not identified but its existence was probable. The third peak appeared in the effluent (5 % ammonium citrate) of which pH was adjusted with hydrochloric acid to be 3.3. This fraction was separated into two parts by passing through a long column of the resine (56cm), as shown in Fig. 4. Fig. 5

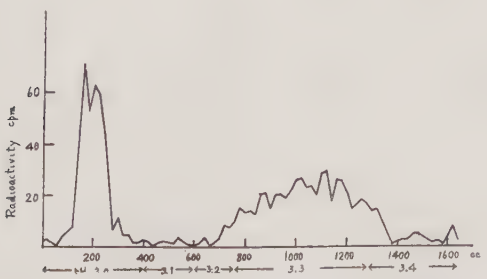

Fig. 4 The elution curves by the ammonium citrate solution for the supernatant sea water sample.

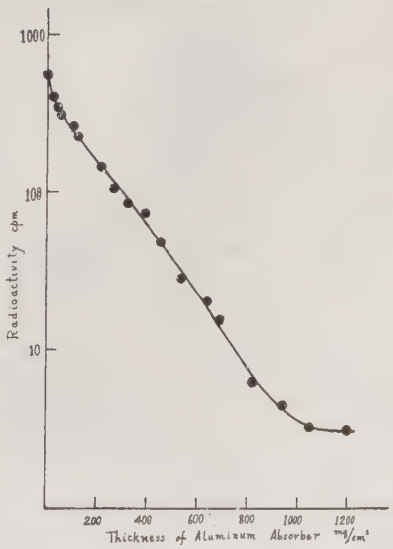

Fig. 5 The β ray energy absorption curves in the effluent from 5% ammonium citrate solution of pH 3.3.

shows an absorption curves of a fraction of the effluent of the ammonium citrate solution in which the existence of Y and rare earths elements were expected. As seen in Fig. 5, it seems that there are two kinds of β rays of different energies. A soft part may be said to be attributed to Ce-141, 144 while a hard one to Y-91 only.

According to Table 2, undoubtedly it may be said that the contributions of yttrium and cerium are dominant. Activities from other nuclides other than Y and Ce are too weak to make a detailed discussion. According to Hunter-Ballou's calculation, the conributions of each radionuclide obtained by bombarding slow neutron to U-235 on 210th day after fission are given in the 8th column in Table 2.

Analytical results show that the contribution in activity of Zr-95 is much lower than the calculation by Hunter-Ballou, on the contrary, Y and Ce much higher. The cause of this discrepancy is not clear. To clarify the reason the study is now in progress.

The authors wish to express their hearty thanks to Dr. K. Kimura, Dr. E. Minami and members of their laboratories in the University of Tokyo for their valuable suggestions and discussions.

Reference

1) Miyake, Y., Sugiura, Y and Kameda, K., 1955: On the Distribution of Radioactivity in the Sea around Bikini Atoll in June, 1954. Pap. Met. and Geophys., 5, p. 253.

Records of Oceanographic Works
in Japan, Vol. 2, No. 2,
October 1955

On the first larva of *Parribucus ursus-major* (Herbst)

By

Hiroaki Aikawa and Kiyoshi Isobe
(Kyushu University)

The first phyllosoma larva was obtained by rearing the berried female of *Parribucus ursus-major* (Herbst) in summer 1950 in Tomari Bay, Kagoshima Pref. (Southern Kyushu). Here a brief description will be given for the larva (Fig. 1).

The large cephalus is pear-shaped with the maximum width of 1.0 mm, the

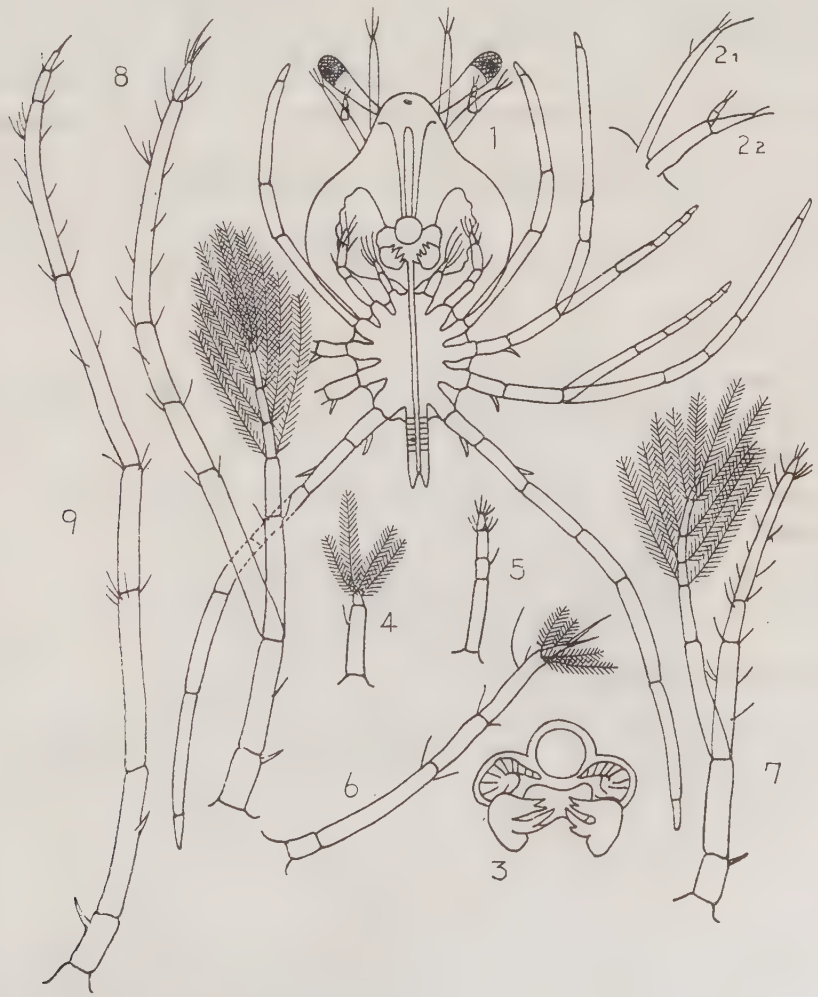

Fig. 1

thorax spherical, and the abdomen rectangular in shape, elongated, and incompletely segmented, being provided with a short spine on each posterior corner. Between these spines anus opens. Body length is 1.8 mm in total.

The 1 st antenna is slender, unjointed, and nearly equal in length to the stalked eye, being provided with three apical setae. The 2 nd antenna rather thick two-jointed, being provided with a single flagellum and a vestigial process. These characteristics are much different from those of the larvae of the Family Parlinuridae. The mandible is bilobed and each lobe ends in two pointed teeth. The 1 st maxilla is single and of two joints: apical joint posseses four apical plumose hairs and basal joint laterally a short smooth hair. The 2 nd maxilla is also single and of four joints: the end joint being provided with five apical hairs on the top, with four plumose hairs a little below them, and in addition, laterally with two unequal hairs; the 2 nd joint also with five hairs and the 3 rd joint only with one hair respectively. The 1 st maxilliped is wholly absent. The 2 nd maxilliped is of four joints: end joint has two smooth hairs on the tip; both 2 nd and 3 rd joints also with two smooth hairs around the anterior end. Three legs are all large, elongated, pigmented with red chromatophores, and posses acoxal spine respectively. Both the 1st and 2 nd legs are two-branched : endopodite of six joints and provided with two plumose setae on each joint except the basal one; exopodite far more elongated than endopodite, of seven joints with short smooth hairs on each joint except the basal two. The 3rd leg is single.

Literature cited

1. Van Bonde, W., 1930, Fish and mar. biol, Survey, U. S. Africa. Report No. 8.
2. Van Bonde, W., and J. M. Marchaud, 1935, Commerce and Industry. Fishery Bull., No. 1.
3. Gilchrist, J. D. F., 1913, Lin. Soc. London, Vol. 31, No. 216.
4. Gurney, R., 1936, Discovery Report., Vol. 12.
5. Orton, J. and E. Ford, 1933, Proc. Zool. London, pt. 1.
6. Oshima, Y., 1942, Bull. Japanese Soc. sci. Fish., Vol. 19, No. 1.

Explanation of figures

1. total view, x 50; 2_1 and 2_2. 1st and 2nd antennae, x 80; 3. mandible, x 120; 4. 1st maxilla, x 120; 5. 2 nd maxilla, x 120; 6. 2 nd maxilliped, x 120; 7. 1st leg, x 120 ; 8. 2 nd leg, x 120; 9. 3rd leg, x 120.

Records of Oceanographic Works
in Japan, Vol. 2, No. 2,
October 1955

Distribution of Plankton Diatoms in Relation to Hydrographic Conditions in the Sea Area East of Honshu in the Summer of 1954

By

Ryuzo Marumo

(Central Meteorological Observatory)

Oceanographical surveys were made in the sea area east of Honshu(Japan Proper) by the ***Ryofu-maru*** of the Central Meteorogical Observatory and by the ***Yushio-maru*** of the Hakodate Marine Observatory in August to September 1954. The present paper is concerned with the surface distribution of plankton diatoms in relation to water masses and currents in these surveys. The method used in this plankton study is detailed by Marumo (1954).

The outline of surface hydrographic conditions (Fig.1) In this season the

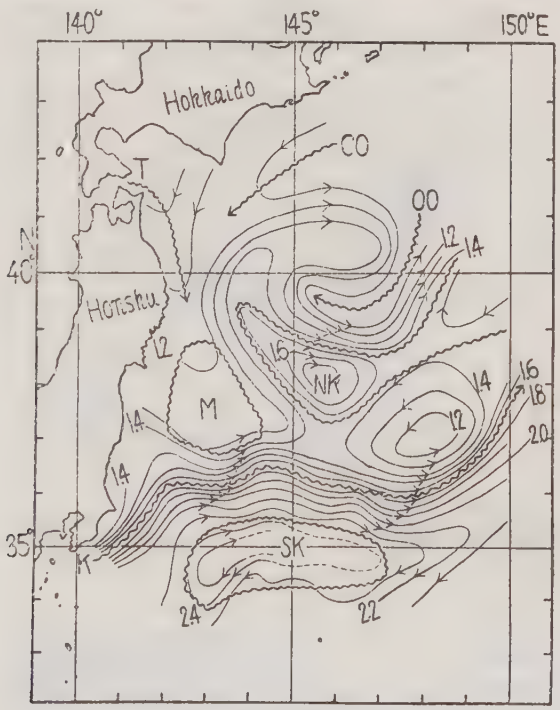

Fig. 1. Surface dynamic anomaly (relative to 1000 db).

surface temperature was fairly uniform and ranged between 24°C and 28°C in the Kuroshio waters. The main Kuroshio current (K in Fig. 1) which showed about 26°C streamed eastward along the latitudinal line of 36°N and changed its course to

the northeast direction at about 148°E. In the Kuroshio water south of the main current (SK) temperature was 26 to 28°C. To the north of the main current the Kuroshio water was cut off around 38°N, 146°E (NK), the temperature of which was 24 to 25°C.

There existed two main Oyashio branches, the one is the coastal Oyashio (CO) and the other the off-shore Oyashio (OO). The surface temperature was 12 to 18°C in the former and 18 to 24°C in the latter.

In coastal areas the Tsugaru warm water (T) showed 18 to 20°C and the mixed water of the Kuroshio with coastal waters (M) showed 20 to 24°C.

Surface distribution of the number of diatom cells (Fig. 2) The cell number of surface water was 10^2 to 10^3 to the liter in the main Kuroshio current, while it decreased to less than 10^2 in the southern and northern Kuroshio waters (SK and NK). Plankton diatoms are scantier in August and September than in each month of March, May and June in 1954 in the Kuroshio waters. Marumo (1954) and Marumo and others (1954) report that the number of diatom cells showed the minium also in summer in the Kroshio water south of Honshu.

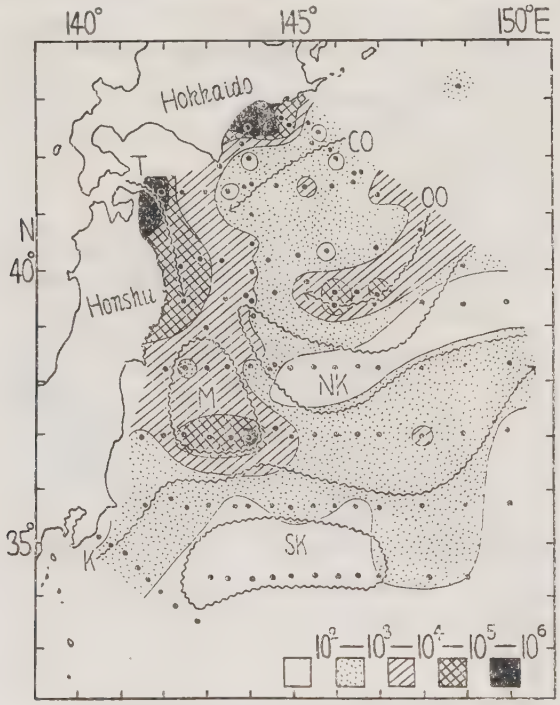

Fig. 2. Surface distribution of the cell number of diatoms to the liter.

The cell number was 10^2 to 10^3 in the coastal Oyashio water characterized by an oceanic community and was very large, 10^5 to 10^6, in the region of a neritic community along the southeast coast of Hokkaido. The cell number in

the off-shore Oyashio was 10^3 to 10^4, to be worthy to note, being larger than in the coastal Oyashio, and especially it increased to 10^4 to 10^5 in its western part where the Oyashio water is considered to have been mixed with the Kuroshio water.

In coastal araes north of 37°N and west of 144°E the cell number was 10^3 to 10^5. And the following two regions possesed large populations of 10^4 to 10^5 cells; the one is a region affected by the Tsugaru current and the other a region where the main Kuroshio current and the coastal mixed water contacted sharply together.

Surface distribution of diatom communities (Fig. 3) Any remarkable distinction was not recognized among communities of the main Kuroshio current, the southern and northern Kuroshio waters. ***Rhizosolenia calcar avis*** was considerably abundant in the whole Kroshio areas in this season, while it was found little in other seasons. And warm-water species such as ***Hemiaulus hauckii***, ***Climacodium***

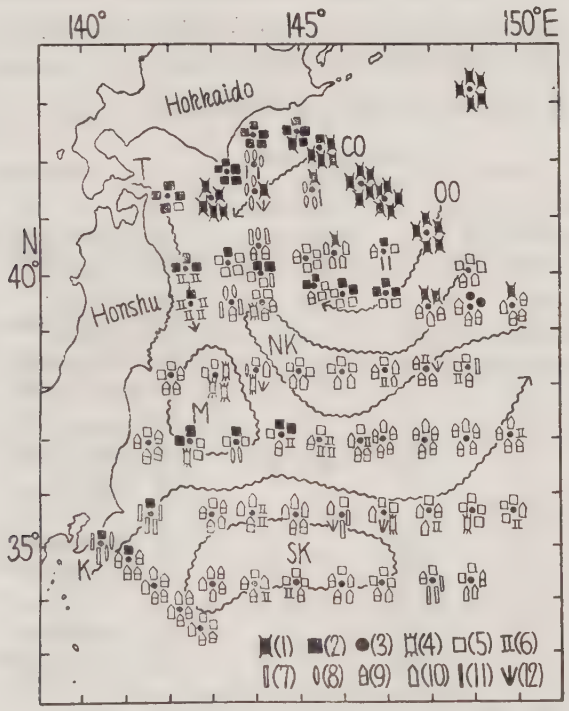

Fig. 3. Surface distribution of diatom communities.

(1) ***Chaetoceros concavicornis, Ch. convolutus, Ch. peruvianus,*** (2) ***Chaetoceros compressus, Ch. debilis, Ch. radicans, Ch. constrictus,*** (3) ***Coscinodicus*** spp., (4) ***Bacteriastrum elongatum, Bac. delicatulum,*** etc., (5) ***Chaetoceros dadayi, Ch. tetrastichon, Ch. affinis, Ch. lorenziaus, Ch. didymus, Ch. curvisetus,*** etc., (6) ***Climacodium biconcavum, Hemiaulus hauckii,*** (7) ***Leptocylindrus danicus,*** (8) ***Nitzschia seriata,*** (9) ***Rhizosolenia calcar avis,*** (10) ***Rhizosolenia styliformis, Rh. st.*** v. ***latissima, Rh. alata,*** (11) ***Talassiothrix longissima,*** (12) ***Thalassionema nitzschioides.***

biconcavum, *Chaetoceros dadayi*, *Ch. tetrastichon*, *Ch. affinis*, *Ch. lorenzianus* *Rhizosolenia alata*, *Rh. styliformis* and *Rh. sty. v. latissima* were widely distributed in these waters. *Chetoceros compressus* was involved in a coastal part of the Kuroshio current.

In the coastal Oyashio, *Chaetoceros concavicornis* and *Ch. convolutus* were most predominant and *Nitzschia seriata* appeared frequently also. By Marumo (1955) this community resembles to that of the Bering Sea in the summer of 1954. Therefore, if the coastal Oyashio water has originated from the Bering Sea, this water is considered to have well maintained its biological characters in the origin. In the densely populated region along the southeast coast of Hokkaido a neritic community was found. Namely, *Chaetoceros radicans*, *Ch. compressus*, *Ch. constrictus* and *Ch. debilis* were leading species. The off-shore Oyashio contained the same cold-water *Phaeoceros* commumity in its eastern part as in the coastal Oyashio, but in its western part the number of species increased and cold-water and warm-water species such as *Chaetoceros affinis*, *Ch. didymus*, *Ch. lorenzianus*, *Ch. compressus* and *Ch. radicans* were present together.

Table 1. Summarized results of distribution of plankton diatoms.

Water mass and current			Number of cells to the liter	Important species
Kuroshio water	Southern Kuroshio(SK)		$10^2>$	*Ch. calcar avis* (most important) *Cl. bicon cavum* *Hem. hauckii* *Ch. dadayi* *Ch. tetrastichon* *Ch. affinis* *Ch. lorenzianus* *Rh. styliformis*
	Main Current(K)		10^2-10^3	
	Northern Kuroshio(NK)		$10^2>$	
Oyashio water	Coastal Oyashio(CO)	Northern Part	10^5-10^6	*Ch. radicans* *Ch. compressus* *Ch. debilis* *Ch. constrictus*
		Southern Part	10^2-10^3	*Ch. convolutus* *Ch. concavicornis* *Nit. seriata*
	Off-shore Oyashio(OO)	Eastern Part	10^3-10^4	*Ch. convolutus* *Ch. concavicornis* *Ch. peruvianus*
		Western Part	10^4-10^5	*Ch. affinis* *Ch. lorenzianus* *Ch. didymus* *Ch. compressus* *Ch. radicans*
Tsugaru Current (T)			10^4-10^5	*Ch. compressus* *Ch. lorenzianus* *Ch. curvisetus* *Hem. hauckii* *Cerat. bergonii* *Rh. styliformis*
Coastal mixed water (M)			10^3-10^5	various

Because any surface temperature below 12°C was not observed in the Oyashio waters in this season, distinctly cold-water species were not found. However, typical cold-water species, ***Chaetoceros atlanticus***, ***Rhizosolenia hebetata*** f. ***hiemalis***, ***Rh. obtusa***, ***Ptychocylis obtusa*** (tintinnid) and ***Parafavella*** spp. (tintinnid), were present in deeper layers, for instance, at the depths of 50 to 150 meters (3.1—1.4°C) at a station, 40.7°N, 148°E.

The community of the Tsugaru warm water indicates the flowing of its current into the Pacific side of Honshu, because of the existence of warm-water species, such as ***Cerataulina bergonii***, ***Hemiaulus hauckii***, ***Chaetoceros lorenzianus***, ***Ch. curvisetus*** and ***Rhizosolenia styliformis*** with ***Chaetoceros compressus***. The densely populated water around 37°N, 143°E was rich in species, involving ***Chaetoceros compressus***, ***Ch. lorenzianns***, ***Ch. affinis***, ***Ch. laciniosus***, ***Ch. curvisetus***, ***Nitzschia delicatissima*** and ***Skeletonema costatum***, and it indiates the neritic Kuroshio water.

Summary The result of these plankton surveys is summarized as in Table 1.

Acknowledgment The writer is indebeted to Dr. Y. Fujii for his invaluable advice and encouragement.

Literatures

Marumo, R. (1954) : Diatom Plankton in the South of Cape Shionomisaki in 1953, *Oceanogr. Mag.*, **5** (3).

Marumo, R., M. Kitou and O. Asaoka (1954) : The Productivity and Its Seasonal Variations of Main Plankton Groups in the Open Sea, *Jour. Oceanogr. Soc. Japan*, **10** (4). (in Japanese)

Marumo, R (1955) : Analysis of Water Masses by the Microplankton (1), *ibid.*, **11**(3).

Records of Oceanographic Works
in Japan, Vol. 2. No. 2,
October 1955

On a Manganese Nodule and *Perotrochus* Dredged from the Banks near the Izu Islands, Japan.

By

Hiroshi Niino

(Tokyo Fisheries University)

1. Introduction.

It is well known that there exisls a series of banks srranged in northeast to southwest in direction on the western side of the Izu Islands, Shizuoka Prefecture, Japan. The northernmost bank is known as the Toshima Tai, the second one as the Torama Guri, and the third is called Hyotan Sho. These are separated from the submatine plantform of the Izu Islands by a channel more than 200 m in depth.

Each bank of the series has a significant flat and broad plain on its top and with inclination less than 2°. The outer margin of the flat surface abruptly descends to the deep sea floor, or in other words, the inclination of the slope of the banks is very steep.

During the years of 1953 to 1955, the training ship of the Tokyo University of Fisheries dredged 22 botton samples from those banks and their environs. It is noteworthy that a manganese concretion was obtained from a station on the alope of the bank and that shells of ***Perotrochus*** were collected from seven stations.

2. The Bottom Character of the Banks.

Although not confirmed, it is proesumed by the records of the echo sounding machine, that rocks are exposed on the steep slope around the banks. the dredged samples consisted mostly of attached organisms.

Gravels and coarse sand were dredged from the flat plain on the banks. the former are well water worn and frequently encrusted with such organisms as calcareous algae, bryozoa, sponges and etc. Of the gravels collected, several were selected at random for petrographical study and their thin sections were examined under the microscope.

Microscopic examination revealed that andesite and basalt were most common. The lithological characters of these volcanic rocks are common to those building the main islands of the Fuji Volcanic Zone.

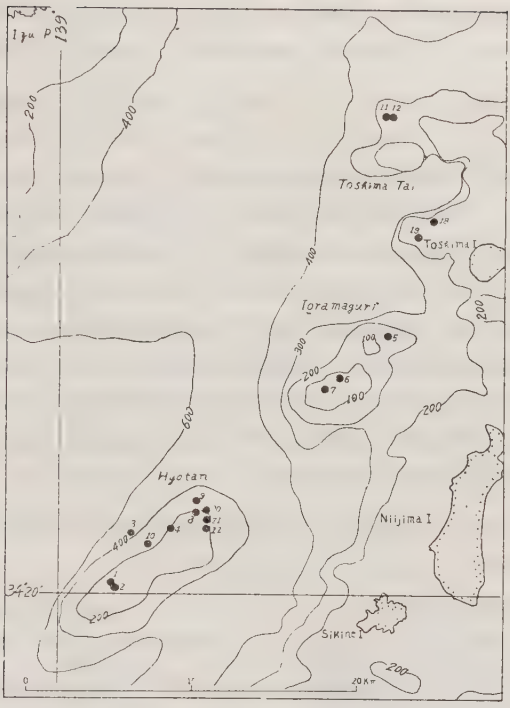

Fig. 1. Bathymetric feature of the banks.
The black spot shows surveying station.

Although the basement rock of the Banks were not obtained at the time of survey, it may be said that, if the gravels on the flat plain of the banks are derived from the basement, the lithological character of the banks may be the same as that of the main islands of the Fuji Volcanic Zone.

It is a noticeable fact that the Izu Islands near the banks above referred to, consist of liparite, thus their lithological characters show a marked contrast with that of the banks.

3. The Manganese Nodule.

The manganese nodules were dredged from St. 9, 34°23.1′ N, 139°05.3′ E, in 260 m depth at the northwestern slope of Hyotanguri, about 15 Km west of Niijima Island. The bottom sample consisted of the manganese nodule, gravels, deep sea corals, Bryozoa, Brachiopoda, calcareous Algae and Mollusca.

The gravels are covered with calcareous algae known as ***Lithothamnium***, and the surface of each gravel is well water worn. The largest gravel measured 5.9 cm in length, 3.5 cm in width and 1.8 cm in thickness, and its lithological characters are those of andesite.

The molluscan remains consisted of ***Tucetona shinkurosensis*** Hatai, Niino, and

Kotaka, *Trichomusculus coralliophaga* (Gmelin), *Lima (Promantellum) basilanica* (Adams and Reeve), *Ctenoides annulatus* (Lamarck), and *Cymatium sp.*

The manganese nodules which were broken into several fragments at the time of collecting, measurd 5.9 cm in length, 3.5 cm in width, 1.8 cm in thickness and weighed 20 gr. The surface is rough and partly covered by encrusting bryozoa and test of annedlids. This indicates that the manganese nodule was exposed on the surface of the sea bottom of the bank. The nodules are very hard and its broken surface shows a black lustre. A thin section of the nodule observed under a microscope shows a thin white-gray layer at the surface. Tests of Foraminifera, sponge spicules, fragmente of fledspar and pyroxene are cemented by black manganese materials, which may also be observed in the inner side of the organic remains. The tests of the organisms consist of aragonite, but some parts of the test are replaced by manganese materills.

The results of chemical analyses of the manganese nodule according to Mr. Tatsumoto, is as follows:

6-N HCl soluble part			6-N HCl insoluble part	
Total oxide	Fe_2O_3, Al_2O_3	2.88%	SiO_2	1.80%
	MnO_2	58.34%	Al_2O_3+Mgo etc	0.34%
	CaO	6.55%		

On the surface of dead shells are found a thin layer of black coated material, which is spread only on one side of the shell, that is to say, that which lies on the sea bottom. The result of chemical analysis of the black layer revealed a moderate content of manganese, viz., Fe_2O_3, Al_2O_3 1.7%, CaO 40.2%, MnO_2 4.5% (6-N HCl soluble part). If the percentage of CaO originated in the shell itself, the percentage of MnO_2 in the coated layer is a little too high. It is uncertain whether the manganese nodule was deposited in situ, but it is certain that the manganese materials were deposited on the bottom of the bank.

Manganese nodules are frequently obtained from the deep sea, but in the present case it was collected from a shallow sea bottom on the bank.

4. *Perotrochus (Mikadotrochus) beyrichi* (Hilgendorff).

Gastropods belonging to the above stated genus are rare in the present seas and are known as "living fossils". There are several species recorded from and rarely obtained in the deep seas around Japan. Previously, the writer recorded a species from the Miocene deposits of Izu Peninsula, Shizuoka Prefecture[1].

From a total of seven stations, many specimens of *Perotrochus beyrichi* were obtained from clean sea bottoms, as shown in the following:

Station	North latitude	East longtude	Depth (in m)	Gravel	Calcium concretion	Coarse sand	Name of Bank
St. 2	34°20.2′	139°02.8′	134	R	A	—	Hyotan

St. 5	34°28.4′	139°12.8′	120	A	—	A	Torama
St. 6	34°27.1′	139°11.0′	104	A	A	A	Torama
St.12	34°35.3′	139°13.4′	88	A	A	—	Toshima
St.20	34°22.5′	139°05.8′	160	A	A	A	Hyotan
St.21	34°22.5′	139°05.8′	160	A	A	A	Hyotan
St.22	34°22.2′	139°05°8′	128	A	A	A	Hyotan

Remarks: A-abundant, R-rare. Organisms are very abundant, viz., calcareous algae, deep sea corals, brachiopods, bryozoas, sponges, etc.

Each dredged sample contained dead shells or fragments of ***Perotrochus veyrichi***, and in the sample form St. 12 was found a perfect living specimen, and from St. 21, an imperfect specimen of a very young living gastropod. The specimen from St. 12 measures 45 mm in height, 47 mm in width and 8 mm in diameter of operculum. The one from St. 21 is more or less broken at the lip, but still preserves the characteristic slit. This seems to be the first record of a young living specimen of ***Perotrochus*** in the world, and it is regretted that it was broken at the time of dredging.

The Kuroshio, the warm current extends throughout the surveyed area, sometimes attaining more than 7 miles perhour. The sea water temperature is very warm, for example, on October 23 rd, 1954, the surface temperature at St. 8 was 23.6^{cw}, and even at 100 meters depth it was recorded at 20.3°C.

The bottom character and associated fauna of the stations where the shells of ***Perotrochus beyrichi*** were dredged are quite the same, therefore, it is certain that they lived on those banks. The following lists are the specific names of the molluscs found in association with ***Perotrochus***, namely:—

Station 2.

Perotrochus (***Mikadotrochus***) ***beyrichi*** (Hilgendorf)
Bolma sp.
Bufonariella ranelloides Sowerby
Chicoreus sp.
Tucetona hanzawai (Nomura and Zinbo)
Limopsis tajimae (Yokoyama)
Miratacar uwaensis (Yokoyama)
Plicatula muricata (Sowerby)
Pecteu albicans (Shröter)
Spondylus acanthus Mawe
Lucinoma spectabilis (Yokoyama)
Vasticardium sp.

Station 5.

Boluma sp.
Bittium sp.
Capulus sp.

Limopsis tajimae Sowerby
Limopsis cumingi A. Adams
Tucetona shikurosensis Hatai, Niino and Kotaka
Tucetona hanzawai (Nomura and Zinbo)
Samarcar pacifica (Nomura and Zinbo)
Acar congenita (E. A. Smith)
Barbatia tenella (Reeve)
Septifer keenae Nomura
Mallens irregularis (Jousseaume)
Plicatula muricate (Sowerby)
Chlamys lemnicate (Reeve)
Aequipecten vesiculosus (Dunker)
Spongylus anacanthus Mawe
Pycnodonta musashiana (Yokoyama)
Crassatellites sp.
Venericardia kiinsis (Sowerby)
Glans sp.
Lucinoma spectabilis (Yokoyama)
Chama sp.

In conclusion the wtier wishes to express his sincere thanks to Dr. Kotora Hatai, for his kind halp.

Reference

1) S. Nomura and H. Niino, Fossil Mollusca from Izu and Hakone. Sci. Rep. Tohoku Imp. Univ., Ser. 2, Vol. XV, No. 3, pl. XII, 1932.

Plate I.

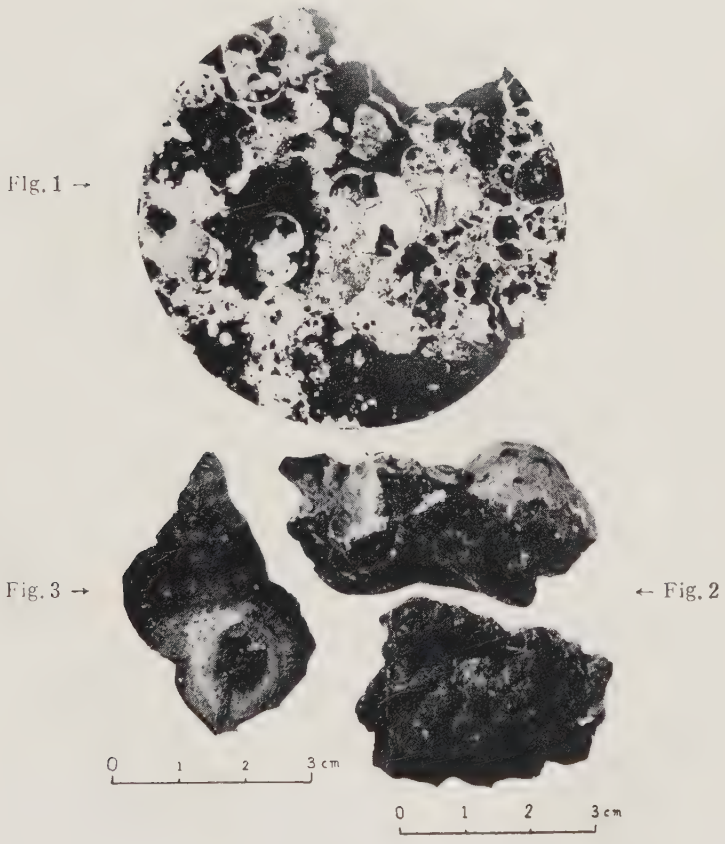

Explanation to Plate I

Figure 1. Photomicrograph of the thin section of manganese nodule. Locality St. 9. x 30.
Figure 2. External view of the manganese nodule partly covered with Bryozoa. Locality St. 9.
Figure 3. A thin black layer covering the surface of the dead shell of *Cymatium* sp. Locality St. 9.

Plate II.

Explanation to Plate II.

Figures 1, 2. ***Perotrochus*** (***Mikadotrochus***) ***beyrichi*** (Hilgendorf). Locality St. 12.
Figures 3, 4. A broken shell of a young specimen of ***Perotrochus*** (***Mikadotrochus***) ***beyrichi*** (Hilgendorf). Fig. 3 External view of the specimens. Fig. 4 Inner view the specimen.

Records of Oceanographic Works
in Japan, Vol. 2, No. 2,
October 1955

Boric Acid in Bittern (I)

Determination of Boric Acid by Barium Borosaccharate, a New Precipitant.

By

Masayoshi Ishibashi, Koichi Emi, Hiroyoshi Kataoka and Seizo Kitadani

(Kyoto University and Okayama University)

I. Introduction

The studies on the separation and determination methods of boric acid have been done by many investigators. As for the separation method, there are the calciumborate method[1], the steam distilation method[1], the boric acid ester method[1], the manganese borate method[1] and the amyl alcohol-extraction method. While, as for the quantitative method, the gravimetric methods have been reported by F. A. Gooch[2], G. Jörgensen[3], L. C. Jones[4], J. Böeseken[5], Treadwell and Hall[6], and L. V. Wilcox[7], many other reports of calorimetric methods have also been made for the determination of a small amount of boric acid[8]. But these methods can not work out well in making the separation and determination of boric acid at the same time, because of their procedures, attendant with various inconveniences as the result of which there is much danger of the loss of boric acid.

As a counter-measure to remove the drawback, J. A. Gautier and P. Pignard[9] succeeded in separation and determination of boric acid by its direct precipitation through the use of a special reagent.

From this consideration the authors have found that the precipitate of the complex boron compound could be separated from the solution of boric acid by adding the saccharic acid and barium ion into the NH_4OH-NH_4Cl buffer solution.

Compared with the quantity of boron, the quantity of this precipitate is so large that this present method, if established, will serve not only as the gravimetric method of boric acid but also as the exploitation of oceanic resources.

II. Experimental

1. Principle of Determination

By adding both bipotassiumsaccharate and barium chloride to a definite concentration of NH_4 OH-NH_4Cl buffering boric acid solution, boric acid can be separated from the solution in a form of a white slightly soluble crystal of barium

borosaccharate. Upon making an analysis of the product, boron has been found to be very small in quantity at a constant ratio. Therefore, the determination of boric acid can be made by weighing it.

2. Preparation of Precipitant

Dissolve the mixture of 5 g of bipotassiumsaccharate, 40 g of ammonium chloride and 15 g of barium chloride in water sufficient enough to bring the volume to approximately one litre and add a small amount of concentrated ammonia water. After filtration, adjust the pH to 8.6—8.8. The solution should be clear in this case. Inasmuch as the pH changes with evaporation of ammonia, care must be taken to keep the same range by adding a concentrated ammonia solution to the solution above-mentioned and also it should be carefully avoided that when the pH exceeds 9 barium saccharate is formed and barium carbonate comes to precipitate by further standing. The one litre of precipitant contains approximately 0.02 mole of saccharic acid and 0.06 mole of barium chloride.

3. Precipitation of Bariumborosaccharate

1) Conditions for Formation

i) Limitation of Concentration of Precipitant

Two kinds of precipitants, A and B are prepared as follows:

Bipotassiumsaccharate (g)	ammonium chloride (g)	conc. ammonia water	total (ml)	pH
0.1	2	small amount	50	8.8
0.1	4	small amount	50	8.8

These two solutions, A and B, have changed to different states - quite clear, turbid, or precipitation - as Table 1 shows the results - when the various amounts of barium chloride are added to the solutions.

Table 1

No.	barium chloride ($BaCl_2 \cdot 2H_2O$) (g)	A	B
1	0.1	−	−
2	0.2	−	−
3	0.3	−	−
4	0.4	+	+
5	0.5	+	+

−: clear solution containing no precipitate
+: turbid or precipitation

As is seen from Table 1, both A and B solutions of No. 4 bring forth the white precipitate after standing overnight, and therefore, more than 4 parts of ammonium chloride should not be added to one part of bipotassiumsaccharate. And an excess of ammonium chloride has also no appreciable effect.

ii) Effect of Drying Temperature and its Time

Since boric acid is designed to precipitate as barium borosaccharate and deter-

mine it by weighing the precipitate, the precipitate should be maintained in a stable condition at a definite temperature. On measuring the changes of the weight by drying temperature and its time upon 0.08 to 0.30 g of sample, the precipitate dried for 3 or 5 hours at 105°C, has attained approximately a constant weight.

In the next procedure, accordingly, the precipitate dried for 4 hours at the same temperature is used as a sample. But it takes more than 7 hours to obtain a constant weight when the quantity of precipitate is larger.

iii) Effect of Barium Chloride and Bipotassiumsaccharate

Within the maximum limit of barium chloride (c. f. 3.1 (i)) which can be added to a definite quantity of bipotassiumsaccharate, the change in the quantity of the precipitate of barium borosaccharate has been examined, as the quantities of barium chloride are changed. As the result it is found that the larger the amount of potassiumsaccharate and barium chloride, the larger the amount of barium borosaccharate is precipitated. However, it should be noted that the previous procedure is limited by the limitation concentration and the pH.

In this way, the authors have come to prepare the precipitant as shown in 2 (preparation of precipitant).

iv) Changes of Amount of Precipitate by Standing Hours

The results shown in Table 2 have been obtained by changing the standing hours, after adding 10 ml of 0.1 M-H_3BO_3 to 50 ml of precipitant.

Table 2

Number of sample	1	2	3	4	5	6
Standing hour	0.5	1.0	2.0	2.0	15	16
Precipitate (g)	0.2949	0.2866	0.3071	0.3047	0.3405	0.3384

It is desirable to allow the samples to stand overnight for the complete formation of the complex boron compound, as the result of which the reaction is considered to be carried out by the slow equilibrium reaction.

v) Changes of Amount of precipitate by Changing the Quantity of Boric Acid to a Definite Amount of precipitant.

According to the change of the quantity of boric acid added to a definite amount of precipitant, the amount of precipitate of barium borosaccharate varies. The results are given in Table 3.

Table 3

A)

Number of sample	1	2	3	4	5	6
Precipitant (ml)	50	50	50	50	50	50
0.1 M-H_3BO_3 (ml)	2	5	7	10	12	15
Precipitant (g)	0.0694	0.1969	0.2669	0.2937	0.3087	0.3208

B)

Number of sample	1	2	3	4	5	6
Precipitant (ml)	50	50	50	50	50	50
0.1 M-H_3BO_3 (ml)	2	4	7	10	12	15
Precipitate (g)	0.0845	0.1793	0.2868	0.3197	0.3200	0.3266

A) Standing for 2 hours
B) Standing overnight

From the results above-mentioned, it seems to be reasonable to assume that the formation of barium borosaccharate depends on the equilibrium reaction.

vi) Changes of Amount of precipitate by Changing Quantity of precipitant to a Definite Concentration of Boric Acid Solution

The results obtained by various experiments have confirmed the fact that when barium borosaccharate brings forth the largest amount of precipitate, the molar ratio of saccharic acid in the precipitant to boric acid is always 2:1. Therefore, the ratio described above should be taken into consideration when boric acid is required to be precipitated quantitatively.

2) Separation, Washing and Drying

Filter the precipitate with a glass filter (G4 or G5) and wash it with water. But, since the white precipitate dissolves to some extent in water, use 25% ethanol solution for washing in consideration of its slight solubility.

Then dry the precipitate at 105°C until it gets constant according to the method described in i) ii).

3) Composition of Precipitate

Upon the precipitate obtained in the treatment above-mentioned the estimation of saccharic acid, barium and boron has been made for the determination of its composition.

Table 4

Component	Quantitative method	found (%)
Sacchatic acid	Periodic acid (10)	46.86±0.58
Barium	Barium sulfate method	44.58±0.09
Boron	Alkalimetry in the presence of mannitol	2.01±0.07

From the results of the experiment, it has been found that the ratio of boron to the complex boron compound in the precipitate is 0.0201:1 and boron is contained in it at a constant ratio.

4) Properties of Precipitate

The precipitate obtained in the experiment has been found to contain 7.64% moisture by standing in the air. This precipitate is slightly soluble in water and

readily soluble in hydrochloric acid, nitric acid and acetic acid, and also the solubilities of the precipitate have been measured in such solvents as shown in Table 5.

Table 5

Kind of Solvent	Solubility (g/100 ml)	Temperature (°C)
Water	0.0322	10.4 0.1
Absolute ethyl alcohol	Decompose	10.7 0.1
Acetone	Insoluble	9.6 0.1
Alcohol solution (25%)	0.0063	9.5 0.1
Acetone solution	0.0084	9.3 0.1
Precipitant	Insoluble	9.4 0.1

4. Application to Qualitative Analysis

The treatment described above has been found to be applicable equally to qualitative analysis for boric acid in a solution.

Sensibility of reaction: Identification limit is 50 γ/ml.
The treatment must be carried out in a condition that such interfering ions as precipitate with Ba^{++} and OH^-, if present simultaneously, should be excluded with a proper method and the pH should be adjusted to 8.0-9.0 in advance.

5. Application to Quantitative Analysis

The determination of boric acid by this method has been found to be possible only in such a condition that its concentration ranges from 0.1 to 0.005 mole/*l*.

From the results of the experiment, the quantitative method of boric acid has been decided to be as follows: Add the precipitant to the solution of boric acid in the condition that the quantity of saccharic acid contained in the precipitant is 2 mole to 1 mole of boric acid (e.g., 10 parts of precipitant are added to 1 part of 0.1 M-H_3BO_3). After allowing the solution to stand overnight, filter it with a glass filter (G4 or G5), wash it twice with a small amount of water and finally 3 or 4 times with 25% ethanol solution until the solution used for washing does not show any reaction of chlorine ion. Cool the precipitate in a desiccator, after being dried (for approximately 4 hours) at 105°C until the precipitate comes constant in weight.

Apply a correction to the quantity of boron in the sample by multiplying the precipitate by the factor 0.0201.

When compared with that of alkalimetry, this method has led to a fairly satisfactory result.

III Summary

By following the afore-said analytical methods, it has been discovered that qualitative and quantitative analysis of boric acid for macro and semi-micro

quantity can be made. It must also be added that this method is distinguished in being applicable to separation and determination of boric acid at the same time.

IV Literature Cited

(1) Shoichiro Nagai, Yoshiaki Kawasumi; Study for Salt Technic, No. 1, 22, 13, 1948.

(2) F. A. Gooch; Proc. Am. Acad. of Arts and Sciences, 22, 167-176, 1886.

(3) G. Jörgensen; Z. Angew. Chem., 549, 1896.

(4) L. C. Jones; Am. J. Sci., [4], 7, 147, 1899.

(5) J. Böescken; Ber., 46, 2612, 1913; Rec., 40 354, 1929.

(6) Treadwell & Hall; Anal. Chem., vol. II. 532, 1924.

(7) L. V. Wilcox; Ind. Eng. Chem., Anal. Ed., 2, 358, 1930.

(8) I. Mellan; Organic Reagents in Inorganic Analysis (1941), F. Feigl; Chemistry of Specific, Selective and Sensitive Reaction (1949).

(9) J. A. Gautier and P. Pignard; Mikrochemie ver. Mikrochim. Acta, 36/37, 793-800, 1951.

(10) W. D. Pohle, V. C. Mehlenbacher, and J. H. Cook; Oil and Soap, 22, 115-119 May, 1945.

Records of Oceanographic Works
in Japan, Vol. 2, No. 2,
October 1955.

Optical properties of the water in the Kuroshio Current

by
Tadayoshi Sasaki*, Noboru Okami**, Seiichi Watanabe**,
and Gohachirō Ōshiba**

2. Introduction

Optical properties of the water in the Kuroshio Current have been investigated by means of a high sensitive under water photometer, described in the preceding report, with monochromatic filters, violet, blue, green, yellow, and red.

In the present case, owing to the limited course of the research vessel the observations were carried out in a region near the coast. Further studies in the open sea are under pursuance.

2. Apparatus and methods

The same underwater photometer described before was employed. In the previous case, owing to the broad spectral sensitivities of the filters, Matsuda color glasses, it was necessary to consider the effective wave-length shift due to the filtering effect of water layer.

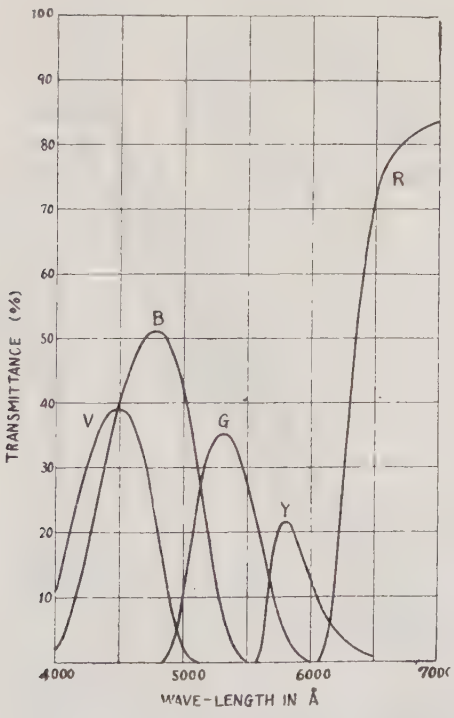

Fig 1. Transmittance Percent of Filters.

This difficulty can be removed to some extent by placing filters which are sensitive to only a narrow range of the spectrum. In the present, Kaken monochromatic filters, violet, blue, green, yellow and red, were used. Transmittances of the filters are shown in Fig. 1. Fig. 2 shows the sensitivities of the photomultiplier with the filters.

From the figure it is noticed that the ranges of transmission are about 1000 Å. The observation was carried out on the observation course of the Shinyo-Mmaru, the training ship of the Tokyo University of Fisheries, east of the Izu Peninsula,

* Tokyo University of Fisheries, Scientific Research Institute.
** Scientific Research Institute, Tokyo.

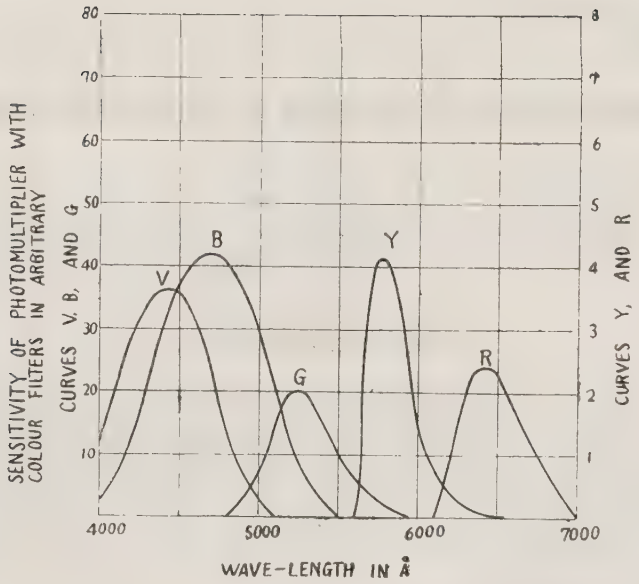

Fig 2. Spectro-Sensitivity curves of Photomultiplier with color filters.

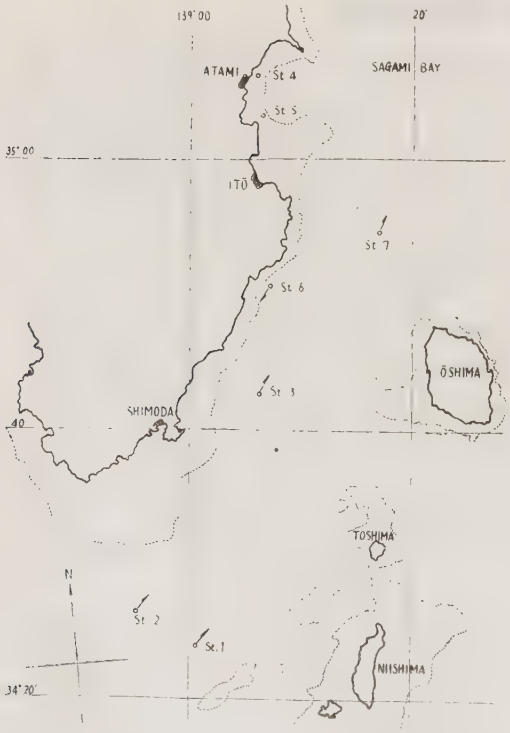

Fig 3. Location of stations where observations were made.

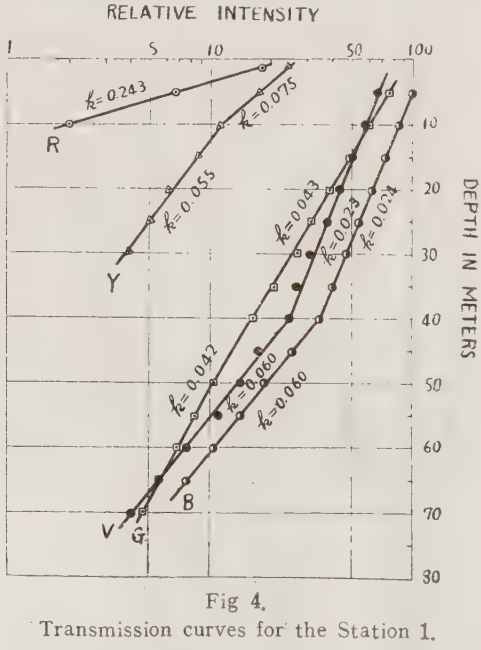

Fig 4.
Transmission curves for the Station 1.

February 1-8, 1955. Fig. 3 shows the observation stations. Observations were made for 1, 3, 5, 7 and 10 m in depth. Below 10 m, data were taken for each 5 m.

For the purpose of obtaining accurate results in the shallow water where red and yellow lights markedly attenuate, the observations were made for relatively short intervals. It was found that the interval of 5 m is sufficient for green, blue and violet lights. Time required to make the observation for five regions in the spectrum at one station was about 40 minutes. The results were expressed by relative intensities using the light intensities measured by a deck photometer as the standards.

3. Observations and Discussion

Extinction coefficients for yellow, green, blue and violet lights obtained at 7 stations are listed in Table 1. Curves in Fig. 4~10 show the light transmissions at the stations. In the figures the relative intensities for every wave length are plotted in logarithmic scale against the depth. The waters at the Stations 1 and 2 on the outward course were the most transparent, the transparency being more than 24 m; color of the water was deep blue. As seen from Figs. 4~5, in the surface layer the penetration of blue and violet lights are the highest. The extinction coefficient (k) for blue light at the Station 2 calculated from the data in Table 1 gives the minimum value, i.e. $k=0.025$. On the homeward course, as it

Table I. Summary of observations

Station	1	2	3	4	5	6	7
Latitude : N	34°-24.8′	34°-26.8′	34°-43.8′	35°-6.4′	35°-30.0′	34°-50.6′	34°-54.7′
Longitude : E	139°-0.5′	138-54.8′	139°-8.5′	139°-7.1′	139°-6.6′	139°-7.2′	139°-17.0′
Date : 1955	Feb. 2	Feb. 2	Feb. 5	Feb. 6	Feb. 6	Feb. 7	Feb. 7
Local sun time	1215~1300	1508~1607	0945~1035	1320~1355	1515~1549	1115~1145	1405~1450
Sky	clear	clear	clear	clear	clear	Over-cast	Over-cast
Av : Altitude of sun	38°00′	18°00′	—	33°19′	17°49′	—	—
Red Light (6100~7000Å)							
Av. Extinction Coefficient (m^{-1})	0.243	0.215	0.349	0.318	0.232	0.369	—
Yellow Light (5600~6600Å)							
Av. Extinction Coefficient (m^{-1})	0.065	0.120	0.087	0.133	0.110	0.106	0.092
Green Light (4800~6000Å)							
Av. Extinction Coefficient (m^{-1})	0.044	0.048	0.047	0.068	0.065	0.068	0.043
Blue Light (3900~5500Å)							
Av. Extinction Coefficient (m^{-1})	0.039	0.025	0.030	0.055	0.055	0.054	0.039
Violet Light (3800~5100Å)							
Av. Extinction Coefficient (m^{-1})	0.040	0.031	0.029	0.061	0.062	0.056	0.036

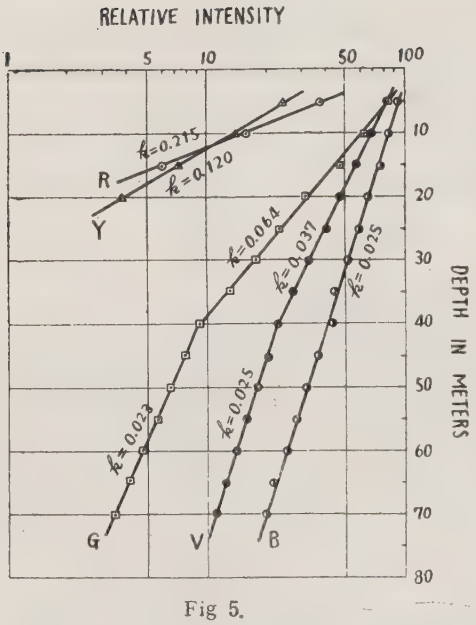

Fig 5.
Transmission curves for the Station 2.

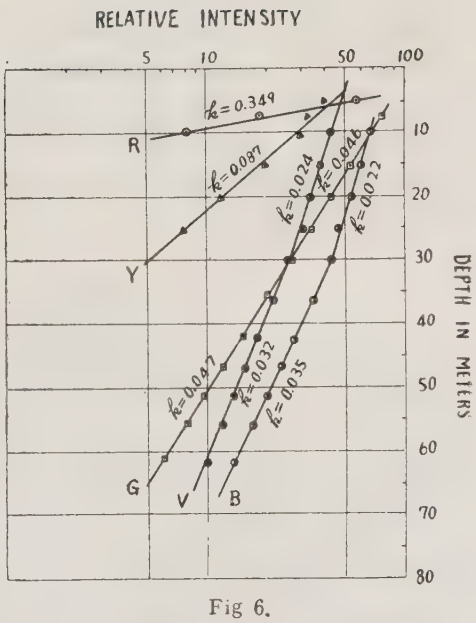

Fig 6.
Transmission curves for the Station 3.

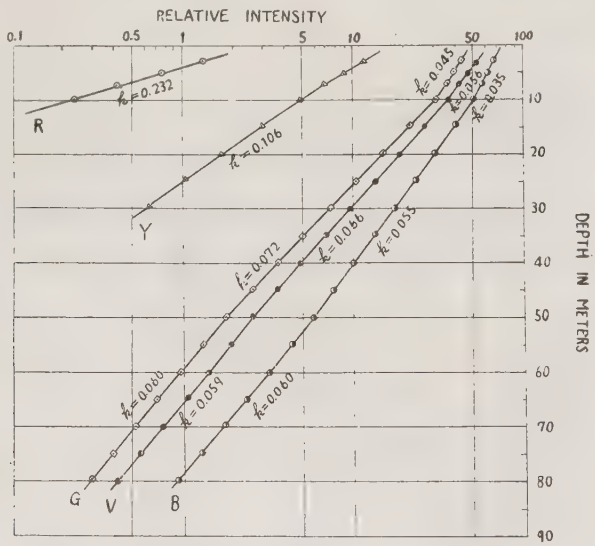

Fig 7. Transmission curves for the Station 4.

was difficult to carry out the observation owing to rough weather only one observation was mabe at the Station 3 lies midway between the Ōshima and the Izu Peninsula. The results are shown in Fig. 6. Transmission for every wave-length has the same tendency as that obtained at the Station 1, e. g. blue and violet lights have the best transmission. The extinction coefficients for short wave-length are similar to those obtained at the Station 1. But the coefficients for long wave length are larger in this case. Exact comparison seems to be unreasonable for the

errors in the measurements due to rolling of the ship.

For the purpose of making measurement at the places near the coast in Sagami Bay, the photometer was transshiped into the Hatsushima-Maru, a research vessel of fisheries laboratory in Shizuoka prefecture, and the observations were carried out February 6, 1955 at the two stations, Stations 4 and 5, 0.5 miles from the shore selected inside the bathymetric line of 200 m. On that day, as the weather was fine and the sea was smooth, the photometer lines were lowered vertically as deep as 80 m. In this place, same as in the oceanic water, blue light has the

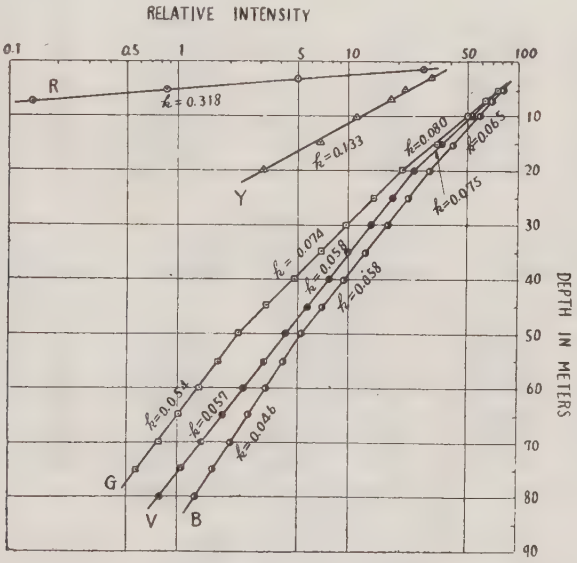

Fig 8. Transmission curves for the Station 5.

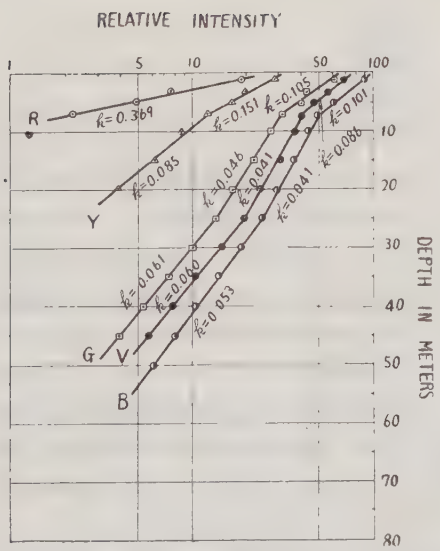

Fig 9.
Transmission curves for the Station 6.

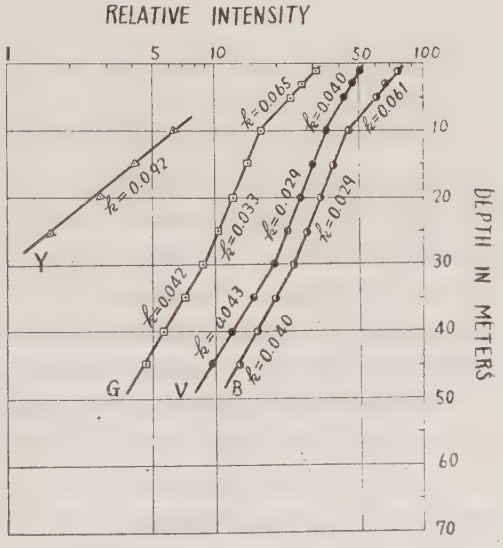

Fig 10.
Transmission curves for the Station 7.

best transmission. But the extinction coefficient was higher than that in the open sea probably due to the effect of inland water. This is also confirmed by the water temperature shown in Table 2, i. e. water temperature of the surface layer in this place is 3 degrees lower than that in the oceanic water.

Table II. Hydrographic observations

Station 1			Station 2			Station 3		
Date : Feb. 2, 1955			Date : Feb. 2, 1955			Date : Feb. 5, 1955		
Depth (m)	Temp. °C	Salinity ‰	Depth (m)	Temp. °C	Salinity ‰	Depth (m)	Temp. °C	Salinity ‰
0	17.9	34.830	0	17.7	34.821	0	16.3	34.740
25	18.07	34.794	25	17.75	34.794	25	17.59	34.740
50	18.02	34.776	50	17.78	34.776	50	17.46	34.722
100	18.05	34.794	100	17.73	34.758	100	16.12	34.650
150	17.06	34.758	150	17.57	34.704	150	15.89	34.632
200	16.17	34.686	200	16.98	34.722	200	15.09	34.596
400	12.18	34.441	400	12.00	34.487	400	13.20	34.469
600	7.41	34.325	600	8.56	34.325			

Station 4			Station 5			Station 6		
Date : Feb. 6, 1955			Date : Feb. 6, 1955			Date : Feb. 7, 1955		
Depth (m)	Temp. °C	Salinity ‰	Depth (m)	Temp. °C	Salinity ‰	Depth (m)	Temp. °C	Salinity ‰
0	14.3	34.903	0	14.9	34.686	0	15.3	34.740
10	14.70	34.632	10	14.57	34.632	25	15.30	34.632
25	14.74	34.596	25	14.59	34.506	50	14.75	34.596
50	14.68	34.578	50	14.56	34.485	100	14.46	34.578
75	14.68	34.524	75	14.59	34.560	150	14.42	34.560
100	14.63	34.480	100	14.68	34.650	200	14.39	34.551
150	13.98	3 .451	150	13.62	34.758	400	10.98	34.397

Station 7		
Date : Feb. 7, 1955		
Depth (m)	Temp. °C	Salinity ‰
0	17.5	34.740
25	17.21	34.749
50	16.87	34.722
100	15.61	34.650
150	14.41	34.596
200	13.50	34.524
400	9.83	34.325

Observations at the Station 6 and 7 were made on the homeward course of the Shinyo-Maru during cloudy weather. The Station 6 was located at 1.5 miles from the coast inside the bathymetric line of 200 m. As seen from Fig. 9 the extinction coefficient of the surface layer, less than 25 m, at the station is higher than that at the Stations 4 and 5, while in the water deeper than 25 m the value of the coefficient almost agrees with that in the oceanic water.

Arrows in Fig. 3 show the directions of currents observed simultaniously with floating plate. It will be seen from the figure that the direction of current at The Station 6 is different from those at other stations indicating the effect of surface water mentioned above.

Fig. 10 shows the results of observation made at the Station 7. Color of the water in the place was also deep blue and the transparency being 23 m.

Taking a wave-length corresponding to the maximum of sensitivity curve of photomultiplier with a filter as the "effective wave-length", the extinction coefficients for every wave-length at each station are plotted against wave-length in Fig. 11. In the figure, the curves seem to be classified into two groups, i.e. the one for transparent oceanic water and the other for the water being effected by inland waters.

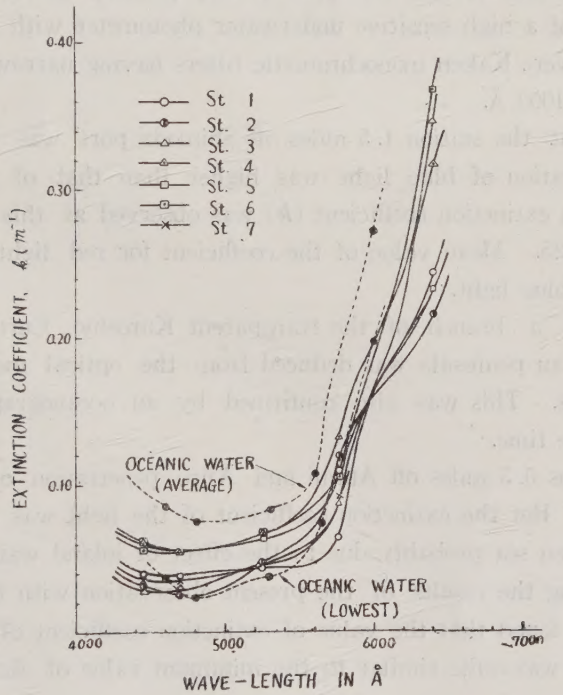

Fig 11. Extinction coefficients per meter for different wave-lengths at 7 stations.

At the same time as our observations, from hydrographic observations Mr. Makoto Ishino has found the northing (Lat. 35° N) of a branch of the Kuroshio Current between the Ōshima and the Izu Peninsula. This oceanographic investigation support our conclusion based on the optical measurements, i. e. the waters at Stations 1, 2, 3, and 7 belong to the same water system.

For the sake of reference, average minimum values of extinction coefficient in the open sea measured by Utterback are shown in Fig. 11. Extinction coefficients obtained at the Station 1~7 lie between the two values. Value of the coefficient in the open sea obtained in the Kuroshio Current is closely similar to the minimum value of the coefficients reported by Utterback. From this fact, it will benoticed that the water in the region of Kuroshio Current has high transparency.

As the present observation was carried out in the season when the water in the Kuroshio Current has the best transparency, the measured extinciton coefficient may be considered to have rather lower value than usual. Observation on the

change in extinction coefficient during all the seasons of the year seemed to be an important problem of the oceanographic investigation.

4. Summary

(1) Transmissions for natural light in a region of Kuroshio Current (Japan current) east of the Izu peninsula were measured for red, yellow, green, blue and violet lights by means of a high sensitive underwater photometer with photomultiplier.

Filters used were Kaken monochromatic filters having narrow ranges of transmission of about 1000 Å.

(2) The water at the station 1.5 miles off Shimoda port was the most transparent. The penetration of blue light was higher than that of violet and green lights. Minimum extinction coefficient (k) was observed at this station for blue light, i.e. $k=0.025$. Mean value of the coefficient for red light was eight times as large as that blue light.

(3) Northing of a branch of the transparent Kuroshio Current between the Ōshima and the Izu peninsula was deduced from the optical measurements made at several stations. This was also confirmed by an oceanographic investigation made at the same time.

(4) In the regions 0.5 miles off Atami and Ajiro penetration of blue light was also the highest. But the extinction coefficient of the light was 1.8 times as large as that in the open sea probably due to the effect of inland waters.

(5) By comparing the results of the present observation with those reported by Utterback it was found that the value of extinction coefficient of the water in the Kuroshio Current was quite similar to the minimum value of that in the oceanic water.

5. Acknowledgement

The Present authors wish to express their hearty thanks to Mr. Keijiro Ozawa, the captain of the Shinyo-Maru, for his kind help and Mr. Makoto Ishino of the Tokyo University of Fisheries who kindly presented the valuable results on the oceanographic investigation.

References

(1) T. Sasaki, N. Okami, S. Watanabe and G. Ōshiba, Records of Oceanographic Works in Japan **2**, 57 (1955)

(2) H. U. Sverdrup, M. W. Johnson, and R. H. Fleming, The Oceans, P. 84. New York (1942)

(3) C. L. Utterback, Consil Perm. Intern. P. I' Explor. de la Mer, Rapp. et Proc-Verb., **101**, pt. 2, No. 4, 15pp (1936)

(4) Jorgensen, Wilhelm and C. L. Utterback, Jour. Marine Research **2**, 30-37 (1939)